CHALMERS

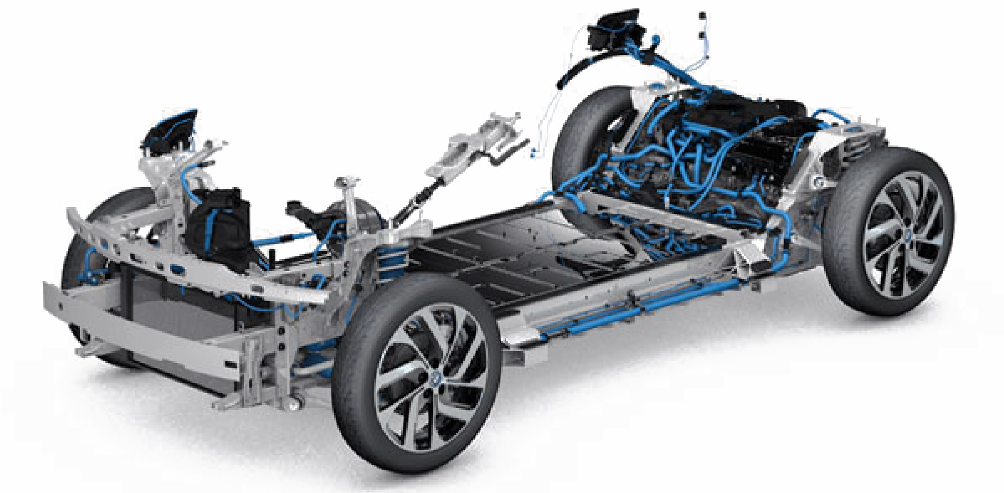

Advanced Control of Future Electric Propulsion Systems for Passenger Vehicles

Master's thesis in Automotive Engineering

VIGNESH ARUMUGAM SUBBIAH
YASHASVI NANDIVADA

Department of Mechanics and Maritime Sciences
CHALMERS UNIVERSITY OF TECHNOLOGY
Göteborg, Sweden 2018

MASTER'S THESIS IN AUTOMOTIVE ENGINEERING

Advanced Control of Future Electric Propulsion Systems for Passenger Vehicles

VIGNESH ARUMUGAM SUBBIAH
YASHASVI NANDIVADA

Department of Mechanics and Maritime Sciences
Division of Vehicle Engineering and Autonomous Systems
CHALMERS UNIVERSITY OF TECHNOLOGY

Göteborg, Sweden 2018

Advanced Control of Future Electric Propulsion Systems for Passenger Vehicles
VIGNESH ARUMUGAM SUBBIAH
YASHASVI NANDIVADA

Industrial Supervisor: Gunnar Olsson and Stefan Karlström, at ÅF Industry, Trollhättan
Examiner: Mathias Lidberg, Associate Professor, Vehicle Dynamics Group, Chalmers University, Gothenburg

Master's thesis 2018:40
Department of Mechanics and Maritime Sciences
Division of Vehicle Engineering and Autonomous Systems
Chalmers University of Technology
SE-412 96 Göteborg
Sweden
Telephone: +46 (0)31-772 1000

Cover:
A BMW i3 Chassis with the high-voltage lithium-ion battery — Source Credits: BMW UK, https://discover.bmw.co.uk

Chalmers Reproservice
Göteborg, Sweden 2018

Advanced Control of Future Electric Propulsion Systems for Passenger Vehicles
Industrial Supervisor: Gunnar Olsson and Stefan Karlström, at ÅF Industry, Trollhättan
Master's thesis in Automotive Engineering
VIGNESH ARUMUGAM SUBBIAH
YASHASVI NANDIVADA
Department of Mechanics and Maritime Sciences
Division of Vehicle Engineering and Autonomous Systems
Chalmers University of Technology

Abstract

Electric Vehicles (EVs) have been around since the 19th century,in fact the EVs were quite popular in that time period and a good number of them were sold during the 1900s but due to the advancement of gasoline engines and the invention of the electric starters for gasoline engines, vehicles powered with internal combustion engines began to dominate the market, thereby the trend for EVs declined until the early 2000s. From the early 2000s on-wards the market share of EVs has begun to rise due to the price rise of gasoline, enactment of stringent environmental policies and advent of cost effective manufacturing capabilities for EVs. The increased demand and environmental benefits of EVs are pushing the automotive companies to invest in the research and development for the Electric Vehicles to initiate the mitigation of global warming.

As the technology is moving towards EVs there is also an increased need to set goals to mitigate the road accidents and improve the vehicle and traffic safety. As a matter of fact it could be stated that Electric propulsion systems have advantages over the conventional propulsion systems since the former has a high-power density, short response time and a better controllability. However, with the ongoing trends, for future vehicles with more sophisticated safety functions, the demand for controllability will be higher. Also new driving cycles used for energy consumption, correlating better with normal driving, will put higher demands on drive-train control.

Thus the main objective of this thesis is to study and implement potential measures to improve controllability of electric drivetrains, in the view of ongoing development trends. As part of addressing the objective, it is envisioned to analyse the strengths and weaknesses in the present and future systems & the possibility of developing principles, methods and solutions to improve the control accuracy, response time, predictability and reliability is investigated.

The first phase of the thesis majorly involved developing a state of the art drive-train based on the electric propulsion technology available in the current market. This model, developed in SIMULINK, is then validated against the real world data. This part of the thesis also involves establishing use cases and sub-system performance targets for a comparative study at a later point of the thesis. The second phase of the thesis involves establishing a relation between the control parameters and sub system performance targets, which would then be the principles of improvement. Subsequently, based on the findings from the technology trends, a Future Drive-train is also proposed during this phase. The third phase involves developing the Future Drive-train and implementing the proposed principles, via a design of experiments approach, on the Future Drive-train to obtain an Optimised Future Drive-train.

On carrying out the process of optimisation on the Future drive-train an Optimised Future drive-train consisting of a Switched Reluctance Motor (SRM) of 93 kW is obtained. The power of the developed SRM is within 7% of the state of the art motor. In terms of acceleration performance (rise time from 0 to 90% of reference velocity) the developed Optimal Future drive-train lags with respect the state of the art drive-train by 2%. This speed dependent characteristic is observed for a 0-35 kmph Step Reference Input. In terms of performance on drive cycles the Optimal Future drive-train, at worst, has a 3% greater deviation from reference velocity when compared to the state of the art drive-train due to its falling power characteristics at higher speeds. In terms of acceleration performance on a transient friction surface, the Optimal Future drive-train performs better on all counts due to the reduction of reflected load inertia stemming from a higher gear ratio.The developed principles of improvement are inline with the expectations to tackle the controllability issue of the future drive-trains.

Keywords: Electrified drive-train, Traction control, Drive cycle, Speed control, Active safety, Vehicle dynamics

Acknowledgements

This thesis was carried out at ÅF Industry and the division of Vehicle Engineering and Automotive Systems at Chalmers University of Technology. We would like to thank our examiner Mathias Lidberg and Industrial Supervisors Gunnar Olsson and Stefan Karlström for their continuous support throughout the thesis, especially for their technical inputs and constructive feedback and helping us understand and implement the thesis deliverables. We also thank Lennart Hasselqvist, the Business Unit Manager - MA Automotive R&D, Jan Tammpere, the Section Manager - Chassis and Vehicle Dynamics and Nicklas Karlsson, the Section Manager - Electricals for their invaluable suggestions during the Gate Presentations. Last but not least we want to thank Ingrid Sjunnesson, Rudolf Brziak and Christopher Routledge from ÅF for their input and suggestions.

Nomenclature

BEV	-	Battery Electric Vehicle
EV	-	Electric Vehicles
PHEV	-	Plug in Hybrid Vehicle
AEA	-	Automatic Emergency Acceleration
DoE	-	Design of Experiments
ICE	-	Internal Combustion Engine
EM	-	Electric Motor
RPM	-	Revolution Per Minute
SRM	-	Switched Reluctance Motor
PMSM	-	Permanent Magnet Synchronous Motor
SPMSM	-	Surface Mounted Permanent Magnet Synchronous Motor
PMSynRM	-	Permanent Magnet Assisted Synchronous Reluctance Motor
RM	-	Reluctance Motor
IPMSM	-	Interior Permanent Magnet Synchronous Motor
RMS	-	Root Mean Square
DT	-	Drive Train
US	-	United States
LDV	-	Light Duty Vehicle
FTP	-	Federal Test Procedure
WLTP	-	Worldwide Harmonised Light-Duty Vehicles Test Procedure
WHVC	-	World Harmonised Vehicle Cycle
NEDC	-	New European Driving Cycle
NYCC	-	New York City Cycle
NVH	-	Noise Vibrations & Harshness
L_q, L_d	-	q and d axis inductances (H)
R	-	resistance of the stator windings (ohm)
i_q, i_d	-	q and d axis currents (A)
v_q, v_d	-	q and d axis voltages (V)
ω_m	-	angular velocity of the rotor (rad/s)
p	-	number of pole pairs
β	-	armature current lead angle from the q-axis
φ_a	-	armature flux linkages due to from permanent magnets along the d-q axis
I_a	-	armature current (A)
m	-	mass of vehicle (kg)
g	-	acceleration due to gravity (m/s^2)
V_x	-	longitudinal velocity of vehicle (m/s)
F_x	-	longitudinal force on tire at contact point (N)
F_d	-	force due to aerodynamic drag (N)
C_d	-	coefficient of drag
A	-	vehicle frontal area (m^2)
β	-	road inclination angle (rad)
ρ	-	density of air (kg/m^3)
F_{zf}	-	vertical load on front axle (N)
F_{zr}	-	vertical load on rear axle (N)
h	-	height of centre of gravity above ground (m)
a	-	distance of front axle from centre of gravity (m)
b	-	distance of rear axle from centre of gravity (m)
κ	-	slip ratio
Rr	-	tire rolling radius (m)
ω	-	wheel angular speed (rad/s)
F_z	-	vertical load on tire (N)

B, C, D, E	-	magic tire formula coefficients
N	-	gear ratio
r_f	-	radius of follower gear (m)
r_b	-	radius of base gear (m)
τ_b	-	torque acting on base gear (Nm)
τ_f	-	torque acting on follower gear (Nm)
τ_{loss}	-	losses in torque transfer calculated based on the efficiency parameter (Nm)
ω_f	-	follower gear angular velocity (rad/s)
ω_b	-	base gear angular velocity (rad/s)
J_f	-	follower gear inertia (kgm^2)
J_b	-	base gear inertia (kgm^2)
$error$	-	velocity error (input to the controller)
$V_{reference}$	-	reference/target velocity for the vehicle (m/s)
P	-	proportional gain
D	-	differential gain
λ	-	amplitude of the flux induced by the permanent magnets of the rotor in the stator phases (Vs)
T_e	-	electromagnetic torque (Nm)
θ_e	-	rotor angle (rad)
T_{ph}	-	torque generated by one phase (Nm)
Ψ_{ph}	-	magnetic flux linkage (Vs)
θ_{ph}	-	rotor angle (degree)
i_{ph}	-	phase current (A)
V_{ph}	-	phase voltage (V)
R_{ph}	-	phase resistance (ohm)
T_f	-	shaft static friction torque (Nm)
T_m	-	shaft mechanical torque (Nm)
F	-	combined viscous friction of rotor and load
J	-	combined rotor and load inertia (kgm^2)
T_M	-	motor torque (Nm)
J_M	-	motor inertia (kgm^2)
J_L	-	load inertia (kgm^2)
J_L^*	-	load inertia including gear-box inertia (kgm^2)
J_{GB}	-	gear box inertia (kgm^2)
J_t	-	total reflected inertia (kgm^2)
N_M	-	number of teeth on base gear wheel
N_L	-	number of teeth on follower gear wheel

Contents

1 Introduction

1.1 Background

Electric vehicles (EVs) have been around since the late 1800s and their popularity has been steadily increasing ever since as seen in Figure 1.1 [IE17], which depicts the growth of EVs between 2011 and 2025.This trend is expected to hold if not increase and BEVs (Battery Electric Vehicles) are forecast to hold 60% of the total electric vehicle (including PHEV & HEV) sales by the year 2025, when the EV stock pile is expected to cross 7 million with annual sales of over 1 million vehicles [CS17]. The increased market share and wider acceptance of

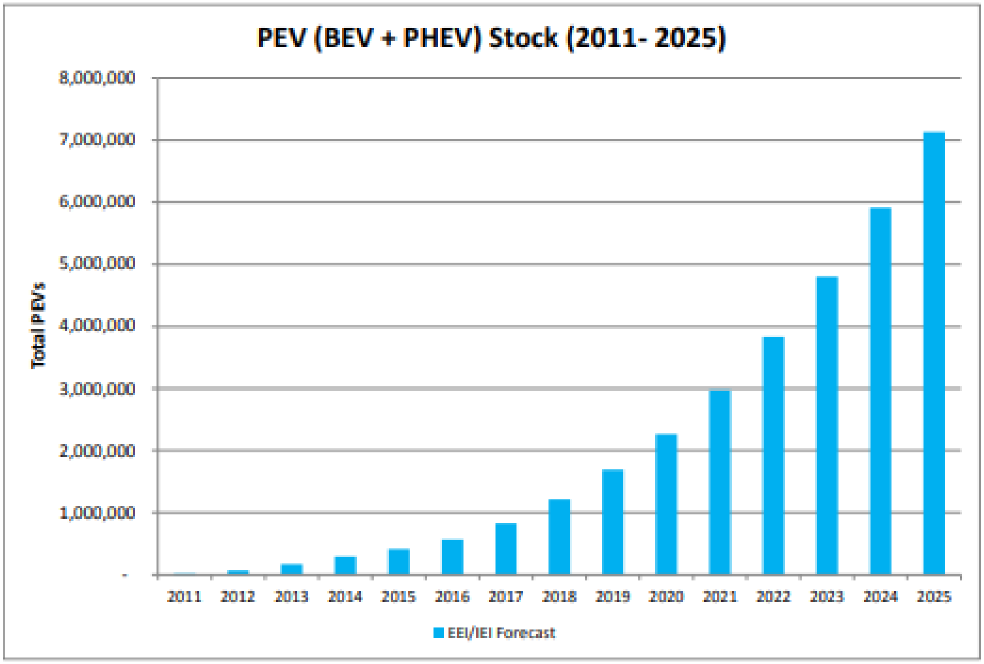

Figure 1.1: Evolution of the Global Electric Car Stock(2011-2025) [IE17]

EVs can be attributed to the factors below:

- ***Cost of Ownership***
  With many countries increasing the taxes on petrol & diesel vehicles and at the same time offering incentives for EVs, consumers are drawn towards ownership of EVs. Adding to this, low running costs (mainly due to lower fuel costs) and lower depreciation rates are making the cost of ownership of EVs lower than it's competitors as seen in Figure 1.2 [Pal+18].

- ***Performance***
  The performance of traditional combustion driven vehicles are typically sub-par when compared to BEVs, the key differences are enumerated below.

  1. **Torque Characteristics**
     Electric Motors(EM),as an inherent characteristic,provide higher starting torque/low end torque when compared to ICE(Internal Combustion Engine) of similar ratings.EMs can provide a constant torque for a greater range of RPMs when compared to ICE.This torque characteristic aids in quicker acceleration times for EVs and also improves performance in cases such as emergency acceleration.

  2. **Response time**
     EMs have lower response times when compared to ICEs. The response time for EMs are in the range of tens of milliseconds while the response time for ICEs is in the order of hundreds of milliseconds [ARI15].This characteristic of EMs improves the performance of the EV is the domains of active safety and stability control.

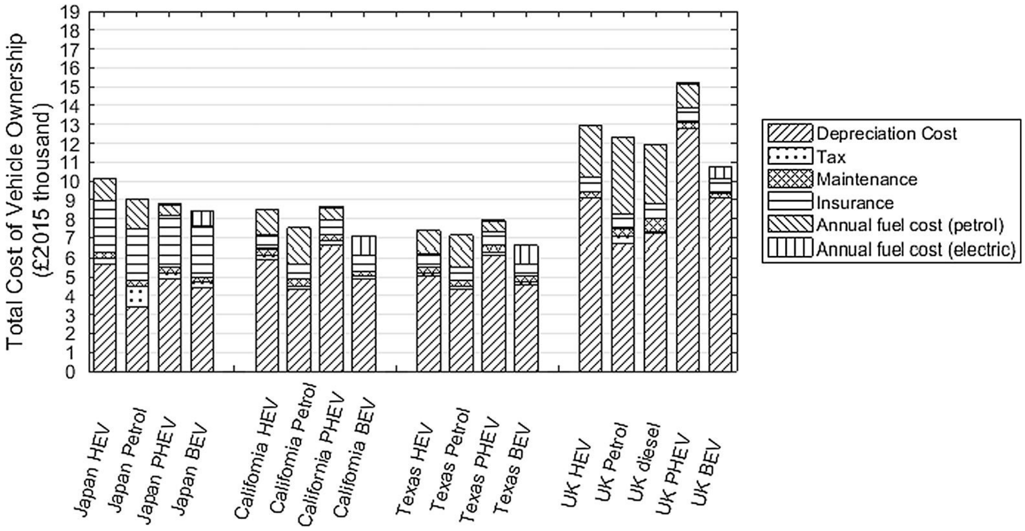

Figure 1.2: Cost of ownership of different vehicle types across 3 countries in FY 2015 [Pal+18]

3. **Emissions & Efficiency**
It is a well known fact that the EM are more efficient in operation offering upto 95% efficiency where as the most efficient ICEs can offer only upto 30% efficiency. Thus BEVs offer a greater energy economy and a better tank to wheel efficiency. This can be summarised in Figure 1.3 [UC07]

Technology	Energy Economy Ratio (EER)			Energy Consumption	
	Baseline	Low	High	(mpgge)	(MJ/mi)
Gasoline, ICEV, 2005 LDA Mix	—	—	—	20.8	5.71
Gasoline, ICEV	1.0	0.92	1.08	22.33	5.33
Gasoline, HEV	1.35	1.22	1.5	30.14	3.95
Gasoline PHEV	1.40	1.35	1.6	31.26	3.81
ULSD, DICEV	1.25	1.21	1.37	28.80	4.13
Biodiesel - BD20, DICEV	1.25	1.21	1.37	28.80	4.13
FT Diesel – FT30, DICEV	1.25	1.21	1.37	28.80	4.13
CNG, ICEV	1.0	0.98	1.08	22.33	5.33
LPG, ICEV	1.0	0.98	1.08	22.33	5.33
E85, FFV	1.03	1.02	1.06	23.00	5.17
Ethanol, dedicated ICEV	1.07	1.03	1.1	23.89	4.98
Hydrogen ICEV/ICHEV	1.3	1.18	1.9	29.02	4.10
Hydrogen FCV/FCHEV	2.0	1.7	2.5	44.65	2.67
PHEV Grid mode	3.6	3.0	4.2	80.38	1.48
Battery EV	3.6	3.0	4.2	80.38	1.48

Figure 1.3: Comparison of energy efficiency of different vehicle types [UC07]

Although EVs offer many advantages, there are certain aspects of their production and manufacturing which have great implications on the environment, especially their demand for exotic and rare materials such as Cobalt and Lithium for batteries, Neodymium, Dysprosium and Samarium for permanent magnets.There do exist alternatives for LiCo batteries such as Fuel Cells, Super Capacitors and alternate chemistry batteries such as Aluminium-Graphite but there exist no such alternatives (which offer the same performance) for Neodymium based permanent magnets.This is a cause for concern as:

- With the increase in demand in EVs(1.1) there is a proportional increase in the demand of high performance Neodymium based permanent magnets. This would increase the price of an already rare and expensive raw material. The trend of demand of permanent magnets is depicted by the projection of US Permanent Magnet Market Size Figure 1.4 [INC]

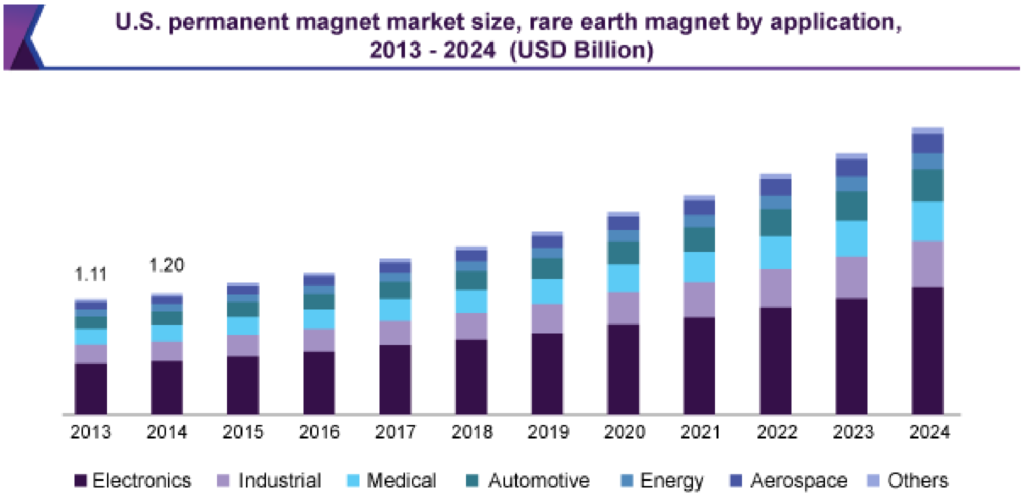

Figure 1.4: Projected demand of permanent magnets in US [INC]

- The production of permanent magnets is dominated by countries such as China, if a situation similar to that of the the Arab Oil Embargo (1973) or Oil Crisis (1979) were to occur, the situation would be dire.
- The production of rare earth metal magnets releases great amounts of toxic acidic waste which is detrimental to the environment

Hence, it can be understood that EVs have become an integral part of modern society but a vast amount of research has to be carried out in order to identify potential alternative technologies which greatly reduce the demand for rare and expensive raw materials.

1.2 Motivation for the Project

As described in the section 1.1, Electric Propulsion systems have advantages over the conventional propulsion systems since the former has a high-power density, short response time and a better controllability. For future vehicles, with more sophisticated safety functions and new driving cycles used for energy consumption evaluation, the demand on the controllability and overall performance of the drive-train will be even higher. However, these increased demands have to be met by recognising the availability and costs of exotic raw materials, hence there is an imminent need to identify possible future electric drive-trains and implement strategies to improve their controllability.

1.3 Objective and Envisioned Solution

The objectives of this project are to determine the trends in electric propulsion technology and based on these trends develop a model of a potential future electric drive-train, on which measures improving controllability are implemented.The potential future electric drive-train will be representative of drive-trains expected to emerge in the market 6 to 7 years hereinafter.

1.4 Deliverables

The major items to be delivered at the conclusion of this study are summarised as:

- A study of the technical, market and social trends in electric propulsion technology
- Define use cases e.g. real-life driving cycles (mainly US, China & Europe), and Automatic Emergency Acceleration (AEA)
- Identify subsystem performance targets
- Develop principles for improving controllability based on identified use cases
- Demonstration of drive-trains with and without the proposed improvements on the identified use cases

1.5 Delimitations

To limit the scope of this study, certain boundaries on the field of study have been imposed:

- No vehicle configurations apart from passenger vehicles are considered
- Vehicle configurations with two driven wheels and no more than four wheels are considered
- Configurations involving hub motors are excluded
- Minimum of one and maximum of two motors are considered to propel the vehicle
- Longitudinal and straight line vehicle manoeuvres are considered

1.6 Work Procedure and Methodology

The work flow adopted can be described using the logical steps taken through the project as:

- ***Step 1: Literature Review, Technology Analysis and Prediction of Future Drive-train***
  Through literature studies and interviews with subject matter experts, status and trends in E-motor technology, transmissions and power electronics were determined.Further,the strengths and weaknesses of the State of the Art and future systems were identified and analysed. The conclusion of this stage included the realisation of:
  1. Current EV technology and establishment of the State of the Art Drive-train
  2. Possible development opportunities for Future Drive-train
- ***Step 2: Modelling of Drive-train and Vehicle Systems(both State of the Art and Future)***
  As mentioned in Step 1, two drive-train models are developed.The development of both the drive-train models followed a 'V' approach which is conceived during the project planning stage of the project and is represented in Figure 1.5. The motivation for such an approach comes from the fact that the V-Model demonstrates the relationships between each phase of the development life cycle and its associated phase of reaching the surface level or the testing phase in this case.
  Once the models are developed, the use cases, on which the drive-trains are to be studied, are identified. Some of the driving scenarios of interest are real life driving cycles, emergency acceleration(to prevent rear end collision), braking on low/stepped friction surface etc.
- ***Step 3: Design of Experiments to obtain Optimised Future Drive-train***
  Using the models developed in Step 2 the effects of parameters,both electrical and mechanical, on the performance of the drive-trains are identified. The effects of these parameters are analysed with the help of Design of Experiments against the vehicle level targets for Velocity. These vehicle level targets include the Rise Time, Peak, Settling Time of the trace signal to the input signal. These targets are identified for a Step reference Input of velocity. These reflect the principles to be developed and implemented on the Optimised Future drivetrain to improve the control accuracy, response time, predictability and reliability of the future drive-train. These principles are adopted with the following restrictions:
  1. Maximum torque on the wheel is to be the same as in the State of the Art drive-train
  2. The maximum motor power is to be similar to the State of the Art drive-train

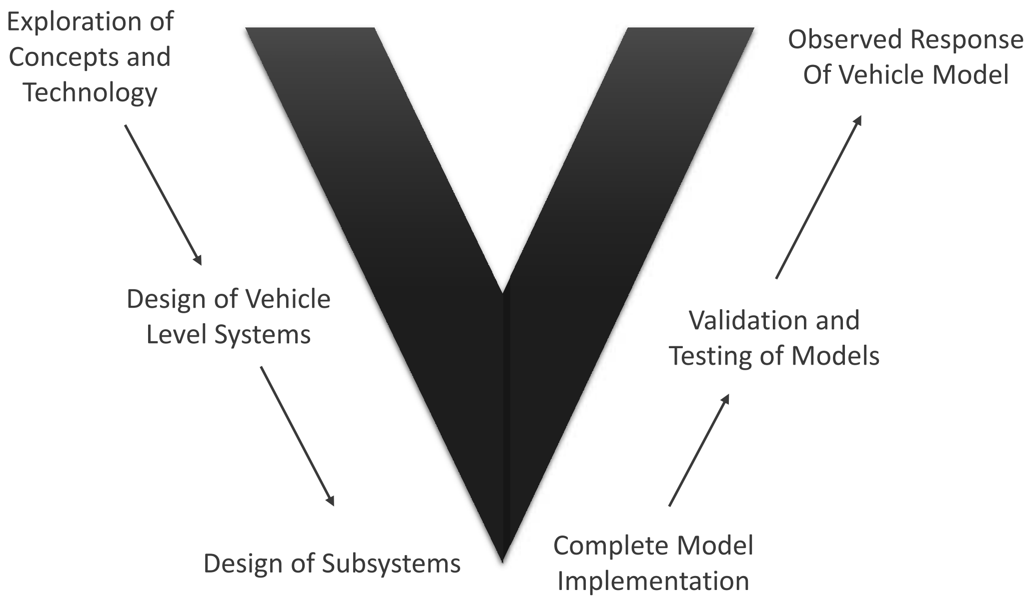

Figure 1.5: Adopted 'V' approach for Model Development

3. The same vehicle level controllers is to be used for both drive-trains
4. The same drive-train layout is to be considered for both drive-trains

- ***Step 4: Simulation/Analysis of drive-trains on use cases***
  The Optimised Future Drive-train obtained in Step 3 is then compared,using the selected use cases, with the State of the Art drive-train.

The above work flow is summarised in Figure 1.6

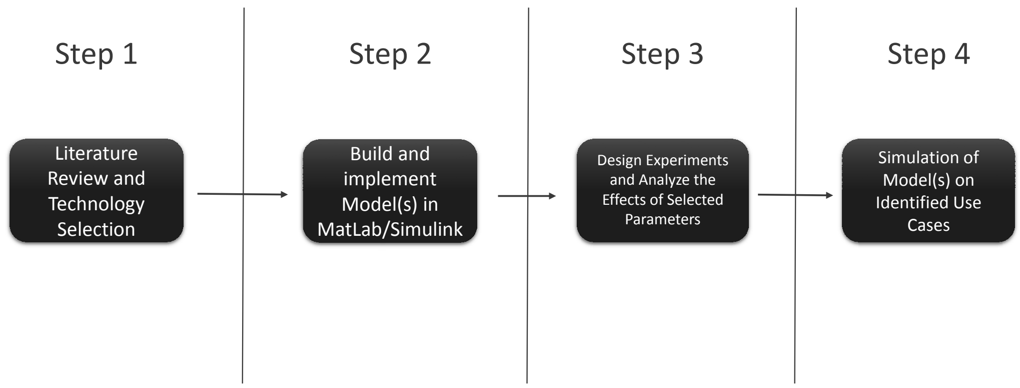

Figure 1.6: Work flow divided into four steps

2 Technology Review

This section briefly discusses the Literature review undertaken during the course of the thesis and the technology analysis pursued in order to establish a connection between the State of the Art and Future Systems. The terms State of the Art corresponds to the Current Day Scenario in Technology.
The priori for Design of Experiments is also discussed in this section, which helps understand the Analysis in the later sections.

2.1 Literature Review

On a surface level, to understand the scope of the thesis better, the major areas of concentration are classified to be studied during the literature review phase. As part of this the areas of major focus are divided as below.

- Electric Vehicle Database - This section intends to identify the current State of the Art electric vehicle technology which enables narrowing down the State of the Art Drive-train.
- Drive Cycles - This section intends to select the Drive Cycles that would put highest demand on the powertrain, thus contributing for a better comparison. This section also establishes the base for Section 3
- Market Trends - This section intends to dwell the the factors driving the EV trend and establish the emerging and future trends.
- Powertrain Technology - This section intends to compare the existing Powertrain Technologies and discuss in brief the reasons for their preference.
- Control & Power Electronics - This section briefly discusses the Power Electronics available and their importance in tackling the scope of this thesis.

2.1.1 Electric Vehicle Database

To understand the State of the Art scenario of Electric vehicles, it is very important to list down the specifications of the vehicles available today. To simplify the search region, as established in the delimitations it is decided to list down the Passenger Electric Vehicles. The parameters of technical importance are identified for each vehicle and their respective values are captured.

The vehicle list here is the list of Highway Capable Passenger electric vehicles available in the market.The vehicle database is as shown in table A.

2.1.2 Drive Cycles & Manoeuvres

As mentioned in Section 1.6, Use Cases are to be selected for demonstrating the performance of the drive-trains. This section briefly describes about the drive cycles that are considered in the scope of this thesis. However the selected drive cycles will be discussed in Section 3.2. The Drive Cycles are studied with the US, EU and China markets as major focus of concentration. The intent is also to select cycles that have higher performance impact on the drive train. The identified drive cycles are described in table 2.1

Table 2.1: Drive Cycles under Consideration

Country	**Drive Cycle**		
US	Federal Test Procedure - 75 (FTP75)	New York City Cycle (NYCC)	US06
EU	New European Driving Cycle (NEDC)	Worldwide Harmonised LDV Test Procedure (WLTP)	
China	WLTP	World Harmonised Vehicle Cycle (WHVC)	

The underlying intent of this thesis is to introduce enhanced possibilities of vehicle dynamics with electric Drive-trains. To demonstrate this core idea, the drive manoeuvre use case is introduced in this section. The term evasion signifies collision avoidance that cannot be performed by braking. The control opportunities for

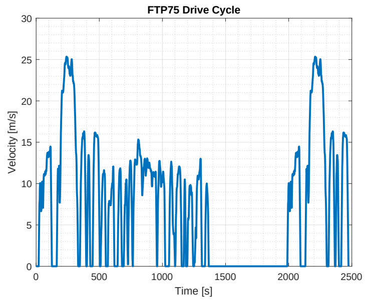

Figure 2.1: FTP75 Drive Cycle

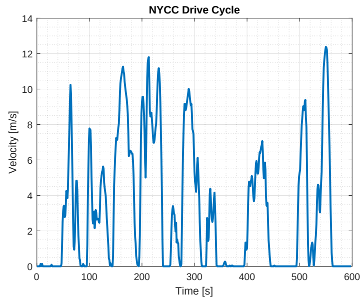

Figure 2.2: NYCC Drive Cycle

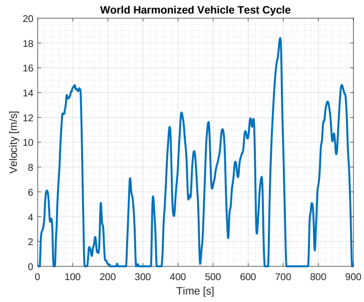

Figure 2.3: WHVC Drive Cycle

each of the manoeuvres are shown in their respective figures.
The possibility of electric Drive-train intervention is briefly discussed in the Appendix.

2.1.3 Market Trends

As for the study of technology trends in the industry, McKinsey as a team with A2Mac1 [Err+17], a supplier of car benchmarking services, led an extensive scale benchmarking of first-and second-generation EV models, which included physically dismantling ten EV models: the 2011 Nissan LEAF, the 2013 Volkswagen e-up!, the 2013 Tesla Model S, the 2014 Chevrolet Spark, the 2014 BMW i3, the 2015 Volkswagen e-Golf, the 2015 BYD e6, the 2017 Nissan LEAF, the 2017 Chevrolet Bolt, and the 2017 Opel Ampera-e. Together these models account for about 40 percent in the market share of Battery Electric Vehicles. This tear down analysis along with publicly available information and subject matter experts revealed key insights into the trend.
The key insights include,

- ***Platform Architecture vs Range***
  The benchmarking demonstrates a gap in bridging driving range and interior space between models with native EV platform architectures and those based out of ICE platforms. OEM's native architecture platforms have better battery packaging where as the non-native platforms have forcefully fit battery packaging which in turn limits the realisable energy capacity. The native EV battery pack, by far, can take a basic, rectangular shape, making native EVs to double the range by more than 300 kilometers per charge and to roughly 400 kilometers for the best performing architectures, as per the Environmental Protection Agency—without constraining up the price (2.4).Also, Native EVs accomplish a larger interior space (up to 10 percent by regression line) for a similar wheelbase compared to the ICE vehicles.

- ***Design to Cost Ratio***
  As similar to the trends in the initial days of ICE development, OEMs are following a similar way of tackling problem for the EVs as well. Once the battle for establishing the leadership for performance and range, OEMs are targeting the design to cost build-up in the second generation EVs being developed. This trend could be mostly noted in component integration and smarter usage of light weight materials and avoiding over design. OEMs are trying to cut down the weight of the vehicle by leaps and bounds to achieve a better range (2.5). However there is always a limit beyond which the OEMs are not willing to cut down the weight to ensure a safe structure. This then brings us to the discussion of cutting down the weight of the powertrain. Generational leaps in powertrain technology are expected to yield significant weight reductions. This would not only reduce the weight but also the Powertrain Manufacturing costs. Although there aren't any external incentives available today for cutting down weight in EVs, it could be a possibility in the near future thus enhancing the market.

- ***Competence and Components***
  The combinations of engine transmission types are very minimal by the current EV industry, as the [Err+17] rightly says there is hardly any differentiation in performance in current EVs compared to their ICE counterparts in the same segment. Base EV's configurations contain many options already unlike the ICEs which evolved over time. This will also imply that the small window for component level

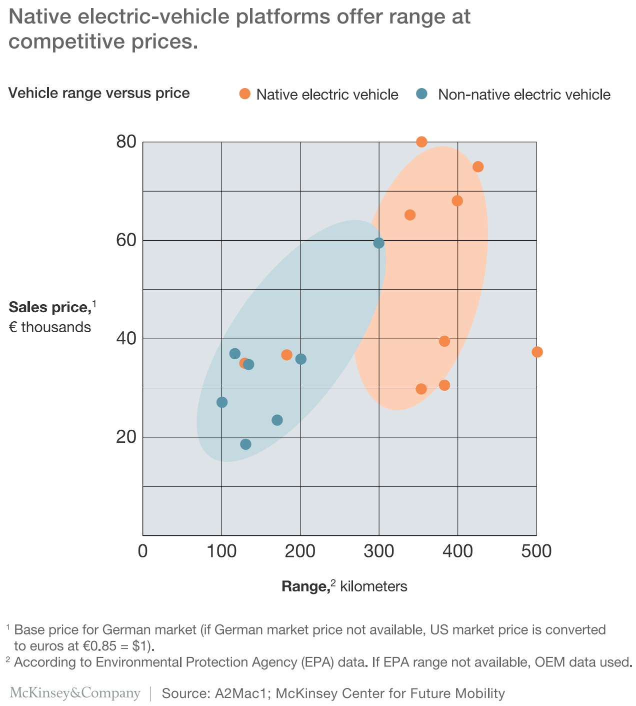

Figure 2.4: Platform Architecture vs Range [Err+17]

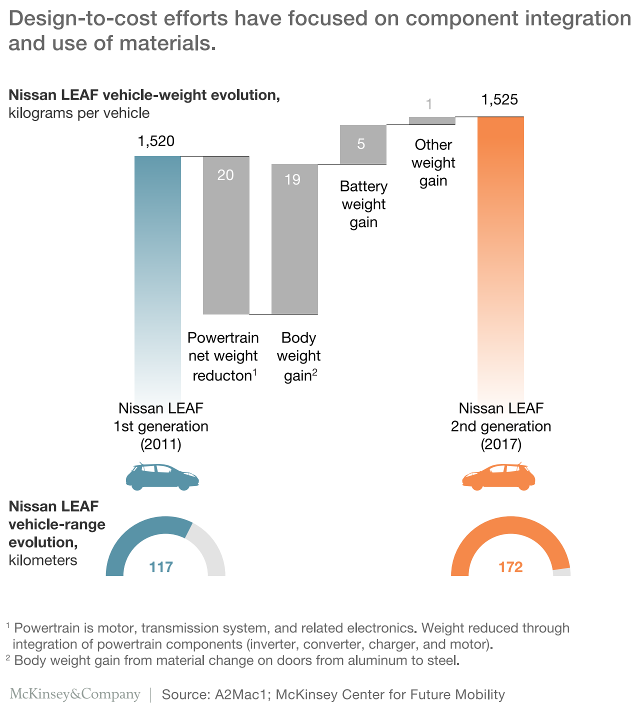

Figure 2.5: Nissan Leaf Vehicle Weight Evolution [Err+17]

improvement against the time which would in turn hit back at the OEM sales. Hence, there is a huge need for having in-house or outsourced competency and supply chain strategies. It is already seen from the current trend that all the manufacturers prefer different supply-chain strategies for their respective powertrain and batteries(2.6).Thus it could be seen that the Market would heavily rely on two-tier and in-house competencies to innovate the available technology and improvise.

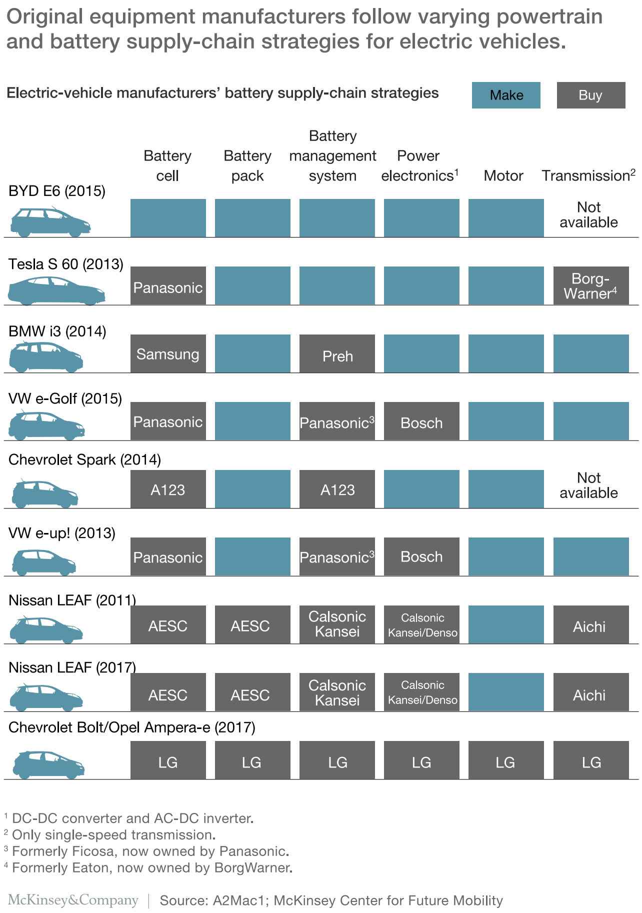

Figure 2.6: OEM's Supply Chain Strategies [Err+17]

2.1.4 Powertrain Technology

EV Powertrain

EVs are usually considered flexible setups due to the fact that they carry less number of intricate mechanical parts in them. Powertrain in an EV refers to the combination of the Electric motor, Transmission and Differentials.

In Figure 2.7, it could be seen that EV is a system incorporating three different sub systems. Energy Source, Propulsion and Auxiliary Systems. The arrows indicate the flow of the entities in question. A backward flow represents actions like regenerative braking. The energy source should be capable to store the energy sent back by regenerative actions. Most of the EV batteries along with capacitors/flywheels are compatible with such energy regeneration techniques. [UnN+17]
The energy source includes the the refuelling system and energy management system. The Propulsion includes the powertrain as well as the Power Electronics controlling the powertrain. The Auxiliary System consists of alternate power supply, cooling systems, temperature systems, power steering etc. In the scope of this thesis, importance is given to the E-Motor technology nevertheless significant study has been performed on the transmission and differential technologies.

Generic Powertrain Configuration

EVs in general can have multiple number of configurations possible based on the type of wheel drives. As an example a front wheel driven vehicle is presented below. It could be seen from figure 2.8, the various possibilities of powertrain arrangements are possible with EVs. Based on the requirement a clutch can be used or avoided, motor-gear-differential can be used as one single unit or in-wheel motors could be used. A detailed

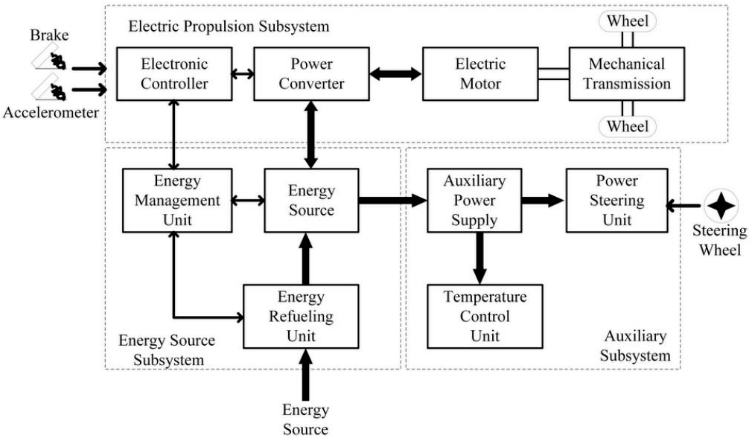

Figure 2.7: EV Powertrain Subsystems [UnN+17]

analysis on the advantages and disadvantages is performed in Section 2.2.

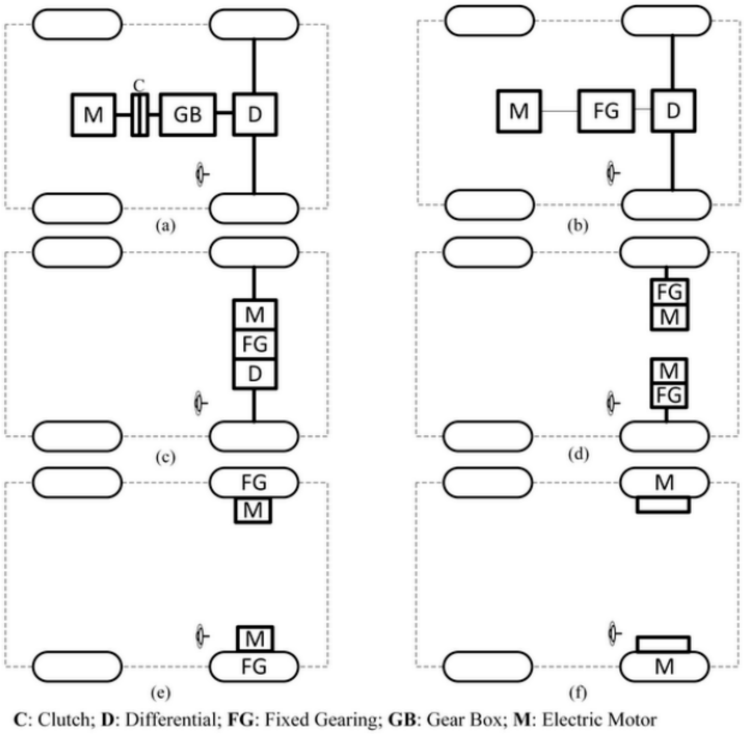

Figure 2.8: EV Powertrain Configurations [UnN+17]

E-Motor Technology

From Table A, it could be seen that the E-Motors that are preferred by the current market are majorly PMSM machines followed by the IM machines. However there are different types of E-Motors that have not yet stepped into automotive markets. The working of the motors currently available and soon to be available below.

PMSM Machine A PMSM or Permanent Magnet Synchronous Machine is an AC Motor which in steady state has synchronised shaft rotation as that of the frequency of the supply current. Ideally, PMSMs contain multiphase AC electromagnets on the stator of the motor that create a magnetic field which rotates in time with the oscillations of the line current. Subsequently the rotor has permanent magnets and turns with the stator field in the same rate. This results in a second synchronised rotating magnetic field. For synchronous motors the voltage equation can be given as equation 2.1. Equation 2.1 relates the d and q axis voltage (v_d & v_q) with d and q axis currents (i_d & i_q),d and q axis inductance (L_d & L_q), motor angular speed (ω_m),armature flux linkages due to from permanent magnets along the d-q axis (φ_a),resistance of the stator windings (R) and number of pole pairs (p).

$$\begin{bmatrix} v_d \\ v_q \end{bmatrix} = \begin{bmatrix} R + pL_d & -\omega_m L_q \\ \omega_m L_d & R + pL_q \end{bmatrix} \begin{bmatrix} i_d \\ i_q \end{bmatrix} + \begin{bmatrix} 0 \\ \omega_m \varphi_a \end{bmatrix} \tag{2.1}$$

The output torque (T) can be given by equation 2.2. In this equation the torque is a function of armature current (I_a) and armature current lead angle from the q-axis (β)

$$T = p\left\{\varphi_a I_a \cos\beta + \frac{1}{2}\left(L_d - L_q\right) I_a^2 \sin 2\beta\right\} \tag{2.2}$$

Depending on the arrangements of the magnets, these motors are further divided into two broad categories.

SPMSM In this type of motor the arc-shaped magnets are mounted on the surface of the rotor core. These magnets are also covered from outside with the help of steel sheets to avoid any magnet fallouts.Lack of magnetic saliency makes this motor use the magnetic torque alone. The maximum torque in this case is achieved at β=0 in equation 2.2. This is considered to be the most efficient phase angle. The motor having a simple construction has a major disadvantage of eddy current losses due to the steel coverings.

IPMSM Unlike the SPMSM, magnets are embedded into the core of the rotor in this type of motor. Due to this fact, the rotor becomes a salient pole and thus both the reluctance as well as magnetic torque can be utilised for the motor operation. The current phase that gives maximum torque is calculated by equation 2.3.

$$\beta = \sin^{-1} \frac{\varphi_a + \sqrt{\varphi_a^2 + 8(L_q - L_d)^2 I_a^2}}{4(L_q - L_d) I_a} \tag{2.3}$$

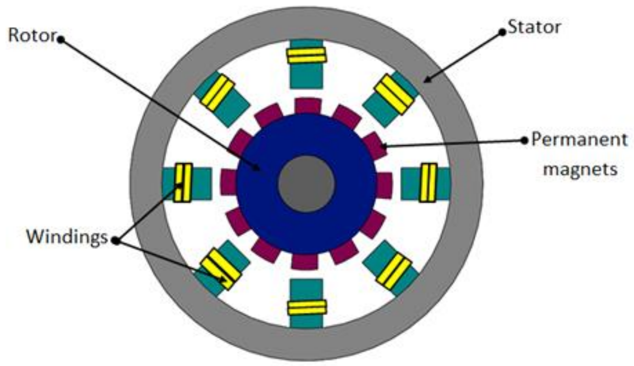

Figure 2.9: PMSM Cross Section [17c]

Induction Motor Machine An induction motor unlike PMSM is an Asynchronous AC electric motor in which the electric current in the rotor produces torque, which is obtained by electromagnetic induction from the magnetic field of the stator winding. This makes it easier for the motor hardware design as IM can be made with zero electrical connections to the rotor. An IM can be either a squirrel cage or a wound rotor type of machine. IMs are preferred in automotive industry due to their capability of being used with Variable Frequency Drives in variable speed applications. In principle both induction and PMSM machiness AC power is supplied to the motor's stator creating a magnetic field that rotates in synchronism with the AC oscillations. The difference being, in a PMSM rotor turns at the same rate as the stator field and in an induction motor rotor turns at a comparatively slower speeds than the stator field.

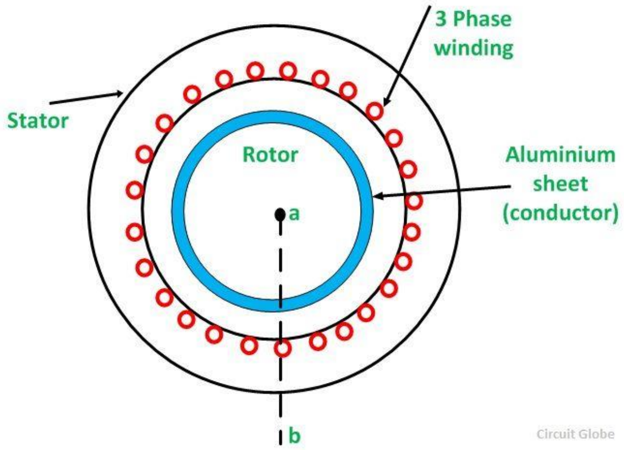

Figure 2.10: IM Cross Section [17b]

Reluctance Motor Machine A reluctance motor induces non-permanent magnetic poles on the ferromagnetic rotor.In this type of motor the rotor does not have any windings. The torque is generated using magnetic reluctance. There exists different types of Reluctance motors.

- ***Switched Reluctance Motor*** This motor works similar to a stepper motor but being driven by reluctance torque. The power is delivered to windings in the stator rather than the rotor. A better switching mechanism needs to be in place as there aren't any electrical connections to the rotor. The wound field coils in Switched Reluctance Motor are similar to that of the DC Motor. The rotor in this case is a solid salient pole rotor having magnetic pole projections. As power is applied to the stator windings the force created by the magnetic reluctance on the rotor aligns the rotor pole with the nearest stator pole. The stator leads the rotor in the forward direction by switching on the windings of successive stator poles by an electronic system.

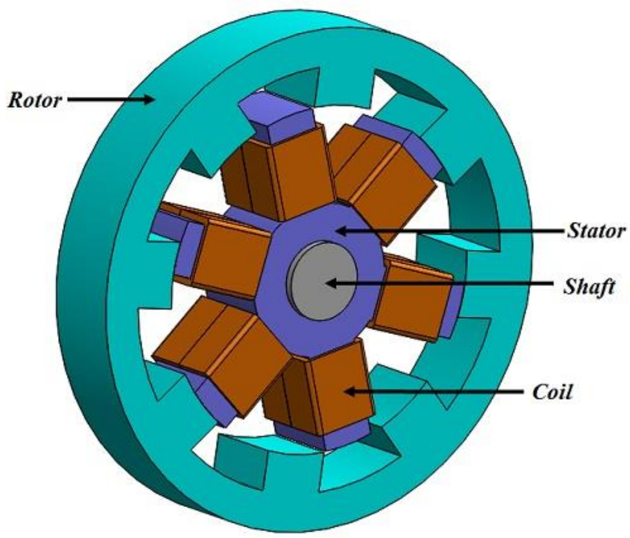

Figure 2.11: Switched Reluctance Motor [17d]

- ***Synchronous Reluctance Motor*** The SynRM, for its torque production, utilizes the reluctance concept and rotating sinusoidal Magneto Motive Force (MMF), which is produced by the traditional IM stator. Synchronous reluctance motors (SynRM) have an equivalent number of stator and rotor poles, unlike the switched reluctance motors. The projections on the rotor are orchestrated to introduce internal flux barriers, openings which direct the attractive transition along the purported direct axis. Typically these motors have 4 and 6 poles.As the rotor is working at synchronous speed the absense of current coinducting parts produces minimal rotor losses compared to the IM. Once began at synchronous speed, the motor can work with sinusoidal voltage. Variable frequency drives are used for a better speed control.

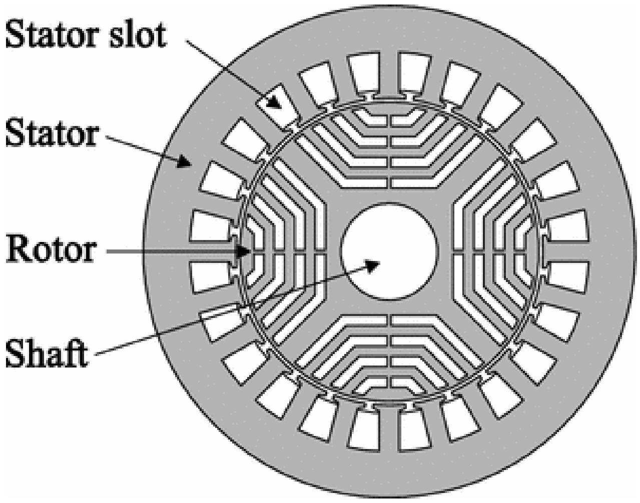

Figure 2.12: Synchronous Reluctance Motor [KF16]

A comparison between motor parameters can be seen in table 2.2

Table 2.2: Parameter values

	SynRM	PMSM	IPMSM
Magnetic Flux Linkage	φ_a=0	$\varphi_a > 0$	$\varphi_a > 0$
d and q-axis inductance	$L_q < L_d$	$L_q = L_d$	$L_q > L_d$

2.1.5 Control and Power Electronics

Power electronics in an EV is a combination of power switching devices, power converter topology with switching strategy and the close-loop control system of the motor. The selection of right semiconductor material, switching strategies and converter/inverter is very much detrimental in an efficient and high performing EV. The challenge of packaging all these components in a compact space would deliver a better system over all. The trend is moving towards having a smaller and low cost power electronic systems [Raj13]. For an EV to stand out, the power electronics also have to withstand the extreme vibrational noise as well as the heavy thermal cycles through the process.
Currently most of the EVs and HEVs are using the 3-phase bridge inverter topology to convert the battery dc voltage to a variable- voltage and frequency to power a 3-phase AC motor. The thre phase hard switched inverter topology seems to be a glorious find as it being used in almost all the EVs in current day. It's a very simple, efficient and proven topology that promises to be the trend for the upcoming years as well.
Back in the day when General Motors released their first prototype EV, IMPACT, it had two 3-phase inverters, each powering a front wheel drive induction motor. The semiconductor device used was a MOSFET, 24 MOSFETS were connected in parallel, making it 48 MOSFETs per phase leg and 144 in total. As the advancement in the semiconductor devices picked up, the 48 MOSFETS per phase leg were replaced by an IGBT. Currently IGBTs are used on almost all the commercially available EVs.

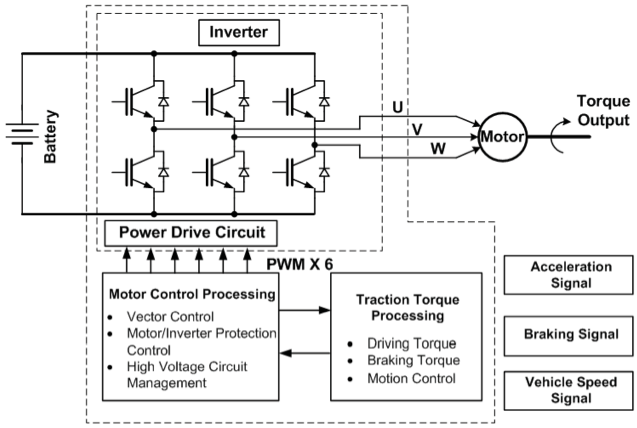

Figure 2.13: Power Electronics Topology in EVs [Raj13]

Differences between MOSFET and IGBT

Table 2.3: Difference between MOSFET & IGBT

Switching Device	**Breakdown Voltage**	**Switching Frequency/Duty Cycle**	**Output Power**	**Remarks**
MOSFET	<250V	>200kHz	<500W	High switching losses at high temperatures
IGBT	>1000V	<20kHz	>5kW	Thermally stable, but higher switching losses at higher frequencies

Future Trends in Semiconductors

The IGBTs wil still continue to be the future until there is commercial availability of silicon carbide and gallium nitride based devices [Raj13]. Although these are available in the curret day, the prices that they cost don't make them viable for the automotive industry. Infact there has been significant progress that's being made in these fields. The major advantages of SiC based inverters when compared to the traditional IGBTs are Sic devices have inherent radiation resistance, high-temperature operating capacity, high voltage and power handling capacity, high power efficiency and flexibility to be used as substrate. These could replace the current Silicon based inverters. GaN devices on the other hand have a better performance than all these discussed due to the fact that they have better material properties such as higher electron mobility and better breakdown field and electron velocity [Raj13]. These devices also have low on resistance and fast switching which reduces the switching losses to a bigger extent and make it viable for better controllability. However until these devices are tested and proved for automotive industry, a conclusion cannot be reached.

2.2 Technology Analysis

In order to weight the advantages and disadvantages in the fields of E-Motor Technology and Transmission, a technology comparison analysis has been performed on the available technology and is graphically shown in a spider chart. The parametrisation used for comparative scaling is described briefly in the Appendix B.2.

2.2.1 E-Motor Technology

The E-motors available in the current day have been studied based on some of the key parameters such as Cost to Power, Power to Weight, Efficiency, Controllability & Architecture and Reliability. The motors analysed were Surface Mounted Permanent Magnet Synchronous Reluctance Motor (SPMSM) ,Reluctance Motor (RM), Permanent Magnet Assisted Synchronous Reluctance Motor (PMSynRM), Induction and Interior Permanent Magnet Synchronous Motor (IPMSM). It could be seen from Figure 2.14 that Cost to Power wise the Reluctance

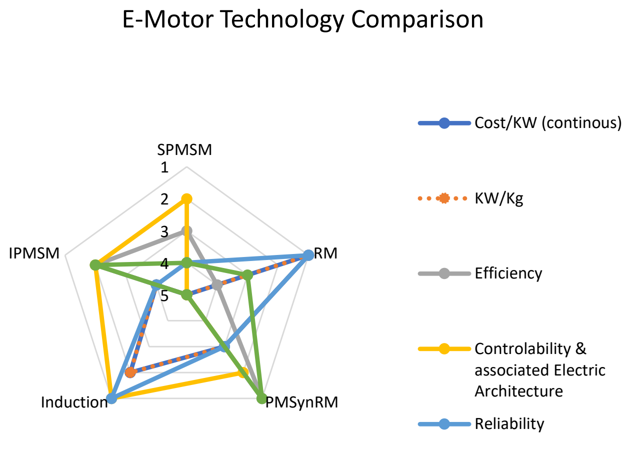

Figure 2.14: E-Motor Technology Comparison

Machine ranks the best followed by Induction Motor and PMSynRM. This could be attributed to the fact that Similarly for the power to weight the reluctance motor tops the chart followed by Induction and PMSynRm. However Eficiency wise PMSynRm tops the list followed by the PMSMs. Induction Machine was found to be easily controllable followed by PMSMs and RM.

Rating the parameters by their importance an overall consensus is achieved as shown in figure 2.15 At an overall level the Reluctance Motor ranks first followed by Induction and PMSynRM. This is based on the parameters that are graded on their importance.

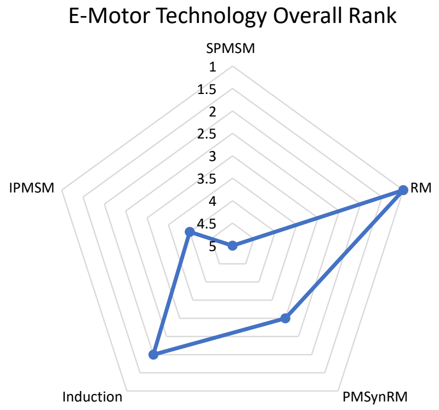

Figure 2.15: E-Motor Technology Overall Comparison

2.2.2 Transmission Technology

The transmission technology in the current day has been studied and has been analysed based on some key parameters such as Cost, Efficiency, Versatality, Weight, Acceleration times, Top Speed and Torque carrying capabilities. The transmissions analysed were CVT, Planetary, Fixed Ratio-Single Ratio Fixed Ratio-Multiple Ratio. It could be seen from figure 2.16 that Fixed Ratio - Single Ratio tops the table of cost efficient models

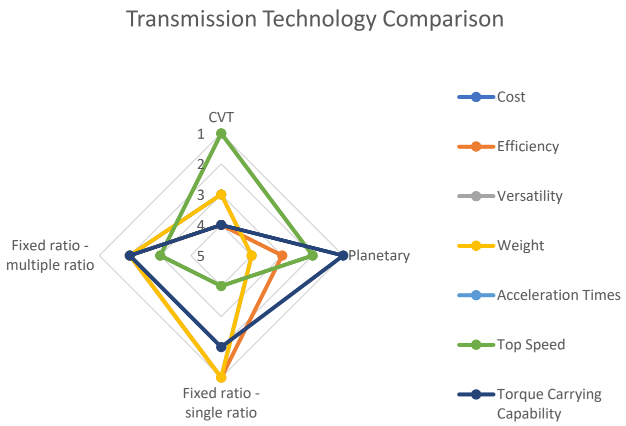

Figure 2.16: Transmission Technology Comparison

followed by Multiple Ratio and CVT. This trend is further noticed in regards to efficiency, the only difference being Planetary ranks better than CVT. CVT, as the name suggests, proves to be a versatile technology followed by Planetary and Single Ratio. Ranking for Weight and Acceleration follow the trends of Cost and Efficiency respectively. While CVT tops the list for top speed followed by Planetary and Fixed Ratio - Multiple Ratio, Planetary does it for Torque carrying Capability followed by Fixed Ratio and CVT.

At an overall level, Fixed Ratios top the list followed by Planetary and CVT based on their significance scores.

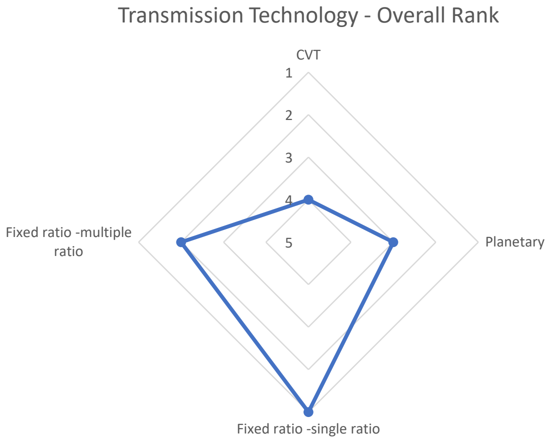

Figure 2.17: Technology Technology Overall Comparison

2.3 Priori for DoE

This section has excerpts from the Statistical e-Handbook. [12]

2.3.1 Intro to DoE

Design of Experiments or DoE is a powerful approach to find the optimal number of experiments that would depict the effect on a desired output response. This is usually preferred when there are higher number of inputs and an effect of these inputs on the desired output response is expected. By manipulating multiple inputs at the once, DOE can identify important interactions that may be missed when experimenting with one factor at a time. This would include the second order or the third order interactions that wouldn't be considered while experimenting with a single input change. Thus a full factorial design is possible with DoE which would depict the effects of the inputs on the output. It could also be noted that different types of designs like fractional factorial design or D-Optimal Design coud also be possible.

Procedure of DoE

In this section the procedure for DoE is explained in brief. It is important to understand the inputs and outputs for a full fledged analysis. The appropriate measure of output should be estimated. It could be noted that measurement should be repeatable and stable. A design matrix can then be created based on the number of factors being selected. The design matrix would show the possible combination of high and low levels for each of the input. The high and low are usually generic coded values as +1 and -1 respectively. Ideally for two level factor investigation there could be 4 experiments created. This could be calculated by 2^n where n is the number of factors. It could look as shown in table 2.4. Then the realisable high and low values can be picked,

Table 2.4: Two level Factor Design - DoE

	Input 1 Level	Input 2 Level
Experiment1	-1	-1
Experiment2	-1	+1
Experiment3	+1	-1
Experiment4	+1	+1

based on the picked values and the number of experiments calculated one can perform the experiments and recording the results for the experiments.The effect of a factor can then be calculated by averaging the data. In a similar fashion the effect of interactions can also be estimated and the corresponding effects of the factors can be found out. This process can be done with a number of statistical tools, and during the course of the project, the tool JMP is used for DoE analysis as well as optimization algorithm. [17a]

2.3.2 Adopted Experimental Design Setup

In this thesis, a D-Optimal design is performed and the classical designs like the factorial and fraction factorial design are not considered due to the fact that the latter design matrices are orthogonal and effect estimates are not correlated. In a D-Optimal design orthogonal design matrices are possible and the effect estimates can be correlated. However the interaction designs can still be performed with this design. The two major reasons for using a D-Optimal design are,

- Classical designs like factorial or fractional factorial need a lot of runs for the amount of resources or time allowed for the experiments
- The design is constrained

Thus when the design has to be constrained, which is the case in this thesis, a D-Optimal Design is favoured.

2.3.3 Model Fitting & Optimisation

Model Fitting

One of the major points in model building is the model validation. One could easily identify if the model fits right with the value of variance. A higher R^2 value ususally signifies a better fit. However this isn't the only way to validate the model. A graphical residual analysis gives a better picture of how well the model fits. Alongside the R^2 statistic a graphical analysis would readily illustrate a broad range of complex aspects of the relationship between the model and the data. The residuals are the differences between the observed value of the combination of inputs and the corresponding prediction of the response computed by a regression analysis.

Optimisation

Before an optimisation process is set to be in place an optimal region needs to be attained. An optimal region is usually achieved with a number of successful experiments performed and a number of empirical models are obtained. Ideally the core intent of performing these experiments is to zero in on the best optimal system response(s). So process point of view, optimisation is to find the operating conditions, the factors, that would yield the maximised or minimised system response as desired. These optimisation techniques are applied on to the previously fit model values. This could be achieved via the JMP tool where the required constraints are set and a best desirability for each of the constraints is achieved. There exists a graphical way of observing the desirability, which is referred as a Desirability Profiler as shown in figure 2.18. The Desirability Profiler for the problem in question in the thesis is discussed at later stages.

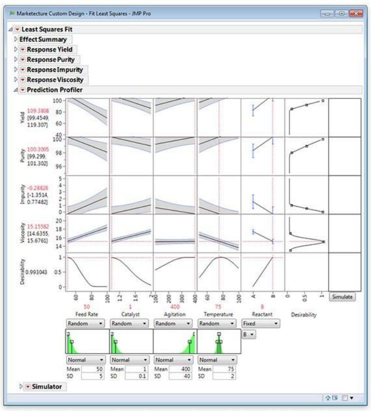

Figure 2.18: Desirability Profiler in JMP

3 Selection of Use Cases

This chapter describes the procedure and rational for the selection of use cases upon which the performance of the drive-trains is compared. A total of three use cases are identified keeping in mind the scope of the thesis,these are described below.

3.1 Cruise Control

The intent of the cruise control use case is to develop a vehicle level controller which would enable the vehicle to track the requested reference velocities. It should be noted here that the same controller is to be used across all drive-trains so as to ensure that one identifies differences in performance only from drive-trains parameters and not differences in performance stemming from the controller. Thus the manoeuvre is a self developed pulse input of velocity. There are two main tasks involved with this use case:

- Development of a PD velocity controller. Details of the developed controller are shown in Section 4.1.6
- Evaluate the performance of the controller on the reference velocity profile shown in Figure 3.1. The specifications of this signals are shown in Table 3.1

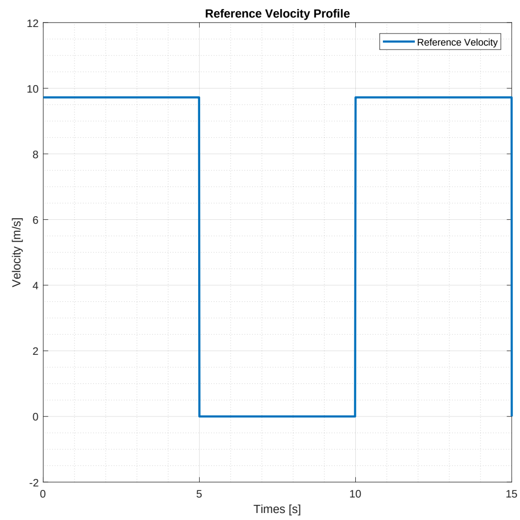

Figure 3.1: Reference velocity profile for cruise control use case

Table 3.1: Specifications of cruise control velocity profile

Parameter	Value
Amplitude	9.72 m/s
Period	10 s
Duty Cycle	50%

3.2 Drive Cycles

This use case is an extension of the cruise control use case, that is to say that the same PD controller developed for the cruise control use cased would be used across all drive-trains and drive cycles so as to obtain a precise comparison of drive-train performance. As seen in Section 2.1.2 many drive cycles were identified for use in this thesis. It was thus necessary to evaluate the drive cycles on their maximum acceleration demand and maximum road load power requirement as it is the intent of this thesis to study the developed drive-trains on the most demanding scenarios in each market.The results of the evaluation of the drive cycles is depicted in Table 3.2.

[1]Tested on standard vehicle

Table 3.2: Comparison of Drive Cycles

Market	Drive Cycle	Maximum Acceleration Requirement (m/sˆ2)	Maximum Power Requirement (kW)[1]
USA	US06	3.241	59.8
	FTP 75	1.475	27.6
	NYCC	2.682	23.3
China	World Harmonised Vehicle Cycle	1.672	23.3
	WLTP Class 3	1.583	38.6
Europe	NEDC	1.389	33.9
	WLTP Class 3	1.583	38.6

It can be seen from Table 3.2 that within the US market the US06 drive cycle is the most demanding cycle both in terms of acceleration and power requirement,where as the NYCC cycle ranks in a close second in terms of acceleration requirement but the FTP75 cycle out ranks the NYCC cycle in terms of power requirement.It was thus concluded that the US06 drive-cycle is the most demanding cycle representing the US market. It was observed that in the Chinese market the WHVC and the WLTP Class 3 cycle have similar acceleration requirement, but in terms of maximum power demand the WLTP Class 3 cycle ranks higher.Thus the WLTP Class 3 drive cycle can be identified as the cycle with a higher demand. Finally, in the European market the current standard NEDC and the forthcoming standard WLTP Class 3 cycle were studied. It was observed that NEDC was inferior to the WLTP Class 3 cycle both in terms of acceleration and power requirement, none the less, the NEDC cycle holds importance as it is the standard cycle upon which all vehicles are juxtaposed within the European market.
The details of the chosen three drive cycles are shown in Sections 3.2.2, 3.2.3 & 3.2.1 respectively.

3.2.1 NEDC

A summary of the NEDC drive cycle is presented in Table 3.3 and the velocity profile is depicted in Figure 3.2. This cycle was selected keeping in mind that as of today NEDC is currently the norm for the comparison of vehicles within the European market.

Table 3.3: Summary of NEDC Drive Cycle [Bar+09]

Distance(m)	Duration(s)	Average Speed(km/h)
11017	1180	33.6

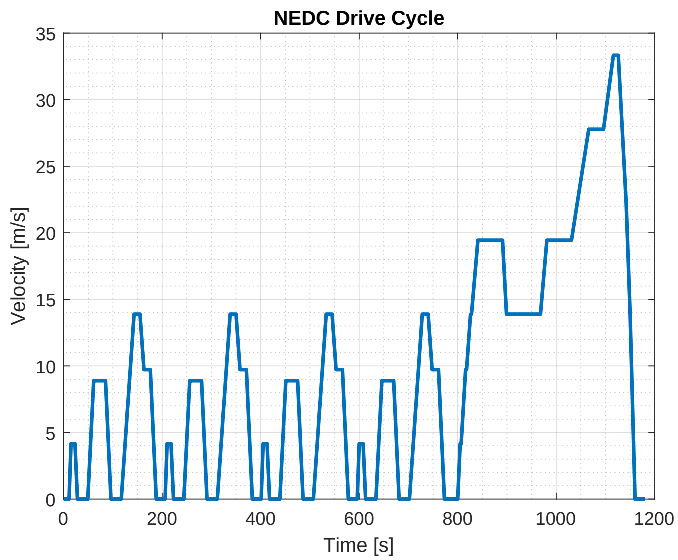

Figure 3.2: NEDC Drive Cycle [Bar+09]

3.2.2 US06

A summary of the US06 drive cycle is presented in Table 3.4 and the velocity profile is depicted in Figure 3.3. This cycle is chosen as it is identified as the most demanding, within the US market, both in terms of acceleration requirement as well as power requirement.

Table 3.4: Summary of US06 Drive Cycle [Bar+09]

Distance(m)	Duration(s)	Average Speed(km/h)
12894	596	77.9

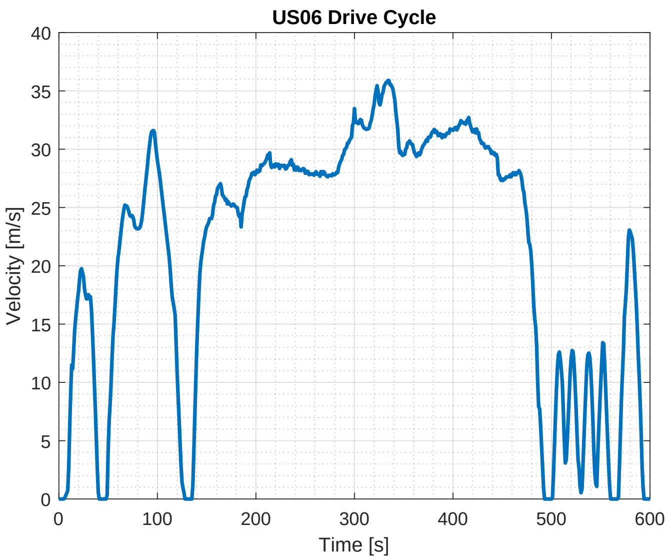

Figure 3.3: US06 Drive Cycle [Bar+09]

3.2.3 WLTP Class 3

A summary of the WLTP Class 3 drive cycle is presented in Table 3.5 and the velocity profile is depicted in Figure 3.4.The WLTP Class 3 cycle is selected as it represented the most demanding cycle not only within the Chinese market but also within the European market. This cycle holds a greater significance as it is slated to become the norm for all vehicle testing not only within Europe (as of September 2019 all new passenger cars placed on the European Union market are to be tested in accordance with the WLTP) and China, but also the entire world.

Table 3.5: Summary of WLTP Class 3 Drive Cycle [Bar+09]

Distance(m)	Duration(s)	Average Speed(km/h)
23266	1800	46.5

It can be seen that a wide array of cycles have been selected covering the markets of China, US and Europe. The selected drive cycles place a great demand on the drive-trains both in terms of power and quick acceleration, hence the drive-cycles would the appropriate use case to study the performance of the different drive-trains.

3.3 Traction Control Use Case

The traction control use case is identified to evaluate the performance of the developed drive-trains in terms of their responsiveness and adaptability when the vehicle experiences a differential friction surface. For this purpose a scenario 10s long was created with surface friction transients as shown in Figure 3.5. The chosen

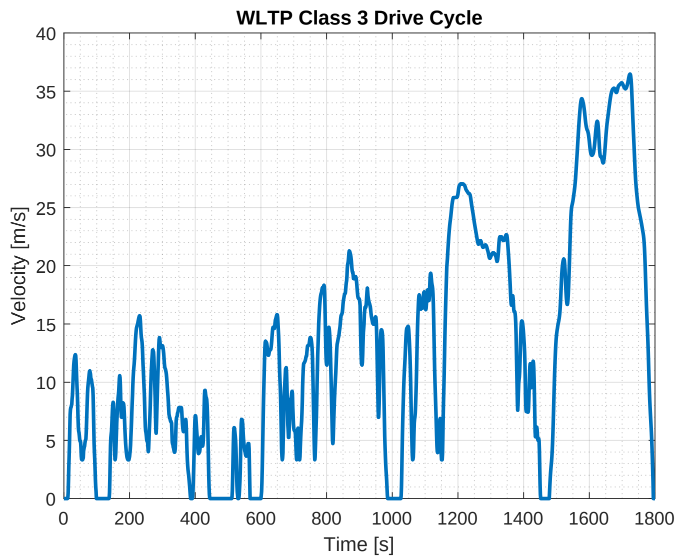

Figure 3.4: WLTP Class 3 Drive Cycle [Bar+09]

surface parameters are shown in Table 3.6. The reference velocity is maintained at 50 kmph across the entire time span.
This use case consisted of two main tasks:

- Development of a wheel slip controller
- Evaluation of the drive-trains on the identified scenario

It should be noted that for the purposes of evaluation of the performance of the drive-trains and the drive-trains alone the same Fuzzy Logic controller will be used on all drive-trains. The details of this controller are shown in 4.1.6. A road friction estimator / model predictive control of road friction was not used to estimate the optimal slip ratio but instead a slip ratio of 15% was considered as optimal across all surfaces.

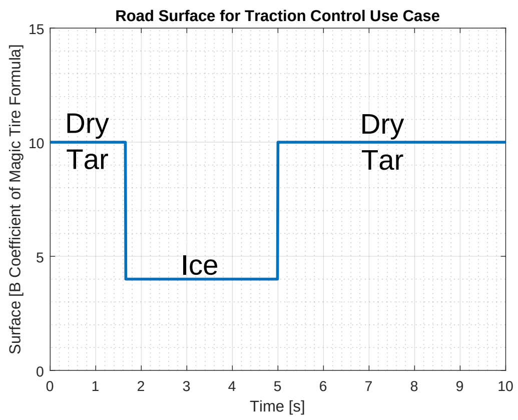

Figure 3.5: Road condition for acceleration scenario

Table 3.6: Surface Parameters

Surface	Magic Tire Formula Coefficients				Co-efficient of Friction
	B	C	D	E	μ
Dry Tar	10	1.9	1	0.97	1
Ice [below 0°C]	4	2	0.1	1	0.1

4 Vehicle and Drive-train Parameterisation

4.1 Vehicle Model

The vehicle model is developed on a MatLab/SIMULINK environment using the SIMSCAPE & powertrain blockset libraries as the SIMSCAPE library enables the creation and simulation of physical systems,an added advantage of SIMSCAPE is the possibility to integrate multiple physical systems domains such as mechanical and electrical within the same model environment.

The following sections will speak of each block within the vehicle model and the equations used within each of them. The model schematics and parameter values used in each block have been shown in the Appendix C.1.4.The blocks common to both the State of the Art as well as the future drive-train will be described in Sections 4.1.1 - 4.1.6. The blocks unique to each of the models will be described in Sections 4.2 & 4.3.

4.1.1 Vehicle Body

The vehicle body is modelled using a single track model i.e. one axle is represented by a single wheel. As within the scope of this thesis only longitudinal straight line motions are of interest, a steering system is not modelled. As only longitudinal dynamics are modelled only pitch dynamics are considered in this model. Also effects of wind and gradient are not considered.The system of equations relate the mass of the vehicle (m), acceleration due to gravity (g), vehicle longitudinal velocity (V_x), longitudinal force on tire at contact point (F_x), force due to aerodynamic drag (F_d),coefficient of drag (C_d), vehicle frontal area (A), road inclination angle (β),density of air (ρ), vertical load on front axle (F_{zf}),vertical load on rear axle (F_{zr}), height of centre of gravity above ground (h),distance of front axle from centre of gravity (a) and distance of rear axle from centre of gravity (b).

The equations used in this block are as follows:

$$m\dot{V_x} = F_x - F_d - mg \cdot \sin\beta \tag{4.1}$$

$$F_d = 0.5 \cdot C_d \cdot \rho \cdot A \cdot V_x^2 \tag{4.2}$$

$$F_{zf} = (-h \cdot F_x + b \cdot mg \cdot \cos\beta)/(2(a+b)) \tag{4.3}$$

$$F_{zr} = (h \cdot F_X + a \cdot mg \cdot \cos\beta)/(2(a+b)) \tag{4.4}$$

To use this model accurately one has to enter the vehicle properties such as mass, frontal area, coefficient of drag etc.

4.1.2 Wheels & Tires

The wheels and tires are modelled using the magic tire formula as this is the closest approximation of real world systems. It is using this formula that the slip ratio at the wheel is calculated, this calculation is of at most importance in the traction control use case. The maximum longitudinal force that one can apply on the tire is dependant on the vertical load acting on it. This vertical load is fed to the tire block form the vehicle body block described above. The system of equations in this block provide a relation between the slip ratio (κ),tire rolling radius (Rr),wheel angular speed (ω),vertical load on tire (F_z),magic tire formula coefficients (B, C, D, E).

The wheels and tires were modelled using the following equations:

$$\kappa = (Rr \cdot \omega - V_x)/|V_x| \tag{4.5}$$

$$F_x = F_z \cdot D\sin(C\arctan(B\kappa - E[(B\kappa) - \arctan(B\kappa)])) \tag{4.6}$$

To utilise this block effectively one must enter the nominal parameters of the chosen tire as well as the threshold velocity below which the solver equates the slip ratio to zero.

4.1.3 Transmission

To model the transmission a simple gearbox is utilised. The gearbox is modelled with two gear wheels a base gear wheel and the follower gear wheel. The base gear wheel is the one which is attached to the motor and the follower gear wheel is the one connected to the differential. Due to limitations within the gear box model The inertia of the gear wheels are not present within the gear box but are connected as an external inertia. It should be noted here that the inertia of the base and follower gear wheels have been calculated based only on their radii and are independent of their masses.The system of equations in this block relate the gear ratio (N),radius of follower gear (r_f),radius of base gear (r_b),torque acting on base gear (τ_b),torque acting on follower gear (τ_f),losses in torque transfer calculated based on the efficiency parameter (τ_{loss}),follower gear angular velocity (ω_f),base gear angular velocity (ω_b),follower gear inertia (J_f) ,base gear inertia (J_b).

The equations used in the modelling of the gearbox are as follows:

$$N = r_f/r_b \tag{4.7}$$

$$N\tau_b + \tau_f - \tau_{loss} = 0 \tag{4.8}$$

$$\tau_b = J_b \cdot \dot{\omega_b} \tag{4.9}$$

$$\tau_f = J_f \cdot \dot{\omega_f} \tag{4.10}$$

To utilise this model effectively one must provide parameters such as efficiency, damping and gear ratio.

4.1.4 Open Differential

The open differential is modelled using an arrangement of a single simple gearbox along with two Sun-Planet bevel gears. The output shafts of the two Sun-planet bevel gears are connected to each of the wheels. The input shaft to each of the bevel gears comes form the simple gearbox. This gear box is fed torque from the transmission system described in Section 4.1.3.To utilise this block effectively one must provide the final drive ratio, inertia of the input shaft/gear arrangement and inertia of the two output gear/shaft arrangement. The equations used in this block are similar to those used in Section 4.1.3

4.1.5 Battery

A simple battery model is used as a part of this thesis as modelling the battery with discharge dynamics, finite charge and non-ideal resistances in beyond the scope of this thesis. The battery is modelled as a constant voltage source of infinite energy, this voltage source is capable of maintaining the required potential irrespective of the current drawn from the battery.

4.1.6 Vehicle Controllers

In this section the developed cruise controller as well as the traction controller will be discussed.

Velocity Controller(Cruise Control)

The velocity controller developed for the cruise control and drive cycle use case is a PD controller. A PD controller is deemed as the optimal controller configuration as the velocity and acceleration of the vehicle are to be controlled and not its position. It can also be understood that the addition of the differential gain and removal of the integral gain tends to decrease the overshoot and the settling time whilst marginally improving the stability of the system. The only draw back is that the derivative system is highly sensitive to noise,this is not a cause of concern within the scope of this thesis as no noise models have been introduced,i.e. a completely deterministic system is studied.

The controller accepts an input of error (formulated in Equation 4.11) and outputs a control signal. The control signal has values between -1 and 1, wherein 1 denotes maximum acceleration (complete depression of accelerator pedal) and -1 denotes maximum braking (complete depression of brake pedal), any positive values(between 0 and 1) represents partial depression of the accelerator pedal and any negative value (between -1 and 0) represents partial depression of the brake pedal.This logic is represented in Equation 4.12 where $V_{reference}$ is the reference/target velocity for the vehicle.

$$error = V_{reference} - V_x \tag{4.11}$$

$$\text{ControllerOutput} = \begin{cases} 1 : MaximumAcceleration \\ (0,1) : PartialAcceleration \\ 0 : NoOperation \\ (-1,0) : PartialDeceleration \\ -1 : MaximumDeceleration \end{cases} \tag{4.12}$$

Furthermore, the tuning of the controller was carried out by studying the linearised plant system at different operating points.The transfer function of the plant at various operating points is shown in Table C.5 Having identified the plant dynamics one can derive the transfer function of the PD controller as in Equation 4.13. The tuned proportional (P) and derivative (D) gains of the controller are presented in the appendix.

$$TransferFunction = P + Ds/(s+1) \tag{4.13}$$

Traction Controller

In this section the traction controller designed to limit wheel slip will be described. To select the type of controller a review of existing literature is carried out from the review of existing literature it is observed that the Fuzzy Logic type of control had the greatest potential in Traction control applications as stated in [Zet07]. [Zet07] also states that "The fuzzy controller, however, performed very well in all the tests. Besides from being nonlinear, it does not need a desired value and manages to localise the peak of the -slip curve by itself. Furthermore, the fuzzy logic, upon which the controller is based, is very easy to understand.", hence it was decided to implement a fuzzy logic controller.

The fuzzy logic controller accepts two inputs:

1. Vehicle Velocity Error
2. Wheel Slip Ratio Error

The vehicle velocity error is calculated by determining the deviation of the vehicle velocity from the reference velocity(represented in Equation 4.11). The slip error is calculated by determining the deviation of the tire's slip ratio from the optimal slip ratio which is assumed to be 15% for all surfaces. It is with these error inputs that the controller determines if an accelerating or braking torque has to be applied on the wheel. In the case that acceleration torque has to be applied the controller outputs a signal between 0 and 1 with 1 denoting maximum acceleration and in the case of braking the controller outputs a signal between -1 and 0 with -1 denoting maximum regenerative braking. The operation of the controller in the acceleration scenario is detailed below, the operation of the controller in the braking scenario is similar to that of the acceleration scenario, the only difference being the controller output membership function. The output membership function for the braking scenario is shown in Figure 4.3.

Once the inputs have been fed into the controller, it determines the level of error as 'high' or 'low' based on the membership functions defined. The membership functions for velocity error and slip error are shown in Figures 4.1 ans 4.2 respectively. Having determined the levels of the inputs, the controller then calculates the degree of membership of the control output using the output membership functions shown in Figure 4.4, once the degree of membership has been determined the centroidal method of defuzzification would be appropriately applied to determine the control output.

4.1.7 Power Electronics

The Power Electronics for State of the Art drive-train as well as Future drive-train are maintained constant. The power electronics in this context refers to the three-phase inverter. In Simulink, a universal bridge

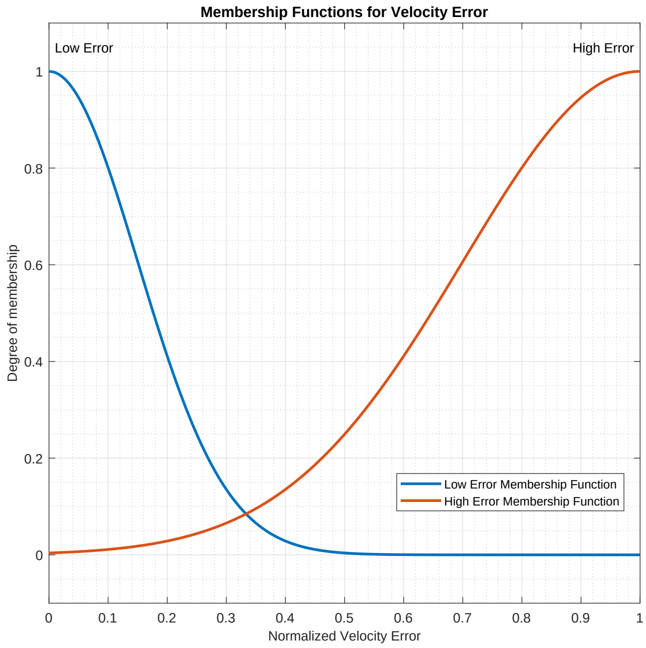

Figure 4.1: Velocity membership functions

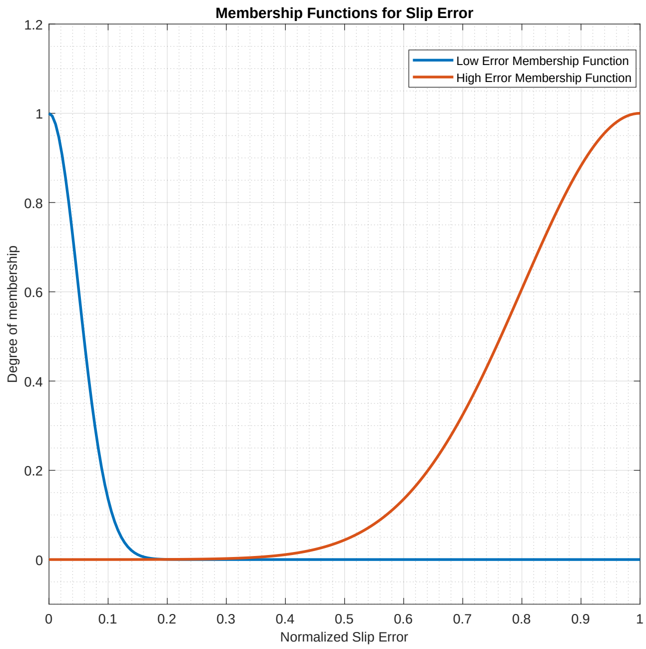

Figure 4.2: Slip membership functions

block has been implemented, which is a three-phase power converter device. It has a six power switches connected in a bridge pattern. The switches selected are the IGBT-Diodes, which reflect the current market trends [Raj13]. The block takes in the DC supply and the Gate Switching pulses as inputs and the resulting three-phase supply is connected to a current measurement unit. Each phase supply is a resultant from a single leg of the bridge consisting of two power switching devices. The architecture is as shown in figure 4.5

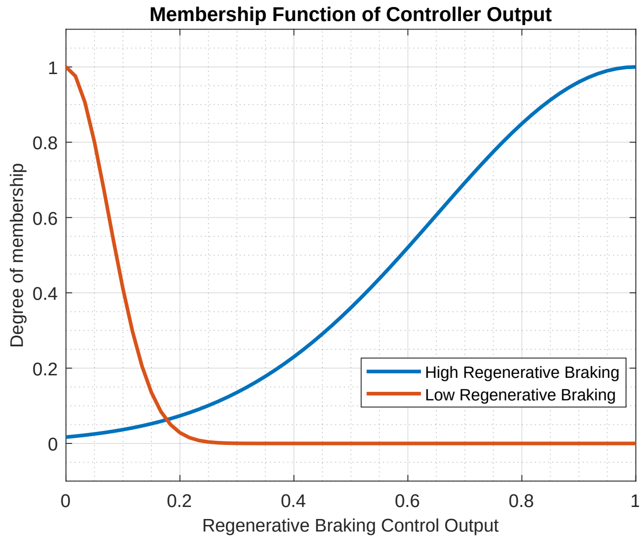

Figure 4.3: Controller output membership function in Deceleration Scenario

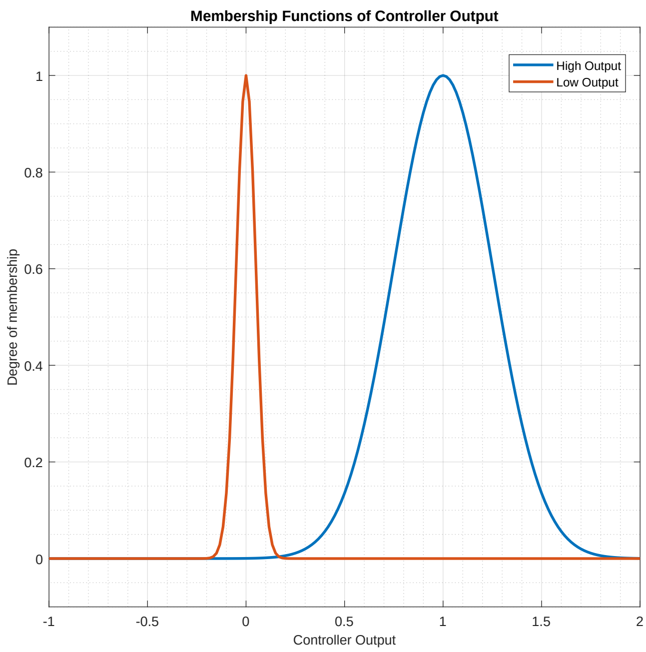

Figure 4.4: Controller output membership function in Acceleration Scenario

4.2 State of the Art Drive-train

In this section Parameters of the components pertaining to the State of the Art drive-train have been discussed briefly, unlike the section 4.1 where the parameters of components common to both drive-trains have been discussed. As the State of the Art drive-train reflects the current day EVs, a conclusion is arrived on the type of components that exist on the drive-train based on the EV Database as shown in the table A. The E-Motor that is currently preferred by most of the manufacturers is the PMSM motor, working of which has been discussed in section 2.1.4. The maximum power of the motor is rated at 100kW and a speed of 12500RPM.

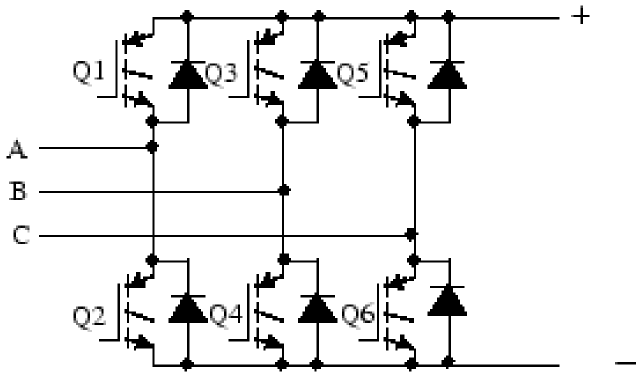

Figure 4.5: IGBT-Diode Bridge Architecture

4.2.1 Motor

The dynamics of a three-phase permanent magnet synchronous machine with sinusoidal back electromotive force have been modelled in Simulink. This model has been utilised from the Simscape Power Systems library. This block has the option of operating in either a motor mode or a generator mode depending on the type of torque being received. The ideal convention is a motor mode for a positive torque, a generator mode for a negative torque. The mechanical and electrical sub parts are mentioned by the state space equations. The back emf model selected on this type of motor could be a sinusoidal or a trapezoidal. The flux established by the permanent magnets in a sinusoidal model is assumed to be sinusoidal by the model, whereas a trapezoidal flux is assumed for a Trapezoidal model. The state space equations for Electrical and Mechanical Systems are described as below. The state space relates the electromagnetic torque (T_e) to amplitude of the flux induced by the permanent magnets of the rotor in the stator phases (λ) and other motor electrical paramters defined in previous sections.
Electrical System:

$$\frac{\mathrm{d}}{\mathrm{d}t} i_d = \frac{1}{L_d} v_d - \frac{R}{L_d} i_d + \frac{L_q}{L_d} p\omega_m i_q \tag{4.14}$$

$$\frac{\mathrm{d}}{\mathrm{d}t} i_q = \frac{1}{L_q} v_q - \frac{R}{L_q} i_q + \frac{L_d}{L_q} p\omega_m i_d - \frac{\lambda p\omega_m}{L_q} \tag{4.15}$$

$$T_e = 1.5p[\lambda i_q + (L_d - L_q) i_d i_q] \tag{4.16}$$

The L_d and L_q inductances signify the relation between the phase inductance and the rotor position due to the saliency of the rotor. The inductance equation for phase a and phase b when phase c is left open (L_{ab}) can be given in terms of rotor angle (θ_e) by,

$$L_{ab} = L_d + L_q + (L_q - L_d)\cos\left(2\theta_e + \frac{\Pi}{3}\right) \tag{4.17}$$

The phase to phase variation against the rotor angle is shown as in figure 4.6

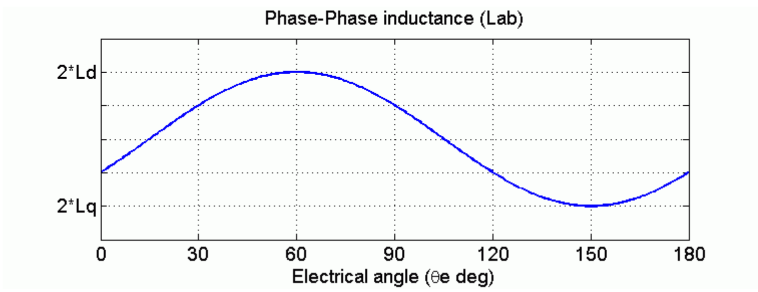

Figure 4.6: Phase vs Rotor Angle

Mechanical System:
The set of equations for Mechanical system provide a relation between rotor angular position (θ), shaft static friction torque (T_f), shaft mechanical torque (T_m), combined viscous friction of rotor and load (F) and combined rotor and load inertia (J) as seen below:

$$\frac{\mathrm{d}}{\mathrm{d}t}\omega_m = \frac{1}{J}\left(T_e - T_f - F\omega_m - T_m\right) \tag{4.18}$$

$$\frac{\mathrm{d}\theta}{\mathrm{d}t} = \omega_m \tag{4.19}$$

All the parameters are matched to a 100kW 288Vdc machine which is the most preferred in the current day according to the EV Database A.

4.2.2 Motor Controller

A Vector Controller is implemented for the PMSM motor selected above.A scalar strategy of controlling has not been considered as it does not cater to dynamic response of the motor. A vector control refers to the magnitude and phase of the controlled variables. The control quantities like Current, Voltage and Flux are represented by Matrices and Vectors. Thus the motor dynamics are considered as a set of mathematical equations. The vector control is also similar to the Field Oriented Control in Induction Machines and also provides similar performance for a sinusoidal PMSMs.

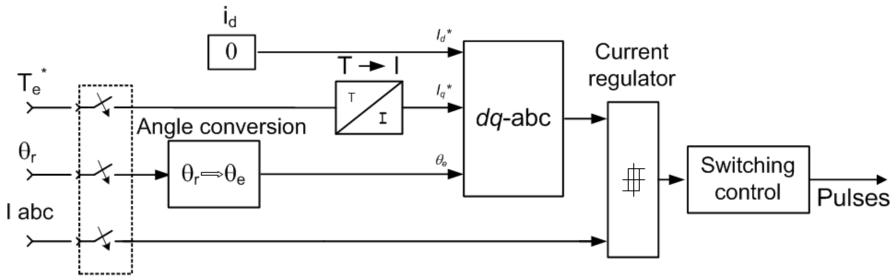

Figure 4.7: Vector Control Block Diagram

In figure 4.7, it could be seen that Vector Control has four major blocks. The figure represents a typical work flow for a three phase system. Typically the dq-abc block performs the conversion of the current components from the motor reference frame to the abc- phase variables.There is a need to convert the electrical rotor angle to a mechanical rotor angle, which is done by the Angle Conversion block. Ideally a hysteresis controller or a bang-bang controller is used in the current regulator block with a variable bandwidth. The inverter-commutation frequency is limited by the switching control, however the maximum value can be varied according to the use.

4.3 Proposed Future Drive-train

Keeping in line with the scope of the thesis and the determined trends it is concluded that the future electric-drive train should have virtually no dependence on permanent magnets, in this regard the Switched Reluctance Motor (SRM) showed the greatest promise. It is an established fact that the SRM does not have a power density as high as that of the IPMSM,but the SRM offers many performance advantages over the PMSM namely:

1. Reduced cost of raw materials, due to the absence of permanent magnets
2. Reduced cost of rotor manufacturing
3. Improved efficiency at higher angular speeds

The last point is of great importance in this study as it was one of the main objectives to develop a high speed to low torque motor(compared to the State of the Art drive-train). Figure 4.8 shows the best efficiency regions of different motors [FFH08], it can be seen that the SRM operates at higher efficiencies when running at higher angular speeds and lower torques, this is due to the fact that at higher angular speeds the IPMSM draws a greater RMS current to induce flux weakening. This phenomenon is depicted in Figure 4.9, here the two motors were run at the same angular speed with varying power requirements at the output, it can be seen that the SRM motor draws a lower RMS current at higher power requirements and hence has better efficiencies in that region for reasons elaborated above.

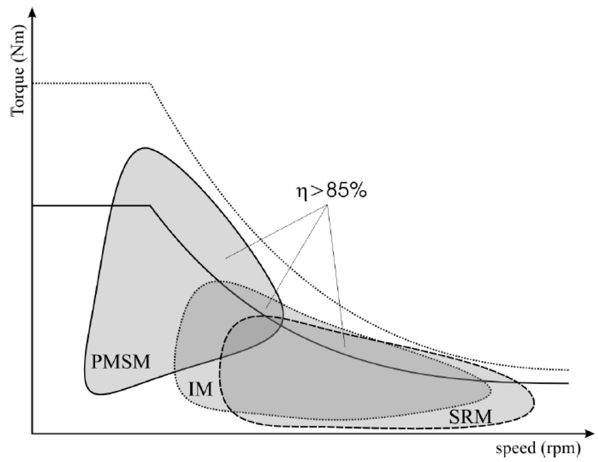

Figure 4.8: Efficiency contour of different motor types [FFH08]

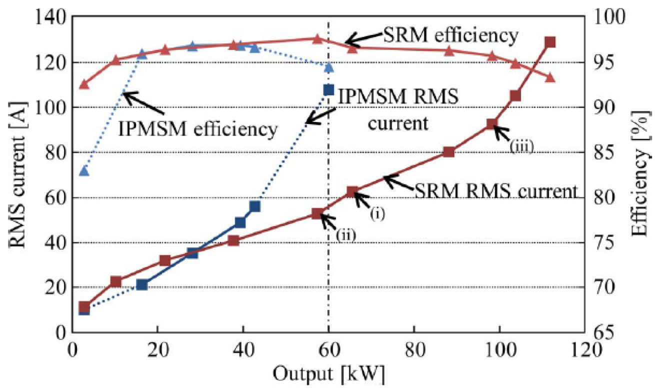

Figure 4.9: Comparison of performance IPMSM and SRM motors at 8100 RPM [KC12]

4.3.1 Motor

This section will elaborate on the dynamics and modelling of the SRM motor. The SRM , as described previously is a synchronous machine with salient rotor and stator poles. When diametrically opposite stator poles are excited , a diametrically opposite rotor pole pair aligns ts self with the excited stator pole, this causes the arrangement to proceed towards minimal reluctance or conversely maximum inductance, this inductance value is termed as aligned inductance (L_a). It follows that when the stator and rotor poles are unaligned they proceed towards the minimum inductance value termed as unaligned inductance (L_u). This variation of inductance over a complete rotor rotation is shown in Figure 4.10, this profile is of great importance when developing the controller.

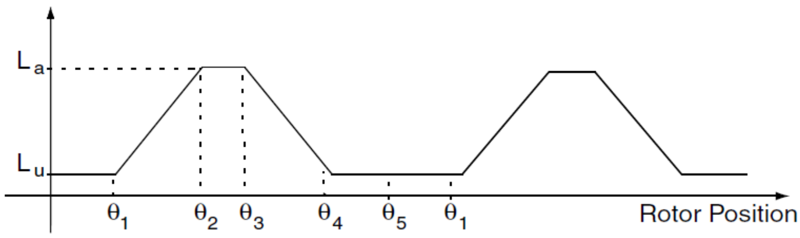

Figure 4.10: Variation of inductance profile [Kri01]

Having studied the operational scheme of the SRM , the dynamics of the system can be easily modelled. The systems of equations representing the SRM which relate torque generated by one phase (T_{ph}), magnetic flux linkage (Ψ_{ph}),phase current (i_{ph}),phase voltage (V_{ph}),phase resistance (R_{ph}) are:

$$T_{ph} = \int \frac{\delta \Psi_{ph}(i_{ph}, \theta)}{\delta \theta} \cdot di_{ph} \tag{4.20}$$

$$V_{ph} = R_{ph} \cdot i_{ph} + \frac{\delta \Psi_{ph}(i_{ph}, \theta_{ph})}{\delta i_{ph}} \cdot \frac{di_{ph}}{dt} + \frac{\delta \Psi_{ph}(i_{ph}, \theta)}{\delta \theta} \cdot \omega_m \tag{4.21}$$

4.3.2 Motor Controller

The motor controller adopted for the SRM was the speed regulated current controlled hysteresis controller [Vis05]. A schematic of this controller is presented in Figure 4.11. Two important variables are required for the proper operation of the controller ,θ_{on} and θ_{off}, i.e. the rotor angles at which the current in a phase has to be turned on and turned of respectively. These angles are dependant on the inductance profile shown in Figure 4.10. The on and off angles are represented by θ_1 and θ_3 respectively in Figure 4.10.

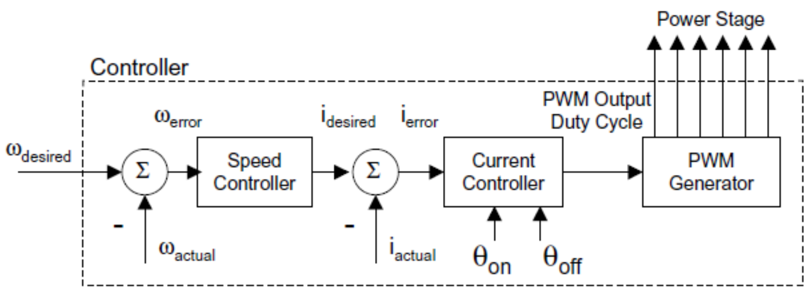

Figure 4.11: Controller schematic for SRM

4.4 Simulation Challenges & Solutions

In the previous sections the modelling of the various blocks were elucidated, it can hence been observed that the mechanical, electrical and vehicle systems were all simulated as though they were all a single system, although this is the true representation of the complete physical system, it posed challenges for the simulation. The challenges arose as a consequence of each of the systems having different operational frequencies, these different frequencies of operation caused the solver to proceed with a time step corresponding to the system/event with the greatest frequency i.e all systems were being solved with a solver step size of ˜˜2e-6 seconds causing a 10 second simulation to run for 40 minutes. The frequencies of operation of the various systems and test events is shown in Table 4.1.

Table 4.1: Frequency of operation of different vehicle events

Event	Frequency of Operation (Hz)
Power electronics switching	1000 - 10000
Motor operation	20 - 350
Short term vehicle events e.g. emergency acceleration/braking	1 - 0.2
Long term vehicle events e.g. drive cycles	0.002 - 5e-4

The envisioned solution to overcome this was to split the electrical and mechanical systems. This separation of the electrical and mechanical systems would allow each of the systems to run at the appropriate step sizes, thus drastically reducing the time of simulation. The separation of the systems was achieved by simulating the electrical system prior to simulating the mechanical system and importing the the torque-speed characteristics of the electrical motor into the mechanical system as a 'look-up table', the look-up table which uses interpolation-extrapolation techniques would thus represent the electrical motor to a reasonable degree of accuracy.

4.5 Design of Experiments and Parameterisation

Having studied the modelling of the proposed future motor, the parameters on which the performance of the motor is dependant on have been identified with this information a list of experiments were generated to study the effects of variation of the identified parameters on the performance of the drive-train. To obtain accurate results one must also define the search region for each of the identified parameters, the parameters and their respective search regions have been identified in Table 4.2.These search regions were identified by varying the parameters manually to different degrees to gauge their effects, this manual process is not presented here.

Table 4.2: Parameters and their ranges

Parameter	Range
Unaligned Inductance	0.000167 to 0.00067 H
Aligned Inductance	0.0059 to 0.0236 H
Saturated Aligned Inductance	0.0000375 to 0.00015 H
Stator Resistance	0.05 to 1 ohm
Flux Linkage	0.486 to 0.6075 Vs
Battery Voltage	400 to 600 V

The consolidated list of experiments is shown in the appendix.It is also necessary to define the targets on which the effects of the parameters are to be studied. Along with defining the targets one must also define the nature of the target, i.e. if it has to be maximised , minimised etc. The targets and their nature have been detailed in Table 4.3.

Table 4.3: Identified targets and their nature

Target	Nature
Motor Torque (RMS)	Match Target - 225 Nm
Maximum RPM	Match Target - 17500 RPM
Length of Motor	Minimise
Rise Time of Vehicle Velocity[1]	Minimise
Settling Time of Vehicle Velocity	Minimise
Peak of Vehicle Velocity	Minimise

The natures of the targets defined above are realised in the JMP tool as a desire-ability index'. This index ranges from 0 to 1 with 1 being most desirable. For example for the target of 'Length', whose nature is that of minimisation, the disability of 1 corresponds to the least value of 'Length'.
It should be noted here that three motor level parameters are selected namely, motor torque,angular speed and axial length and three vehicle level parameters are selected namely, rise time , settling time and peak value of velocity trace of the vehicle with reference to a step input of velocity.

[1]Tested at vehicle level with velocity step reference input

5 Results

5.1 DoE and Optimisation of Future Drive-train

In the previous section we have seen the parameters and targets selected for the DoE, with these parameters and targets in mind a list of experiments are generated as shown in the appendix. Once the proposed future drive-train is simulated on the set of experiments three major results are obtained namely,

1. ***Parameter effects***
   An important outcome of the DoE is to gauge which parameters are the most influential on the performance of the drive-train, this influence is ascertained based on the Log worth as well as the P-Value (a P-Value closer to zero signifies greater influence) of the parameters. The P-Value of all parameters and their second order interactions is shown in Figure 5.1.

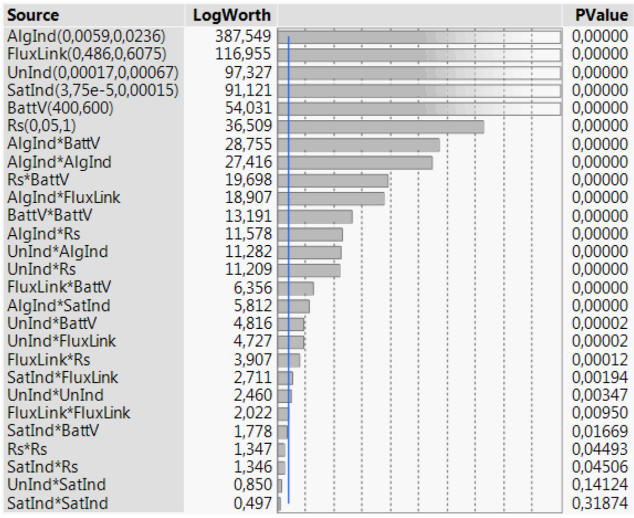

Source	LogWorth	PValue
AlgInd(0,0059,0,0236)	387,549	0,00000
FluxLink(0,486,0,6075)	116,955	0,00000
UnInd(0,00017,0,00067)	97,327	0,00000
SatInd(3,75e-5,0,00015)	91,121	0,00000
BattV(400,600)	54,031	0,00000
Rs(0,05,1)	36,509	0,00000
AlgInd*BattV	28,755	0,00000
AlgInd*AlgInd	27,416	0,00000
Rs*BattV	19,698	0,00000
AlgInd*FluxLink	18,907	0,00000
BattV*BattV	13,191	0,00000
AlgInd*Rs	11,578	0,00000
UnInd*AlgInd	11,282	0,00000
UnInd*Rs	11,209	0,00000
FluxLink*BattV	6,356	0,00000
AlgInd*SatInd	5,812	0,00000
UnInd*BattV	4,816	0,00002
UnInd*FluxLink	4,727	0,00002
FluxLink*Rs	3,907	0,00012
SatInd*FluxLink	2,711	0,00194
UnInd*UnInd	2,460	0,00347
FluxLink*FluxLink	2,022	0,00950
SatInd*BattV	1,778	0,01669
Rs*Rs	1,347	0,04493
SatInd*Rs	1,346	0,04506
UnInd*SatInd	0,850	0,14124
SatInd*SatInd	0,497	0,31874

Figure 5.1: Summary of effects

   It can hence be seen that all the parameters and their second order interactions are highly influential on the six selected targets. It can also be seen that the interactions of saturated aligned inductance-battery voltage,stator resistance-stator resistance,saturated aligned inductance-stator resistance,unaligned inductance-saturated aligned inductance and saturated aligned inductance-saturated aligned inductance hold the least influence over the targets while the first order parameters hold the greatest influence.

2. ***Model fitting of targets and their corresponding prediction formulation***
   The next important result from the DoE is the model for the prediction of each of the selected targets. This model is based on a predictor formula (not shown), before the model/predictor formula can be implemented for the purposes of optimisation one should determine if the predicted model explains the given data satisfactorily. The model is analysed with respect to its summary of fit, most notably its $R^2 - Adj$ value, where an $R^2 - Adj$ value closer to 1 denotes a well fitted model. The summary of fits for the six targets are shown in Tables 5.1 - 5.6

Table 5.1: Summary of fit for Motor Torque

Model Fit Parameter	Value
R^2	0.999973
$R^2 - Adj$	0.999959
Root Mean Square Error	0.121975
Mean of Response	169.0852
Observations (or Sum Weights)	80

Table 5.2: Summary of fit for Motor Angular speed

Model Fit Parameter	Value
R^2	0.996462
$R^2 - Adj$	0.994625
Root Mean Square Error	215.0716
Mean of Response	13639.4
Observations (or Sum Weights)	80

Table 5.3: Summary of fit for Rise time of vehicle velocity

Model Fit Parameter	Value
R^2	0.996451
$R^2 - Adj$	0.994608
Root Mean Square Error	0.028648
Mean of Response	2.652645
Observations (or Sum Weights)	80

Table 5.4: Summary of fit for Settling time of vehicle velocity

Model Fit Parameter	Value
R^2	0.996717
$R^2 - Adj$	0.995012
Root Mean Square Error	0.033287
Mean of Response	3.285015
Observations (or Sum Weights)	80

Table 5.5: Summary of fit for Peak of vehicle velocity

Model Fit Parameter	Value
R^2	0.997967
$R^2 - Adj$	0.996912
Root Mean Square Error	0.000186
Mean of Response	9.764759
Observations (or Sum Weights)	80

Table 5.6: Summary of fit on motor length

Model Fit Parameter	Value
R^2	1
$R^2 - Adj$	1
Root Mean Square Error	1.169e-8
Mean of Response	0.529339
Observations (or Sum Weights)	80

It can be seen for the above tables that the $R^2 - Adj$ value ˜=1, hence the models explain the given data very well. These model can therefore be used for the purposes of optimisation.

3. ***Optimisation***
   Using the models detailed above one can now proceed to maximise the desirability of the targets (elaborated in Section 4.5). The result of the maximisation of the desirability is the optimal values of the parameters of the proposed future drive-train these values are shown in the appendix.

5.2 Comparison of Motors

In this section the proposed optimised future motor will be compared with the State of the Art motor. The characteristics of the State of the Art motor is shown in Figure 5.2 and the characteristics of the Optimal Future are shown in Figure 5.3.

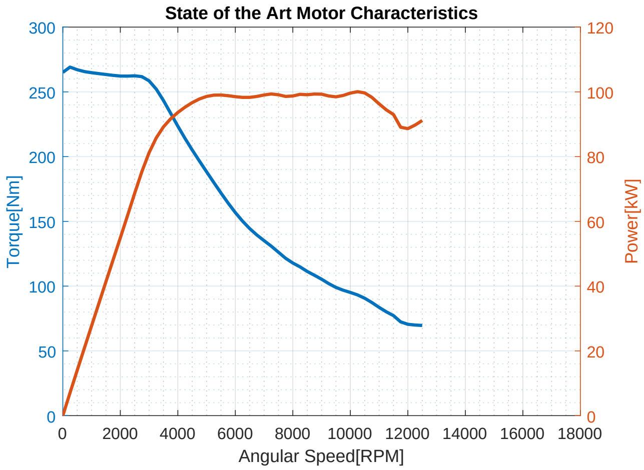

Figure 5.2: State of the Art motor torque and power characteristics

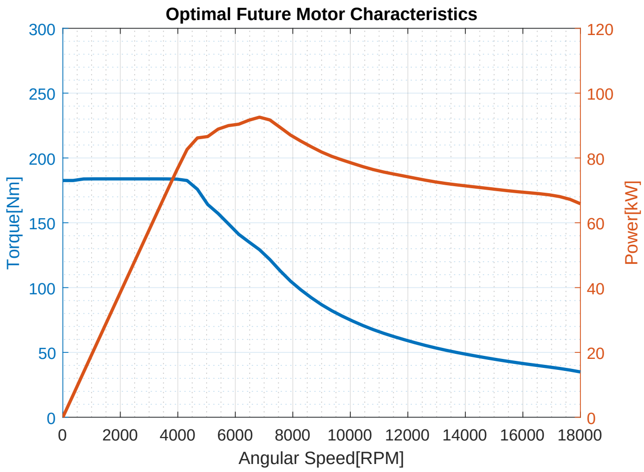

Figure 5.3: Optimal Future motor torque and power characteristics

It can be seen form the above figures that the State of the Art motor provides a greater maximum torque but a lower rated speed when compared to the Optimal Future motor. It can also be seen that the Optimal Future motor has a greater period of constant torque i.e. the constant torque is provided is provided for a greater range of angular speeds. In the case of the optimal motor the constant torque is provided upto ~5000 RPM where as in the State of the Art motor the constant torque is provided for ~3000 RPM. On the other hand it should be noted that the State of the Art motor has a greater span of angular speeds in which it provides constant power. These characteristics are typical of the motor technologies chosen.

It is a delimitation/constraint within the scope of the thesis to maintain similar peak power characteristics of both motors and also to maintain identical maximum wheel torques across all drive-trains. The latter is achieved by adjusting the gear ratio of the transmission.The comparison of motor power characteristics can be seen in Figure 5.4. It can be observed that the peak powers of the motors are within 10% of each other. Figure 5.5 compares the torque applied on the wheel by both the drive-trains for different wheel velocities. As discussed before the maximum torque on the wheel was maintained identical across all drive-trains by adjusting

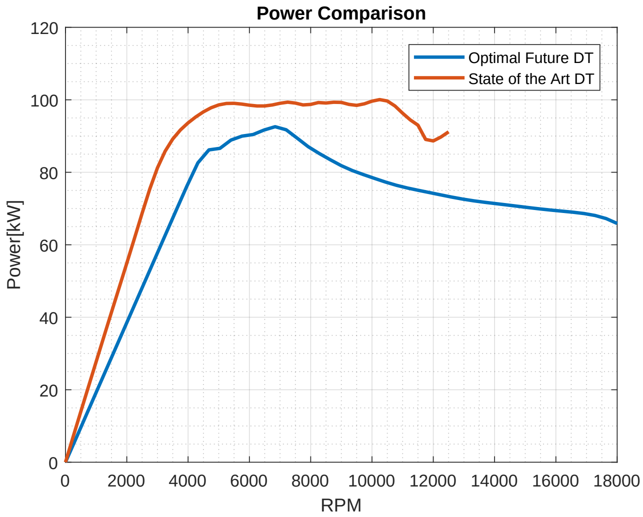

Figure 5.4: Comparison of motor powers

the gear ratio of the transmission according to the torque characteristics of the motors.It can be observed that the Optimal Future drive-train provides lower torque on the wheel at higher speed due to the fact that at higher angular speeds the Optimal Future motor is power limited i.e. it outputs a lower power when compared the the State of the Art drive-train.

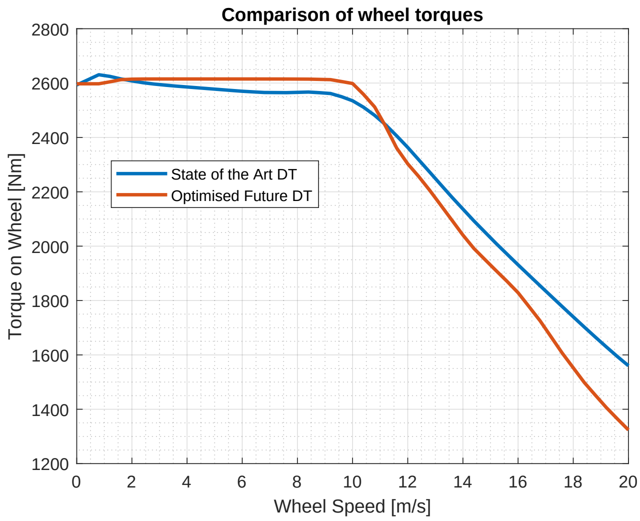

Figure 5.5: Comparison of wheel torques

The summary of the characteristics of each of the motors is shown in Table 5.7.

Table 5.7: Comparison of State of the Art and Optimised motors

Parameter	State of the Art E-Motor	Optimised Future E-Motor
Peak Torque (from motor)	270 Nm	185 Nm
Peak Power	100 kW	93 kW
Gear Ratio	2.71	3.95
Maximum Torque on Wheels	~2640 Nm	~2640 Nm

5.3 Use Case-Cruise Control

In this section the results of the cruise control use case will be described. As detailed in previous sections the reference velocity for the cruise control use case is a pulse input with an amplitude of 35 kmph and a period of 10 s.

5.3.1 Performance of State of the Art Drive-train

In this section the performance of the State of the Art drive-train will be studied, to analyse its performance Figure 5.6 will be decisive.

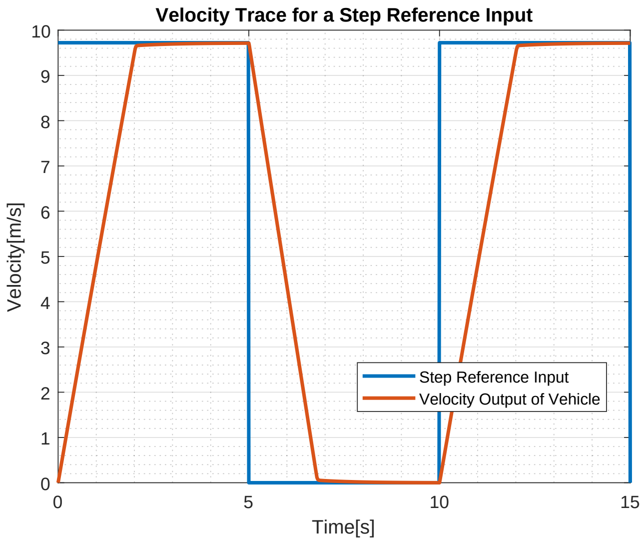

Figure 5.6: Performance of State of the Art DT for a Pulse Input of 35kmph

It can be seen from Figure 5.6 that the State of the Art drive-train traces the reference velocity quite well. This would imply that the developed cruise controller functions well in conjunction with the State of the Art drive-train. It should be noted here that the acceleration characteristic of the drive-train is validated with real-world test data from vehicles with similar vehicle and drive-train characteristics. Further, it should also be noted that the braking is achieved solely with regenerative braking. The dynamic behaviour of the system is described in Section 5.3.3.

5.3.2 Performance of Optimised Future Drive-train

In this section the performance of the Optimal Future drive-train will be studied, to analyse its performance Figure 5.7 will be decisive.

It can be seen from Figure 5.7 that the Optimal Future drive-train traces the reference velocity quite well. This would imply that the developed cruise controller functions well in conjunction with the Optimal Future drive-train. It should also be noted that the braking was achieved solely with regenerative braking in a similar manner to that of the State of the Art drive-train. The dynamic behaviour of the system is described in Section 5.3.3.

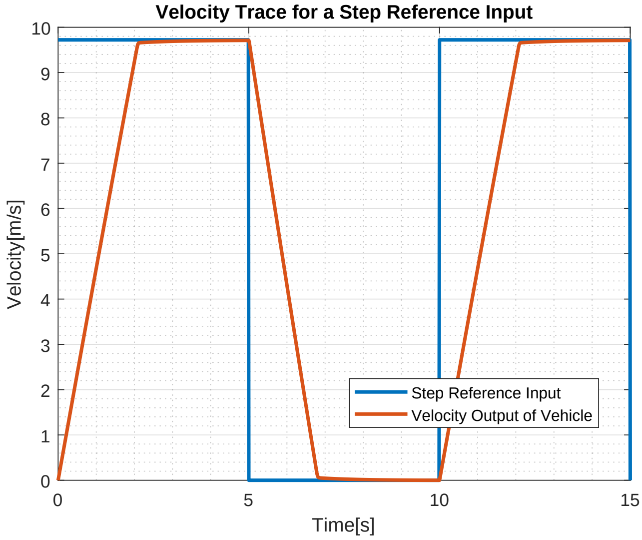

Figure 5.7: Performance of Optimised DT for a Pulse Input of 35kmph

5.3.3 Comparison and Validation

In this section the differences in performance between the drive-trains will be studied. To study the comparative velocity tracing of the drive-trains Figure 5.8 would prove to be useful. It can be seen from Figure 5.8 that the Optimal Future drive-train, in the acceleration phase, attains the reference velocity of 35 kmph later/ at a time after the State of the Art drive-train. It can also be seen from the figure that the deceleration characteristics of both the vehicles are similar. The dynamic characteristics of both the vehicles and the reasons for their behaviour will be dealt with in the upcoming sections.

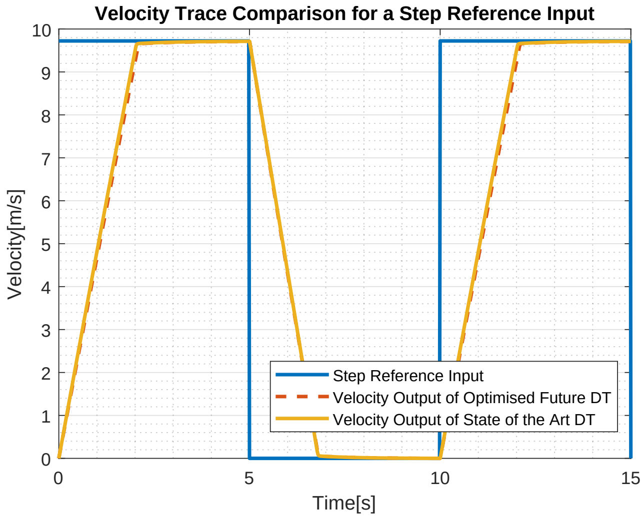

Figure 5.8: Performance Comparison of Both DT for a Pulse Input of 35kmph

Within the scope of the thesis the acceleration characteristics of the drive-trains are of utmost importance as it is these characteristics which are predominately dependant on the motor characteristics. Hence the performance of the drive-trains between 0 and 2.5 s should be the focus of study. Figure 5.9 shows the comparative performance of the drive-trains between 0 and 2.5 s.

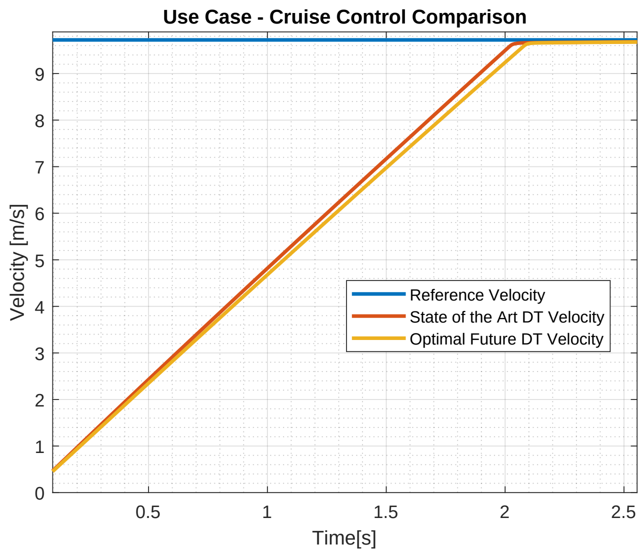

Figure 5.9: Performance Comparison of Both DT for a Pulse Input of 35kmph (0 - 2.5 s)

It could be easily understood from Figure 5.9 that the tracing of velocity between 0 and 2.5 s in both the drive-trains is akin to that of a step response of a signal, hence the dynamic characteristics of the drive-trains could be characterised in terms of step response parameters. The dynamic response characteristics for both drive-trains is shown in Table 5.8.

Table 5.8: Comparison of dynamic characteristics of DTs

Parameter	State of the Art DT	Optimal Future DT
Rise Time	1.6377 s	1.6825 s
Settling Time	2.0048 s	2.0619 s
Peak	9.7132 m/s	9.7106 m/s
Steady State Error	0.033 m/s	0.037 m/s

It can be seen from Table 5.8 that both the drive-trains perform quite similar as the performance was targeted to be similar while running the simulations, however the Optimal Future drive-train is inferior to the State of the Art drive-train in all regards with respect to dynamic characteristics. Optimal Future drive-train performs 3% lower than the State of the Art in terms of Rise Time and Settling time. The Optimal Future drive-train has 10% higher error than the State of the Art drive-train. To understand this very similar but a bit different performance, one must understand the exact phenomena occurring at the wheel across both the drive-trains. This is explained briefly in E.1

5.4 Use Case-Drive Cycle

The performance of the drive-trains for different inputs of drive cycle sources has been discussed in this section. Each of the results is shown as a velocity trace and as error analysis comparison for drive-trains.

5.4.1 NEDC

In this section the performance of the drive-trains on the NEDC cycle will be studied. First the performance of the State of the Art drive-train will be studied followed by the Optimal Future drive-train.

Performance of State of the Art Drive-train

The tracing of the request velocity performed by the State of the Art drive-train is shown in Figure 5.10. It can be seen that the State of the Art drive-train traces the requested velocity very well, with a standard magnification of the velocity plot no inherent differences between the the reference and actual vehicle velocity can be seen. In order to analyse if there is indeed a difference between the requested and actual velocity a

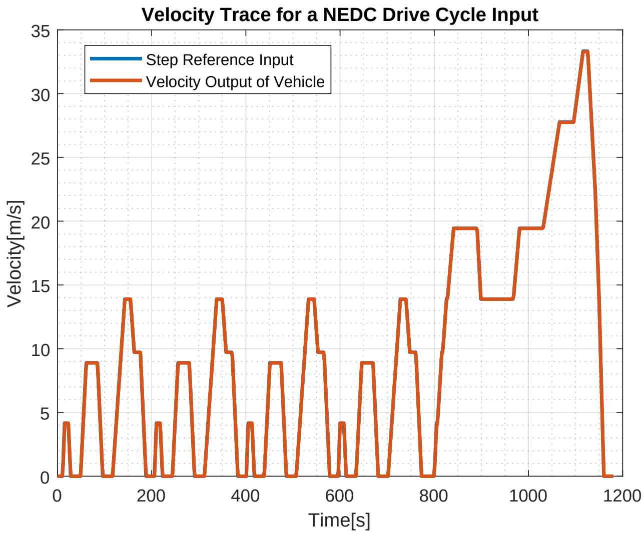

Figure 5.10: Performance of State of the Art DT for NEDC Input

magnified image of the velocity plot is studied. The order of magnification was ˜10 and even at this scale no considerable difference between the requested and vehicle velocity could be found. This magnified velocity plot is shown in Figure 5.11.

Performance of Optimal Future Drive-train

The tracing of the request velocity performed by the Optimal Future drive-train is shown in Figure 5.12. It can be seen that the Optimal Future drive-train traces the requested velocity very well, with a standard magnification of the velocity plot no inherent differences between the the reference and actual vehicle velocity can be seen. In order to analyse if there is indeed a difference between the requested and actual velocity a magnified image of the velocity plot is studied. The order of magnification was ˜10 and even at this scale no considerable difference between the requested and vehicle velocity could be found. This magnified velocity plot is shown in Figure 5.13.

Comparison and Validation

To understand the differences in performance of the two drive-trains on the NEDC cycle one must study the deviation of the vehicle velocity from the requested velocity i.e. the velocity error. The convention followed was that a positive error signified that the requested velocity was higher than the actual vehicle velocity. The plot

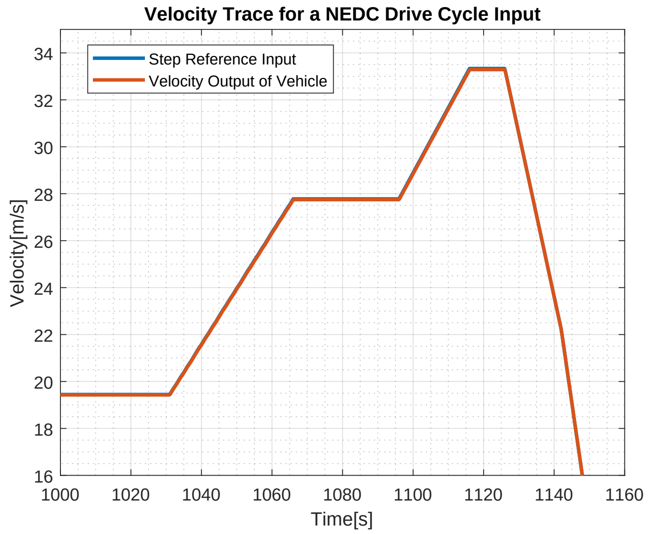

Figure 5.11: Performance of State of the Art DT for NEDC (Magnified)

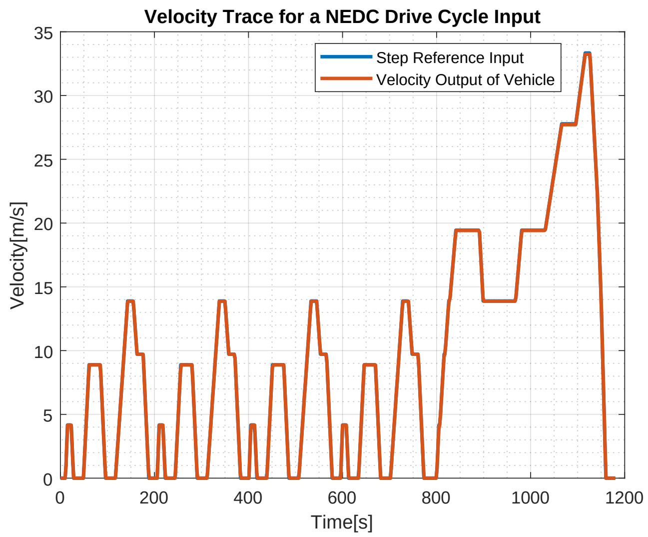

Figure 5.12: Performance of Optimised DT for NEDC Input

of error on both drive-trains is shown in Figure 5.14. It can be seen that the maximum magnitude of error for the drive-trains is 0.12 m/s, which can be considered as a lower error as it closely represents the targeted velocity. It can also be seen that at low vehicle velocities, the errors of the State of the Art drive-train and the Optimal Future drive-train are remarkably similar, it is at high velocities that they begin to deviate with the Optimal Future drive-train having higher error (seen in the time span of 1000 - 1200 s). This is due to the fact that the Optimal Future drive-train is power limited at higher velocities due to its motor power characteristics discussed in previous sections.

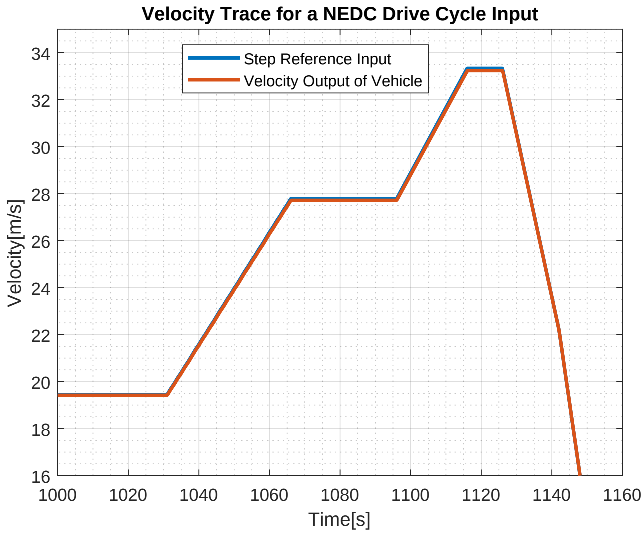

Figure 5.13: Performance of Optimised DT for NEDC (Magnified)

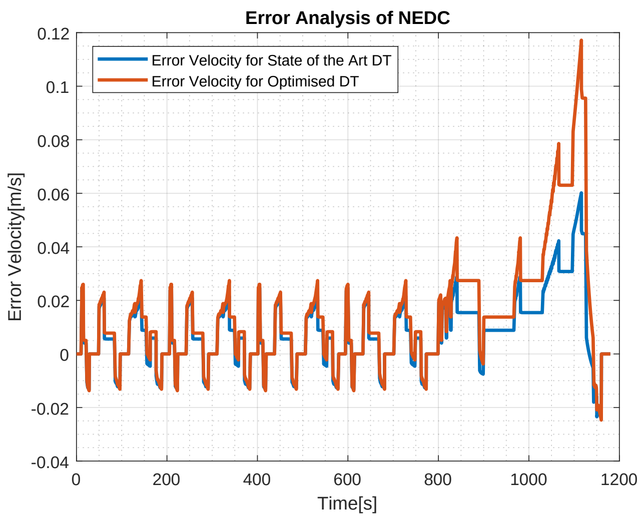

Figure 5.14: Error Analysis of Both DT for NEDC Input

5.4.2 US06

In this section the performance of the drive-trains on the US06 cycle will be studied. First the performance of the State of the Art drive-train will be studied followed by the Optimal Future drive-train.

Performance of State of the Art Drive-train

The tracing of the request velocity performed by the State of the Art drive-train is shown in Figure 5.15. It can be seen that the State of the Art drive-train traces the requested velocity very well, with a standard magnification of the velocity plot no inherent differences between the the reference and actual vehicle velocity can be seen.

In order to analyse if there is indeed a difference between the requested and actual velocity a magnified image of the velocity plot is studied. The order of magnification was ~10 and even at this scale no considerable difference between the requested and vehicle velocity could be found. This magnified velocity plot is shown in Figure 5.16.

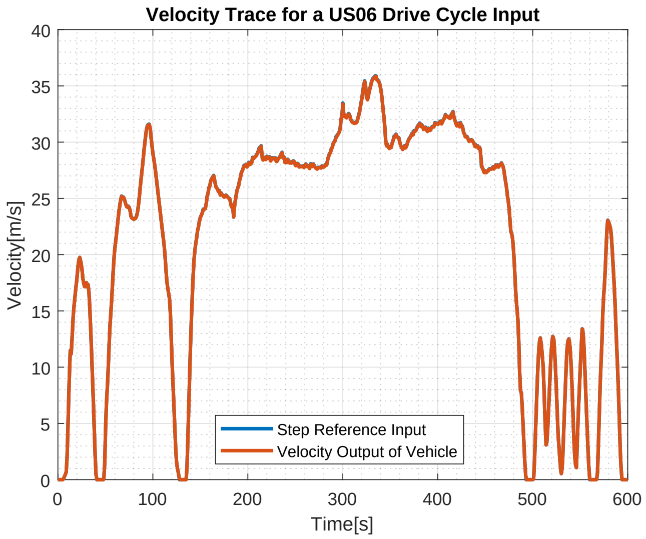

Figure 5.15: Performance of State of the Art DT for US06 Input

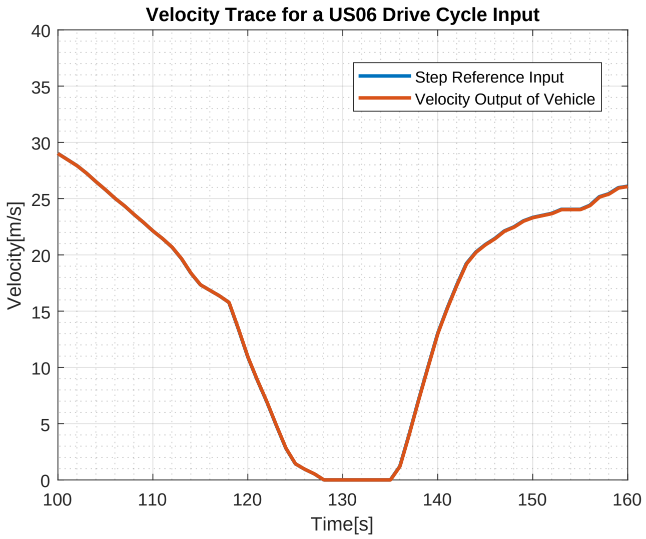

Figure 5.16: Performance of State of the Art DT for US06 (Magnified)

Performance of Optimal Future Drive-train

The tracing of the request velocity performed by the Optimal Future drive-train is shown in Figure 5.17. It can be seen that the Optimal Future drive-train traces the requested velocity very well, with a standard magnification of the velocity plot no inherent differences between the the reference and actual vehicle velocity can be seen.

In order to analyse if there is indeed a difference between the requested and actual velocity a magnified image of the velocity plot is studied. The order of magnification was ˜10 and even at this scale no considerable difference between the requested and vehicle velocity could be found. This magnified velocity plot is shown in Figure 5.18.

Comparison and Validation

To understand the differences in performance of the two drive-trains on the US06 cycle one must study the deviation of the vehicle velocity from the requested velocity i.e. the velocity error. The convention followed was that a positive error signified that the requested velocity was higher than the actual vehicle velocity. The plot of error on both drive-trains is shown in Figure 5.19. It can be seen that the maximum magnitude of error for the drive-trains is 0.2 m/s, this is a low error and is within tolerance limits. It can also be seen that at low vehicle

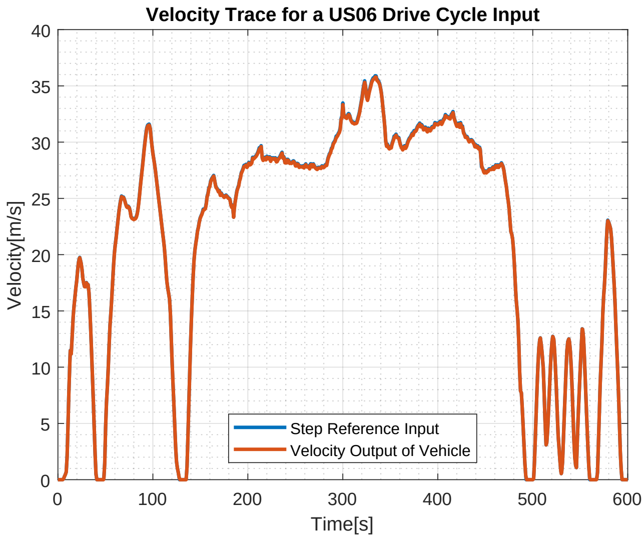

Figure 5.17: Performance of Optimised DT for US06 Input

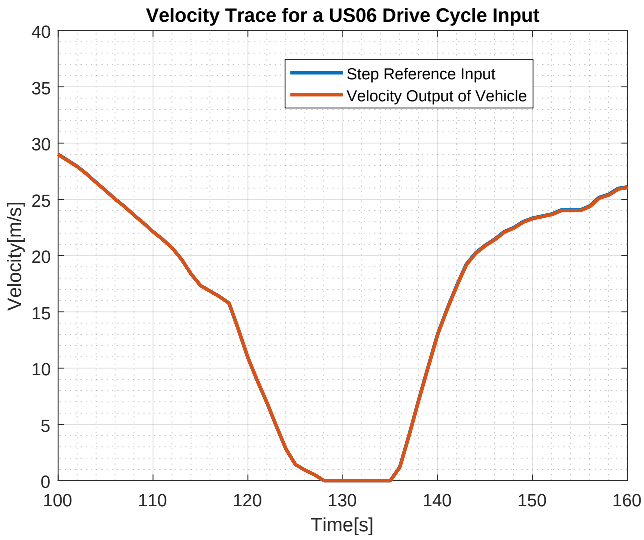

Figure 5.18: Performance of Optimised DT for US06 Input (Magnified)

velocities, the errors of the State of the Art drive-train and the Optimal Future drive-train are remarkably similar, it is at high velocities that they begin to deviate with the Optimal Future drive-train having higher error, this is represented by peaks in the error plot of the Optimal Future drive-train, these peaks can be seen in the regions around 100 s, 330 s and 580 s, it is at these times that there is a high velocity/acceleration demand. This error trend is due to the fact that the Optimal Future drive-train is power limited at higher velocities due to its motor power characteristics discussed in previous sections.

5.4.3 WLTP Class 3

In this section the performance of the drive-trains on the WLTP Class 3 cycle will be studied. First the performance of the State of the Art drive-train will be studied followed by the Optimal Future drive-train.

Performance of State of the Art Drive-train

The tracing of the request velocity performed by the State of the Art drive-train is shown in Figure 5.20. It can be seen that the State of the Art drive-train traces the requested velocity very well, with a standard magnification of the velocity plot no inherent differences between the the reference and actual vehicle velocity can be seen.

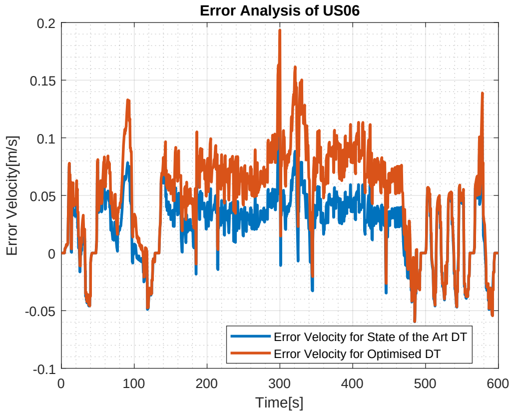

Figure 5.19: Error Analysis of Both DT for US06 Input

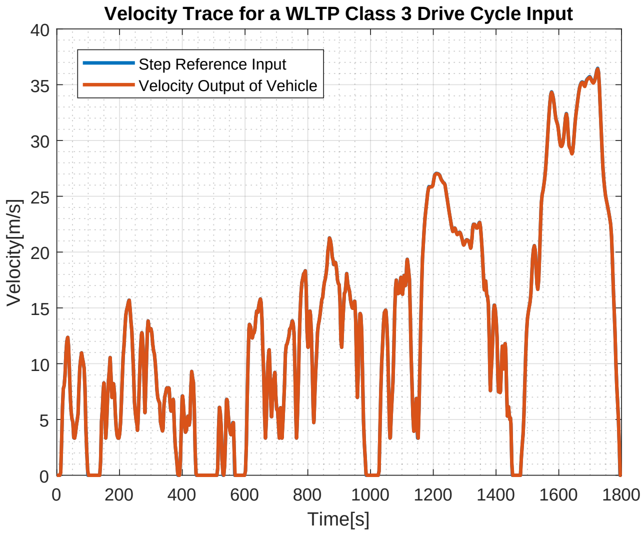

Figure 5.20: Performance of State of the Art DT for WLTP Class 3 Input

In order to analyse if there is indeed a difference between the requested and actual velocity a magnified image of the velocity plot is studied. The order of magnification was ˜3 and even at this scale no considerable difference between the requested and vehicle velocity could be found. This magnified velocity plot is shown in Figure 5.21.

Performance of Optimal Future Drive-train

The tracing of the request velocity performed by the Optimal Future drive-train is shown in Figure 5.22. It can be seen that the Optimal Future drive-train traces the requested velocity very well, with a standard magnification of the velocity plot no inherent differences between the the reference and actual vehicle velocity can be seen.

In order to analyse if there is indeed a difference between the requested and actual velocity a magnified image of the velocity plot is studied. The order of magnification was ˜3 and even at this scale no considerable difference between the requested and vehicle velocity could be found. This magnified velocity plot is shown in Figure 5.23.

Comparison and Validation

To understand the differences in performance of the two drive-trains on the WLTP Class 3 cycle one must study the deviation of the vehicle velocity from the requested velocity i.e. the velocity error. The convention followed

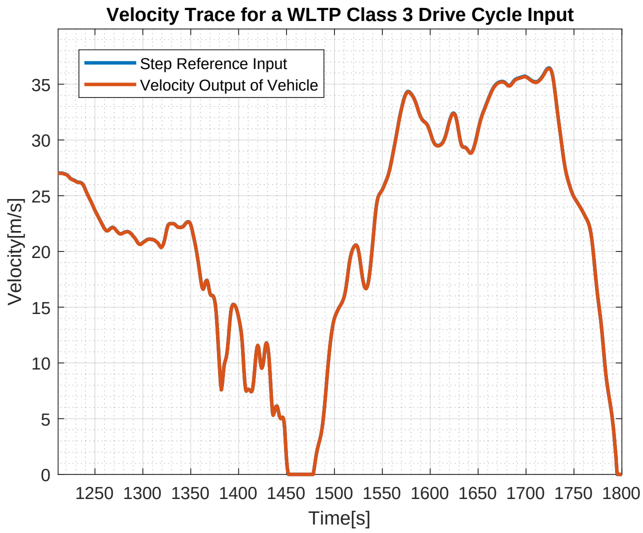

Figure 5.21: Performance of State of the Art DT for WLTP Class 3 Input (Magnified)

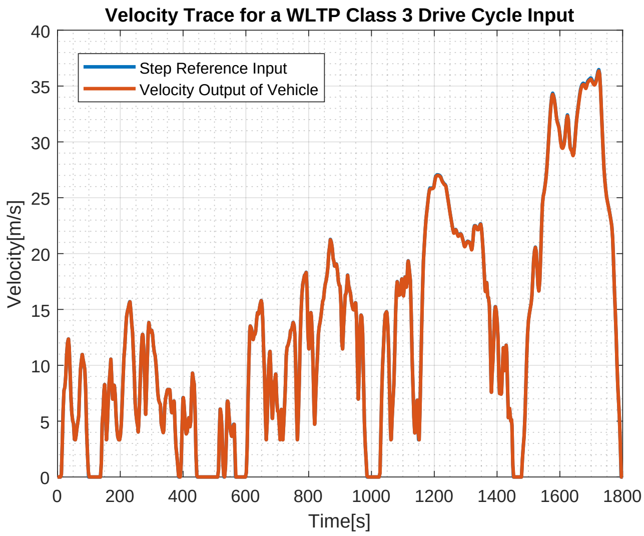

Figure 5.22: Performance of Optimal Future DT for WLTP Class 3 Input

was that a positive error signified that the requested velocity was higher than the actual vehicle velocity. The plot of error on both drive-trains is shown in Figure 5.24. It can be seen that the maximum magnitude of error for the drive-trains is 0.12 m/s, this is a low error and is within tolerance limits. It can also be seen that at low vehicle velocities, the errors of the State of the Art drive-train and the Optimal Future drive-train are remarkably similar, it is at high velocities that they begin to deviate with the Optimal Future drive-train having higher error, this is represented by peaks in the error plot of the Optimal Future drive-train, these peaks can be seen in the regions around 1200 - 1400 s and 1600 - 1800 s, it is at these times that there is a high velocity/acceleration demand. This error trend is due to the fact that the Optimal Future drive-train is power limited at higher velocities due to its motor power characteristics discussed in previous sections.

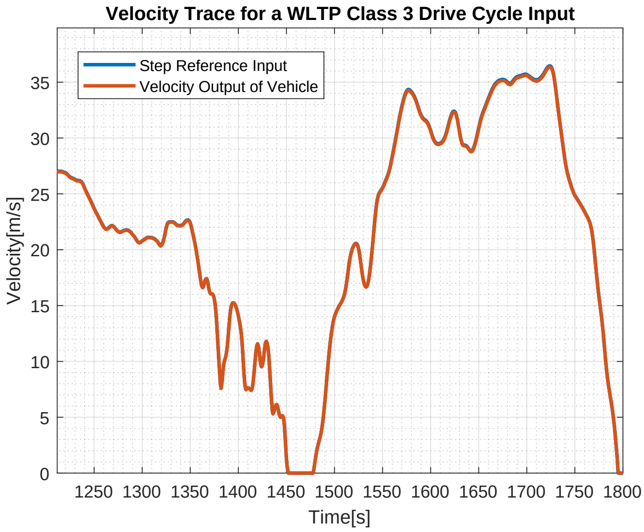

Figure 5.23: Performance of Optimal Future DT for WLTP Class 3 Input (Magnified)

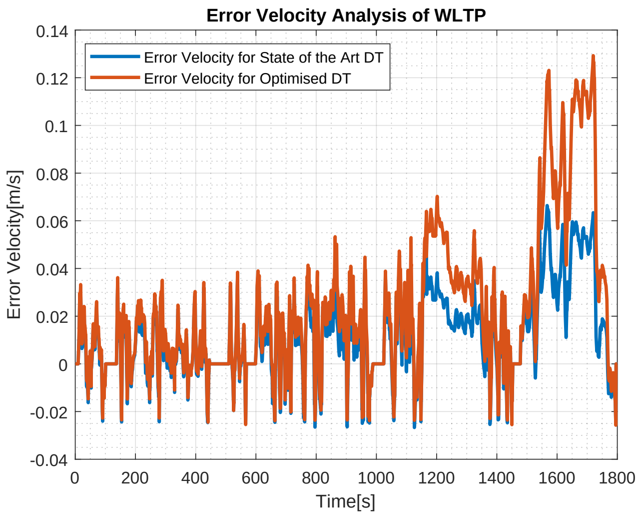

Figure 5.24: Error Analysis of Both DT for WLTP Class 3 Input

5.5 Use Case-Traction Control

The traction control use case performance for different drive-trains has been discussed in this section. The comparison is drawn and explained in brief. The test criteria is discussed in section 4.1.6 and the test surfaces are described in 3.6. The drive-trains were subjected to start in a Dry Asphalt condition and then move in to Icy condition and comes back to Dry Asphalt. Thus it could be regarded as a Traction Control Acceleration use case.

5.5.1 Performance of State of the Art Drive-train

The performance of the State of the Art drive-train is shown with the help of Vehicle Velocity Trace and Vehicle Wheel Slips in figures 5.25 and 5.26 respectively. It could be seen from figure 5.25 that the velocity trace for an input of 50kmph is being achieved during the manoeuvre. The velocity trace appears to be increasing in the first 1.5s, where the transition to Ice starts, after which the velocity drops when compared to the trend. As the contact surface changes to Ice, the tractive force reduces resulting in a reduction in velocity at vehicle level. This trend is an expected phenomenon. The velocity tries to follow the initial trend at 5s, where the second transition to Dry Asphalt starts, after which it reaches the targeted velocity with a steady state error.

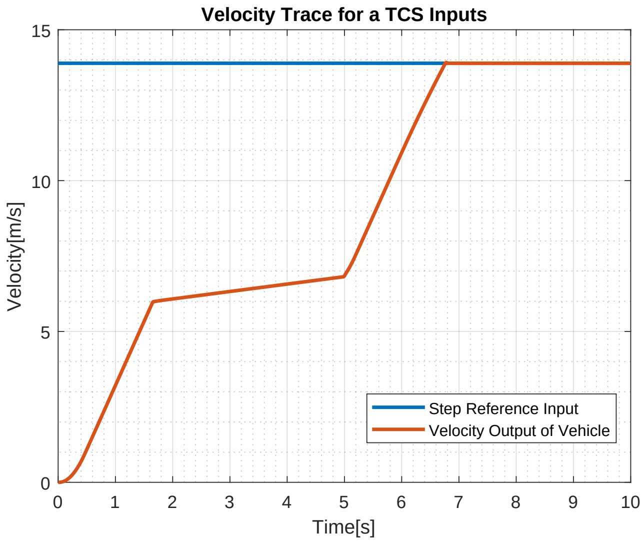

Figure 5.25: Velocity Trace of State of the Art DT for TCS Inputs

The targeted wheel slip for the manoeuvre is 0.15 or a 15% slip, as also can be seen from figure 5.26. When the vehicle is in the Dry Asphalt region, the slip tends to increase to 0.15 and is maintained by the controller at 0.15 till it reaches 1.5. As it moves into the Ice surface the wheel slip shoots up beyond 0.2, which is an expected trend, after which the controller tries to even out the slip back to 0.15. At 5s, as the vehicle enters the Dry Asphalt region the wheel slip dips down towards zero slip, indicating a reduction in tractive force. The controller pitches in to maintain the slip at 0.15 until the vehicle reaches the requested velocity. As the vehicle reaches the requested velocity, the wheel slip fluctuates around zero slip due to the steady state error in velocity of the vehicle when compared to the requested velocity.

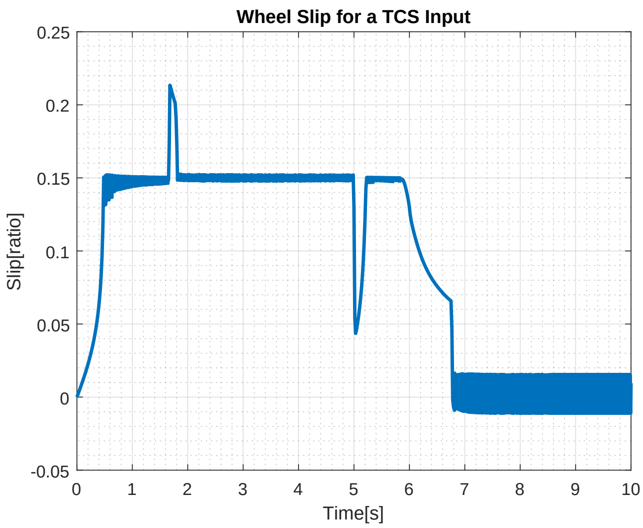

Figure 5.26: Wheel Slip Trace of State of the Art DT for TCS Inputs

5.5.2 Performance of Optimised Future Drive-train

The performance of the Optimised Future drive-train is shown with the help of Vehicle Velocity Trace and Vehicle Wheel Slips in figures 5.27 and 5.28 respectively. The velocity trend follows the same trend as discussed in section 5.5. However the velocities reached with respect to time is different compared to State of the Art drive-train. This will however be discussed in the next section. The targeted wheel slip for the manoeuvre is 0.15 or a 15% slip, as also can be seen from figure 5.28. The Wheel Slip trend matches to the trend depicted for the State of the Art drive-train, however the slip ratios being traced are a bit different from the State of the Art drive-train and this would be discussed in the next section.

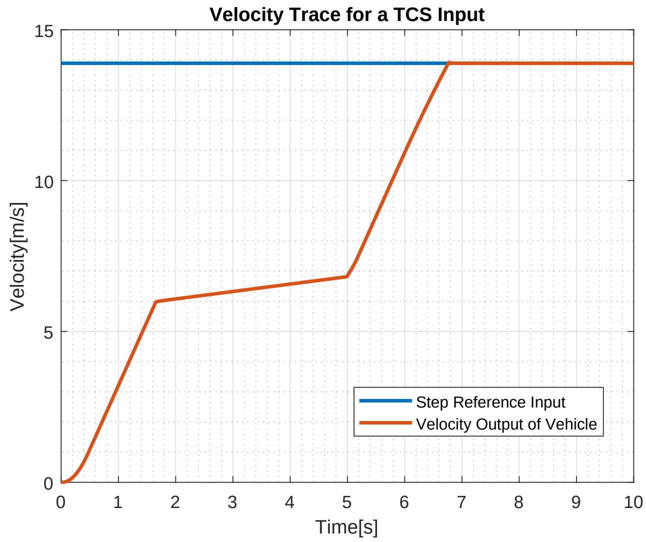

Figure 5.27: Velocity Trace of Optimised DT for TCS Inputs

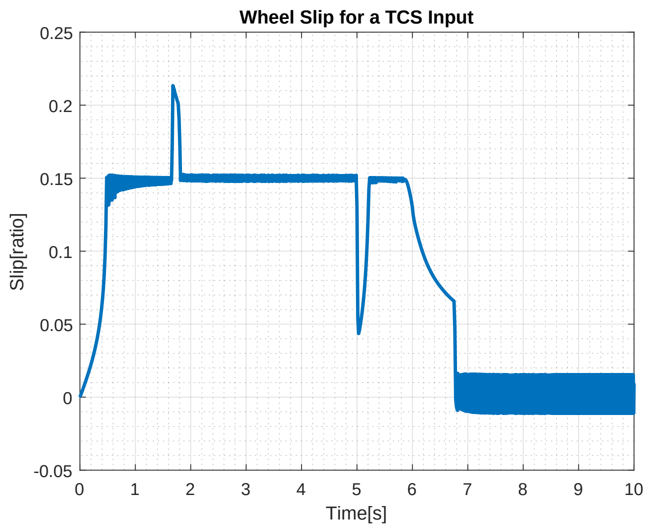

Figure 5.28: Wheel Slip Trace of Optimised DT for TCS Inputs

5.5.3 Comparison and Validation

The comparison of the Traction Control System Manoeuvre is depicted with Wheel Slip Comparison, Wheel Torque Comparison, Vehicle Velocity Comparison and Wheel Velocity Comparison as shown in figures 5.29,5.30, 5.31 and 5.32 respectively.
Before the results are discussed in brief, a comparison analysis at the system level and a better understanding regarding the motor characteristics is provided with the help of figure E.5 in the Appendix E.2

0s-1.5s Having established that fact, if the results of wheel slip are to be seen in the figure 5.29, the optimised future drive-train reaches the target slip of 0.15 or 15% much faster than the State of the Art drive-train. It could be noted that in the first 1.5s the vehicle is accelerating in Dry Asphalt. The first 0.5s in figure 5.30 show that the torque at the wheel is much lower in State of the Art drive-train and as a result the optimised drive-train spools up faster compared to the State of the Art drive-train. However once the targeted slip is reached by the State of the Art drive-train the slip ratio fluctuates around 0.15.

The similar trend as discussed above could be seen in the Vehicle Velocity traces as well as the Wheel velocity traces in figures 5.31 and 5.32

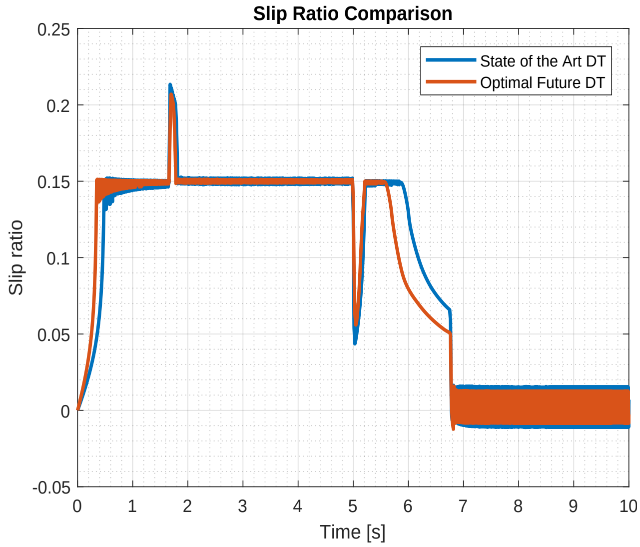

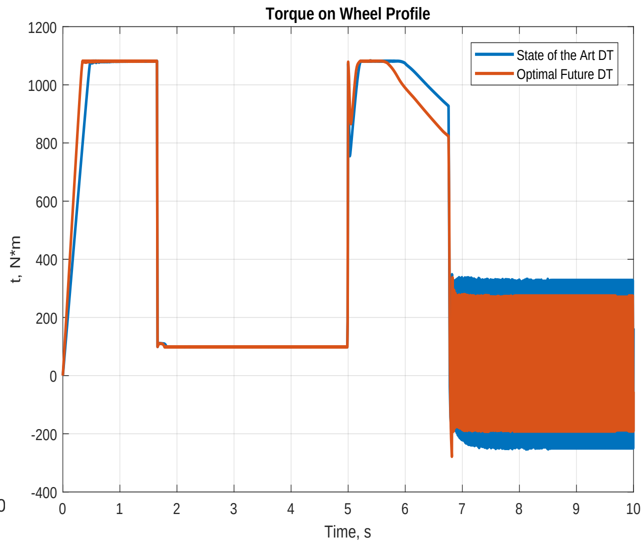

Figure 5.29: Slip Comparison for Both DT for TCS Inputs

Figure 5.30: Torque on Wheel Comparison for Both DT for TCS Inputs

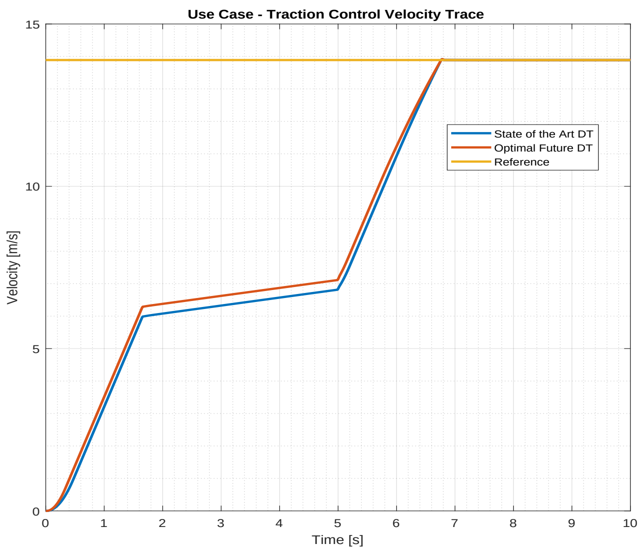

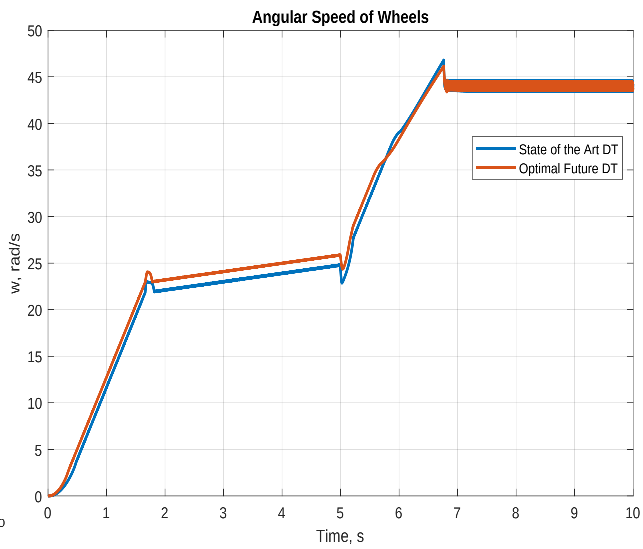

Figure 5.31: Vehicle Velocity Comparison for Both DT for TCS Inputs

Figure 5.32: Wheel Velocity Comparison for Both DT for TCS Inputs

1.5s-5s As the vehicle enters the Ice Patch from the Dry Asphalt region, a sudden spike could be seen in the slip comparison figure 5.29 in both the drive-trains. This certainly suggests the loss of tractive force, however it could be seen that the optimised future drive-train has a better accuracy and traces back to slip of 0.15 much faster than the State of the Art drive-train. This could be attributed to the motor characteristics. The torque on the wheel drops down to slightly lower values than that of State of the Art drive-train.

5s-10s In this phase the vehicle is entering back into the Dry Asphalt region from Ice. From the Velocity figure 5.31 it could be seen that both the drive-trains have similar trend till 5.8S. However both the velocity lines converge as they near the requested velocity. It could be seen from the figure 5.32 that there is a crossover in the angular velocities of the wheel. The main reason for this could be seen in the figure 5.30, where the Torque drops off at 5.8s for the Optimised Future drive-train when compared to the State of the Art drive-train. This is typically the motor characteristic, as the Optimised Future Motor lacks the ability to provide the torque required at higher speeds as compared to the State of the Art drive-train. It could however be seen as a trade-off between a faster response in an Icy patch and faster drop-off of torque at a higher speeds as the targeted velocity is approached.

6 Conclusion

The principles developed to improve the controllability, i.e. the response time and accuracy, that is encountered due to an inferior motor technology were applied on the Future Technology and the results substantiated the principles.
A summary of the advantages and disadvantages of the drive-trains could be seen in the table below 6.1, where '+' signifies 'Better', '-' signifies 'Worse' and '0' signifies 'Reference'.

With respect to the Motor Size the Optimal Future drive-train is typically larger at the expense of losing the Permanent magnet technology. However, within the scope of this thesis the length on an approximation was found to be 1.5 times the Permanent Magnet Technology (with equal stator inner diameter maintained across both motor technologies). In terms of ease of fabrication, the Optimal Future drive-train takes the edge due to it's simple design geometry and operating costs. The Acceleration Performance was retained similar and the Drivecycle Performance is found to be similar in both the drive-trains. The Traction Control Performance was found to be better in Optimal Future drive-train than the State of the Art drive-train due to the fact that the optimised future drive-train has higher angular acceleration when considering the inertial effects on to the motor. The State of the Art drive-train has a higher constant power region where as the Optimal Future drive-train has higher Constant Torque region.

To summarise, barring the NVH (Noise,Vibrations & Harshness) issue due to the torque ripple, the Reluctance motor Technology has all probability to be a leading alternative although it is inferior in terms torque density (with all other factors being equal) and the principles developed in optimisation can be clubbed with better motor geometries (generated through FEM analysis) to negate the shortcomings in Vehicle Dynamic opportunities. In conclusion, the controllability of the Optimal Future Drive-train performs similarly to that of the State of the Art Drive-train despite losing on the permanent magnets. The advancement in controllability with an inferior technology can thus be achieved with the developed principles.

Table 6.1: Drive-train Comparison Summary

	State of the Art drive-train	**Optimal Future drive-train**
Motor Size	0	-
Ease of Fabrication(inc costs)	0	+
Acceleration Performance	0	0
Drive Cycle Performance	0	0
Traction Control Performance	0	+
Constant Power	0	-
Constant Torque	0	+
Torque Ripple	0	-
Inverter Cost	0	+
Inverter availability in current market	0	-
Motor Response Characteristics	0	-
Region of Efficient Operation	0	+

7 Future Work

The scope of further development based on this thesis can be divided into two categories namely,

- Development of electrical systems
- Development of vehicle systems

Under the domain of electrical systems the following research and development activities can be performed:

1. Development of a control methodology/ algorithm to minimise torque ripple in the Switched Reluctance Motor - this would then overcome the principal disadvantage of NVH in the Switched Reluctance Motor.
2. Perform FEM & thermal efficiency analysis on the proposed SRM - a well defined FEM simulation could be used to obtain a well defined rotor geometry and stator constructional details, where as a thermal efficiency analysis would provide the efficiency contours of the proposed SRM so that one may study its energy consumption characteristics.

Under the domain of vehicle systems the following research and development activities can be performed:

1. Development of a two track vehicle model enabling the application of lateral dynamic use cases. The performance of the proposed future drive-train, both in longitudinal and lateral scenarios, could be further augmented by studying various motor-transmission topologies.
2. Optimisation of the gear ratio of the proposed drive-train by taking into consideration efficient regions of operation in the drive cycles use case.

References

[12] *NIST/SEMATECH e-Handbook of Statistical Methods. Market Research.* NIST/SEMATECH, 2012. URL: http://www.itl.nist.gov/div898/handbook/.

[17a] *DESIGN OF EXPERIMENTS (DOE) TUTORIAL. Tutorial.* ASQ, 2017. URL: http://asq.org/learn-about-quality/data-collection-analysis-tools/overview/design-of-experiments-tutorial.html.

[17b] *Linear Induction Motor. Market Research.* Circuit Globe, 2017. URL: https://circuitglobe.com/linear-induction-motor.html.

[17c] *Permanent Magnet Synchronous Motor (PMSM) Market is Expected to Garner $31.1 Billion, Globally, by 2022. Market Research.* Allied Market Research, 2017. URL: https://alliedmarketresearch.wordpress.com/2017/02/03/permanent-magnet-synchronous-motor-pmsm-market-is-expected-to-garner-31-1-billion-globally-by-2022/.

[17d] *Switched Reluctance Motor (SRM). Market Research.* EMWorks, 2017. URL: https://www.emworks.com/blog/motor-design/switched-reluctance-motor-electric-vehicles.

[ARI15] A. ARIKERE. Vehicle Dynamic Opportunities in Electrified Vehicles for Active Safety Interventions (2015).

[Bar+09] T. J. Barlow et al. A Reference Book of Driving Cycles for Use in the Measurement of Road Vehicle Emissions (2009).

[CG17] P. Cazzola and M. Gorner. Global EV Outlook 2017 (2017).

[CS17] A. Cooper and K. Schefter. Plug-in Electric Vehicle Forecast: 2016-2025. *IEI Report* (2017).

[Err+17] M. Erriquez et al. Trends in Electric Vehicle Design (2017).

[FFH08] T. Finken, M. Felden, and K. Hameyer. Comparison and design of different electrical machine types regarding their applicability in hybrid electrical vehicles. *18th International Conference on Electrical Machines, 2008. ICEM 2008.* (2008).

[IE17] A. C. (IEI) and K. S. (EEI). *Plug-in Electric Vehicle Forecast: 2016-2025.* Institute for Electric Innovation, 2017.

[INC] G. V. R. INC. Permanent Magnet Market Size, Share Trend Analysis Report By Product (Ferrite Magnet, Rare Earth), By Application (Automotive, Electronics, Industrial) By Region, And Segment Forecasts, 2018 - 2024. *Global Permanent Magnet Market Share, Industry Report, 2018-2024* ().

[KC12] K. Kiyota and A. Chiba. Design of Switched Reluctance Motor Competitive to 60-kW IPMSM in Third-Generation Hybrid Electric Vehicle. *IEEE TRANSACTIONS ON INDUSTRY APPLICATIONS* (2012).

[KF16] B. Kerdsup and N. H. Fuengwarodsakul. Performance and cost comparison of reluctance motors used for electric bicycles (2016).

[Kri01] R. Krishnan. SWITCHED RELUCTANCE MOTOR DRIVES (2001).

[Pal+18] K. Palmera et al. Total cost of ownership and market share for hybrid and electric vehicles in the UK, US and Japan. *Applied Energy* **209** (2018), 108–119.

[Raj13] K. Rajashekara. Present Status and Future Trends in Electric Vehicle Propulsion Technologies (2013).

[UC07] S. Unnasch and M. Chan. Full fuel cycle assessment Tank to wheels emissions And energy consumption (2007).

[UnN+17] F. Un-Noor et al. A Comprehensive Study of Key Electric Vehicle (EV) Components, Technologies, Challenges, Impacts, and Future Direction of Development (2017).

[Vis05] R. Visinka. 3-Phase Switched Reluctance (SR) Sensorless Motor Control Using a 56F80x, 56F8100 or 56F8300 Device (2005).

[Zet07] C. Zetterqvist. *Powertrain modelling and control algorithms for traction control.* Department of Electrical Engineering,Linköpings Universitet, 2007.

A EV Database

Manufacturer	Model	Top speed	Acceleration	Capacity	Nominal Range	Number of Motors	Motor Size	Motor Type	Transmission Type	Drive
BMW	i3	150 km/h (93 mph)	8 s	4	183 km (114 mi)[1]	1	125kW	HSM	Single Speed with Fixed Ratio	RWD
Bolloré	Bluecar	130 km/h (81 mph)		4	250 km (160 mi) in urban use	1	50kW	DC(Assumed as there isn't any inverter)	Automatic	FWD
BYD	e6	140 km/h (87 mph)	8 s	5	300 km (186 mi)	1-2	or - 160kW2 I	PM Synchronous Motors	CVT	AWD
Chevrolet	Bolt EV	150 km/h (93 mph) (speed limited)	6.5 s	5	383 km (238 mi)	1	150kW	Permanent magnet motor/generator, torque 266 lb.ft./360 Nm	Electronic Precision Shift, final drive ratio 7.05:1	FWD
Citroën	C-Zero	130 km/h (81 mph)	15.9 s	4	150 km (93 mi)	1	47kW	PM Synchronous Motors	Automatic	RWD
Ford	cus Elect	135 km/h (84 mph)	9.9 s	5	185 km (115 mi)[21]	1	107kW	AC Synchronous Motor	1 Speed	FWD
Hyundai	Ioniq	185 km/h (115 mph)	10.8 s	4	169–250 km (105–155 mi)	1	88kW	PM Synchronous Motors	1 Speed	FWD
JAC Motors	EV/JAC	120 km/h/130 km/h	11.5 s	5	170 km / 300 km @ 60km/h	1	85kW	PM Synchronous Motors	NA	NA
Kia	Soul EV	145 km/h (90 mph)	11.2	5	150 km (93 mi) EPA,	1	81.5kW	AC Synchronous Motor	1 Speed	FWD
Mahindra	e2o plus	82 km/h (51 mph)		4	110–140 km (68–87 mi)	1	19KW	AC Induction Motors	Direct Drive 2 Speed	RWD
Mahindra	e-Verito	85 km/h (52 mph)		5	110 - 180 km (68 -111 mi)	1	30.5kW	AC Induction Motors	Direct Drive 1 Speed	FWD
Mercedes-Benz	s Electric	160 km/h (99 mph)	7.9 s	5	200 km (124 mi)	1	132kW	AC Induction Motors - Powered by Tesla	Direct Drive 1 Speed	FWD
Mitsubishi	i-MiEV	130 km/h (81 mph)		4	170 km (106 mi)	1	47kW	PM Synchronous Motors	Automatic	RWD
Nissan	Leaf	150 km/h (93 mph)		5	121 km (75 mi) EPA / 200 km (120 mi) (NEDC)	1	80kW	AC Synchronous Motor	Single Speed with Fixed Ratio	FWD
	QBeak	90 km/h (56 mph)		4	250 km (155 mi)	2	4+35.4 (70.8k	PM Synchronous Motors - In Wheel	Single Speed with Fixed Ratio	RWD
Peugeot	i0n	130 km/h (81 mph)	15.9 s	4	150 km (93 mi)	1	47kW	PM Synchronous Motors	Automatic	RWD
Renault	luence Z	135 km/h (84 mph), electronically limited		5	135 km (84 mi) + 15 km limp home mode	1	70kW	AC Synchronous Motor	Single Speed Auto	FWD
Renault	Zoe	135 km/h (84 mph), electronically limited	13.5 s	5	400 km (250 mi) 41 kWh battery	1	66kW	AC Synchronous Motor	Single Speed with Fixed Ratio	FWD
Sono Motors	Sion	140 km/h (87 mph)	11.5 s	5	250 km (160 mi)	1	80kW	AC Synchronous Motor	Single Speed with Fixed Ratio	RWD
Stevens[42]	Zecar	90 km/h (56 mph)[42]		5[43]	80 km (50 mi)	2	52kW Peak	Twin AC induction brushless and maintenance-free motors	Automatic	RWD
Volkswagen	e-Golf	145 km/h (90 mph)	10.4 s	5	190 km (118 mi)	1	100kW	PM Synchronous AC Motor	Single Speed Automatic	FWD
Volkswagen	e-Up!	130 km/h (81 mph)	12.4 s	4	160 km (99 mi)	1	60kW	PM Synchronous AC Motor	Single Speed Transmission	FWD

B Technology Analysis

This section presents the rational behind the evaluation and subsequent identification of the best technology for the proposed application within the scope of the thesis. The various technologies were scored and then ranked (with rank 1 being the best) based on various parameters, each parameter was assigned a significance score i.e. how important said parameter is within the scope of the thesis. The technology analysis was carried out for the various E-Motor and Transmission technologies as seen in the sections below.

B.1 E - Motor

Table B.1: Ranking of E-motor Technologies based on Cost/kW

Serial Number	Type	Parameter	Significance Score	Score	Total Score	Rank
1	SPMSM	Cost/kW (continuous)	9	1	9	5
3	RM	Cost/kW (continuous)	9	5	45	1
4	PMSynRM	Cost/kW (continuous)	9	3	27	3
5	Induction	Cost/kW (continuous)	9	4	36	2
6	IPMSM	Cost/kW (continuous)	9	2	18	4

Table B.2: Ranking of E-motor Technologies based on kW/kg

Serial Number	Type	Parameter	Significance Score	Score	Total Score	Rank
1	SPMSM	kW/kg	9	1	9	5
3	RM	kW/kg	9	5	45	1
4	PMSynRM	kW/kg	9	3	27	3
5	Induction	kW/kg	9	4	36	2
6	IPMSM	kW/kg	9	2	18	4

Table B.3: Ranking of E-motor Technologies based on Efficiency

Serial Number	Type	Parameter	Significance Score	Score	Total Score	Rank
1	SPMSM	Efficiency	8	0.92	7.36	3
3	RM	Efficiency	8	0.89	7.12	4
4	PMSynRM	Efficiency	8	0.94	7.52	1
5	Induction	Efficiency	8	0.87	6.96	5
6	IPMSM	Efficiency	8	0.93	7.44	2

Table B.4: Ranking of E-motor Technologies based on Controlability & associated Electric Architecture

Serial Number	Type	Parameter	Significance Score	Score	Total Score	Rank
1	SPMSM	Controlability & associated Electric Architecture	10	4	40	2
3	RM	Controlability & associated Electric Architecture	10	3,5	35	5
4	PMSynRM	Controlability & associated Electric Architecture	10	4	40	2
5	Induction	Controlability & associated Electric Architecture	10	5	50	1
6	IPMSM	Controlability & associated Electric Architecture	10	4	40	2

Table B.5: Ranking of E-motor Technologies based on Reliability

Serial Number	Type	Parameter	Significance Score	Score	Total Score	Rank
1	SPMSM	Reliability	6	4	24	4
3	RM	Reliability	6	5	30	1
4	PMSynRM	Reliability	6	4.5	27	3
5	Induction	Reliability	6	5	30	1
6	IPMSM	Reliability	6	4	24	4

Table B.6: Ranking of E-motor Technologies based on kW/Litre

Serial Number	Type	Parameter	Significance Score	Score	Total Score	Rank
1	SPMSM	kW/Litre	7	3.9	27.3	4
3	RM	kW/Litre	7	4	28	3
4	PMSynRM	kW/Litre	7	4.2	29.4	1
5	Induction	kW/Litre	7	2.5	17.5	5
6	IPMSM	kW/Litre	7	4.1	28.7	2

Table B.7: Overall ranking of E-Motor technologies

Serial Number	Type	Total	Overall Rank
1	SPMSM	117	5
3	RM	190	1
4	PMSynRM	158	3
5	Induction	176	2
6	IPMSM	136	4

B.2 Transmission

Table B.8: Ranking of Transmission Technologies based on Cost

Serial Number	Type	Parameter	Significance Score	Score	Total Score	Rank
1	CVT	Cost	7	3	21	3
2	Planetary	Cost	7	2	14	4
3	Fixed ratio -single ratio	Cost	7	5	35	1
4	Fixed ratio -multiple ratio	Cost	7	4	28	2

Table B.9: Ranking of Transmission Technologies based on Efficiency

Serial Number	Type	Parameter	Significance Score	Score	Total Score	Rank
1	CVT	Efficiency	9	0.88	7.92	4
2	Planetary	Efficiency	9	0.96	8.64	3
3	Fixed ratio -single ratio	Efficiency	9	0.98	8.82	1
4	Fixed ratio -multiple ratio	Efficiency	9	0.97	8.73	2

Table B.10: Ranking of Transmission Technologies based on Versatility (measure of variability in gear ratio)

Serial Number	Type	Parameter	Significance Score	Score	Total Score	Rank
1	CVT	Versatility	8	5	40	1
2	Planetary	Versatility	8	4	32	2
3	Fixed ratio -single ratio	Versatility	8	2	16	4
4	Fixed ratio -multiple ratio	Versatility	8	3	24	3

Table B.11: Ranking of Transmission Technologies based on Weight

Serial Number	Type	Parameter	Significance Score	Score	Total Score	Rank
1	CVT	Weight	8	2	16	3
2	Planetary	Weight	8	1.75	14	4
3	Fixed ratio -single ratio	Weight	8	5	40	1
4	Fixed ratio -multiple ratio	Weight	8	4	32	2

Table B.12: Ranking of Transmission Technologies based on Influence on acceleration capability

Serial Number	Type	Parameter	Significance Score	Score	Total Score	Rank
1	CVT	Influence on acceleration capability	7	2	14	4
2	Planetary	Influence on acceleration capability	7	3	21	3
3	Fixed ratio -single ratio	Influence on acceleration capability	7	5	35	1
4	Fixed ratio -multiple ratio	Influence on acceleration capability	7	4	28	2

Table B.13: Ranking of Transmission Technologies based on Achievable Top Speed

Serial Number	Type	Parameter	Significance Score	Score	Total Score	Rank
1	CVT	Achievable Top Speed	5	5	25	1
2	Planetary	Achievable Top Speed	5	4	20	2
3	Fixed ratio -single ratio	Achievable Top Speed	5	2	10	4
4	Fixed ratio -multiple ratio	Achievable Top Speed	5	3	15	3

Table B.14: Ranking of Transmission Technologies based on Torque Carrying Capability

Serial Number	Type	Parameter	Significance Score	Score	Total Score	Rank
1	CVT	Torque Carrying Capability	8	3	24	4
2	Planetary	Torque Carrying Capability	8	5	40	1
3	Fixed ratio -single ratio	Torque Carrying Capability	8	4	32	2
4	Fixed ratio -multiple ratio	Torque Carrying Capability	8	4	32	2

Table B.15: Overall Ranking of Transmission Technologies

Serial Number	Type	Total	Overall Rank
1	CVT	148	4
2	Planetary	150	3
3	Fixed ratio -single ratio	177	1
4	Fixed ratio -multiple ratio	168	2

C Vehicle & Motor Specifications

C.1 Vehicle Specifications

This section outlines the schematic diagram of each subsystem with the corresponding inputs and outputs. The values of the subsystem parameters have also been presented here.

C.1.1 Vehicle Body

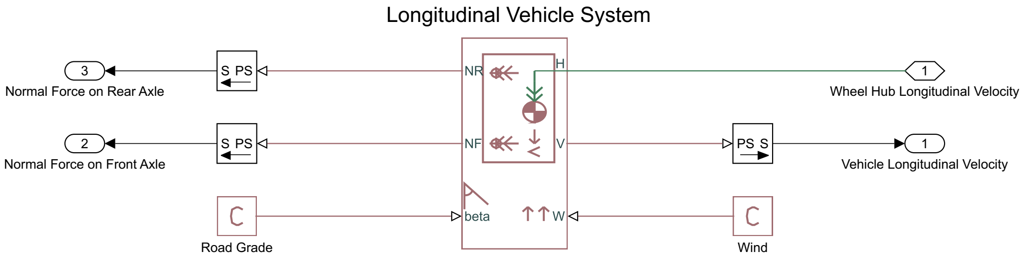

Figure C.1: Vehicle Body model schematic

Table C.1: Parameter values of the Vehicle Body

Parameter	Value
Mass of Vehicle	1547.65 kg
Frontal Area	1.978 m^2
Drag Co-efficient	0.281
Centre of gravity height from ground	0.3 m
Horizontal distance from CG to front axle	1.544 m
Horizontal distance from CG to rear axle	1.511 m

C.1.2 Wheels and Tires

Driven Wheels

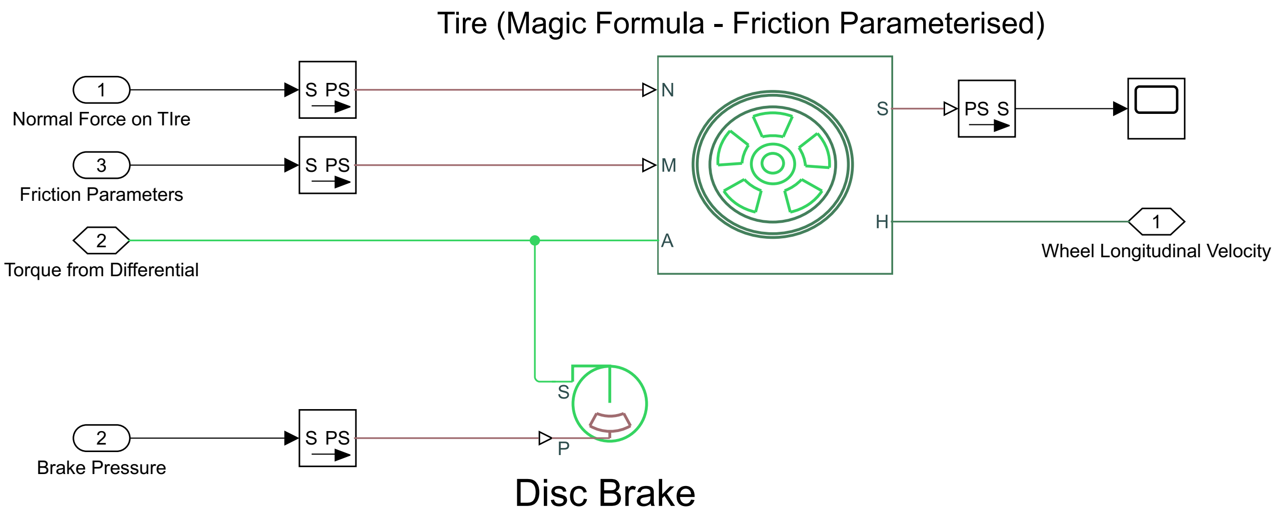

Figure C.2: Drive Wheel model schematic

Undriven Wheels

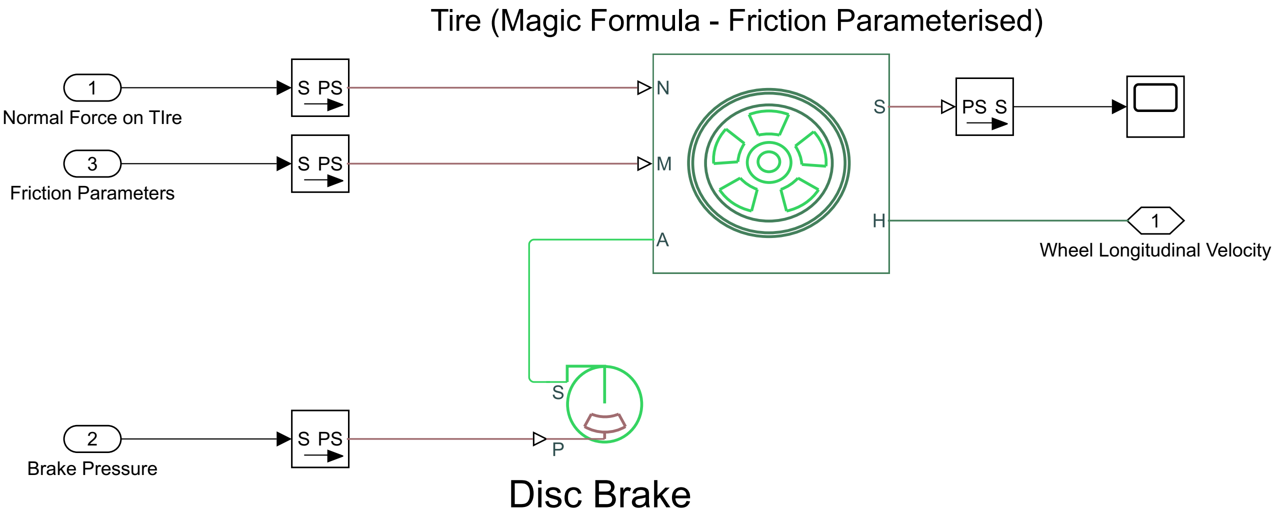

Figure C.3: Undriven Wheel model schematic

Table C.2: Parameter values of the Wheels

Parameter	Value
Rolling radius	0.31623 m
Mass	10 kg

C.1.3 Transmission

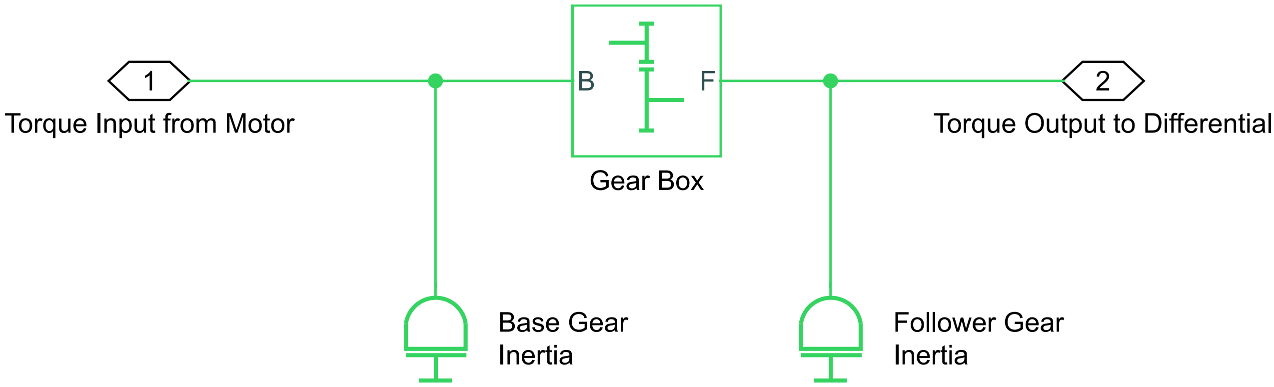

Figure C.4: Gear Box model schematic

Table C.3: Parameter values of the Gear Box

Parameter	Value
Radius of Base gear wheel	0.05 m
Inertia of Base gear wheel	0.0013 kgm^2
Radius of Follower gear wheel - State of the Art DT	0.135 m
Radius of Follower gear wheel - Optimal Future DT	0.197 m
Inertia of Follower gear wheel - State of the Art DT	0.0092 kgm^2
Inertia of Follower gear wheel - Optimal Future DT	0.0194 kgm^2
Gear ratio - State of the Art DT	2.71
Gear ratio - Optimal Future DT	3.95
Transmission efficiency	98%
Base gear wheel viscous friction coefficient	0.02 Nms/rad
Follower gear wheel viscous friction coefficient	0.02 Nms/rad

C.1.4 Open Differential

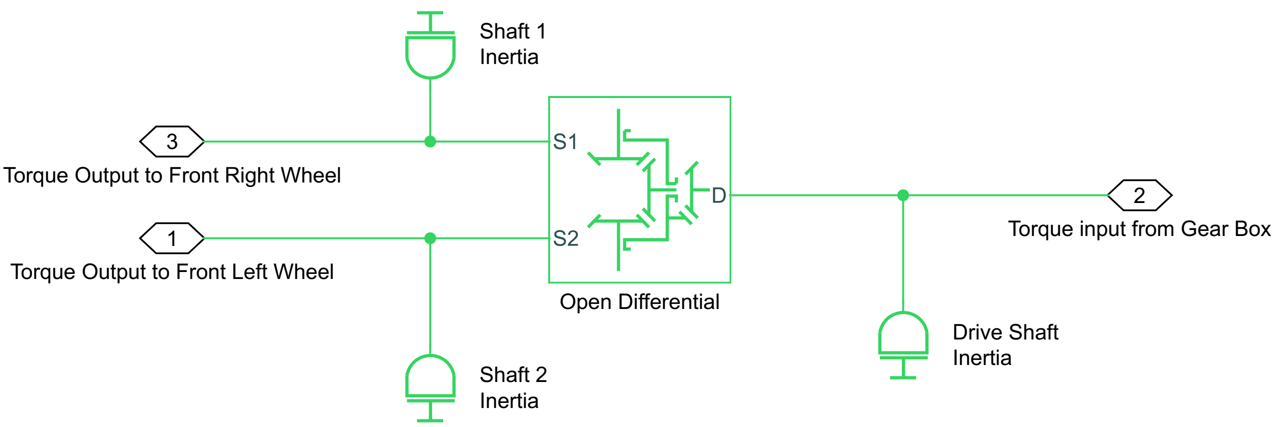

Figure C.5: Open differential model schematic

Table C.4: Parameter values of the Open Differential

Parameter	Value
Drive Shaft Inertia	0.05 kgmˆ2
Shaft 1 Inertia	0.05 kgmˆ2
Shaft 2 Inertia	0.05 kgmˆ2
Carrier to Drive-shaft Gear Ratio	3.61

C.1.5 Cruise Controller

This section presents the transfer function of the linearised vehicle model at different operating velocities. The tuned values of the PD controller are also presented in this section.

Table C.5: Linearised plant at different operating points

Operating Point[1] Velocity (kmph)	Transfer Function
50	$(2.971e-07s^6+6.74e-07s^5-1.363e-06s^4+2.837e-07s^3+1.803e-07s^2$ -1.646e-09s+1.302e-26)/ $(\mathrm{s}^8-4.449s^7+7.897s^6-6.984s^5+3.074s^4$ $\text{-0.5338s}^3-0.002618s^2)$
35	$(1.41e-07s^6+3.384e-07s^5-6.636e-07s^4+8.434e-08s^3+1.404e-07s^2$ -1.899e-08s-2.359e-26)/ $(\mathrm{s}^8-4.368s^7+7.49s^6-6.193s^5+2.326s^4-0.1908s^3-0.06357s^2$ +2.562e-18s)
15	$(2.493e-07s^6+6.627e-07s^5-9.556e-07s^4-2.83e-09s^3+$ $\text{1.758e-07s}^2-2.183e-08s+1.407e-26)/$ $(\mathrm{s}^8-4.081s^7+6.46s^6-4.841s^5+1.584s^4-0.08046s^3$ $\text{-0.04162s}^2-2.578e-20s)$

Table C.6: Parameter values of the Cruise Controller

Parameter	Value
Proportional Gain	10
Derivative Gain	0.2
Filter Coefficient	1

C.2 State of the Art Motor

The specification of the State of the Art motor are presented in this section.

Table C.7: Specifications of State of the Art motor

Parameter	Value
Battery Voltage	323 V
Number of pole pairs	4
Flux Linkage by magnets	0.071 Vs
Stator Resistance	0.008296 ohm
d-axis inductance	0.00017 H
q-axis inductance	0.00029 H
Stator Inner Diameter	0.17 m
Axial Length	0.18 m [2]

[1]Tested only on State of the Art drive-train
[2]Averaged value taken from motors available in the market currently

C.3 Optimal Future Motor

The specifications of the Optimal Future motor are presented in this section along with a schematic diagram of the proposed Switched Reluctance Motor.

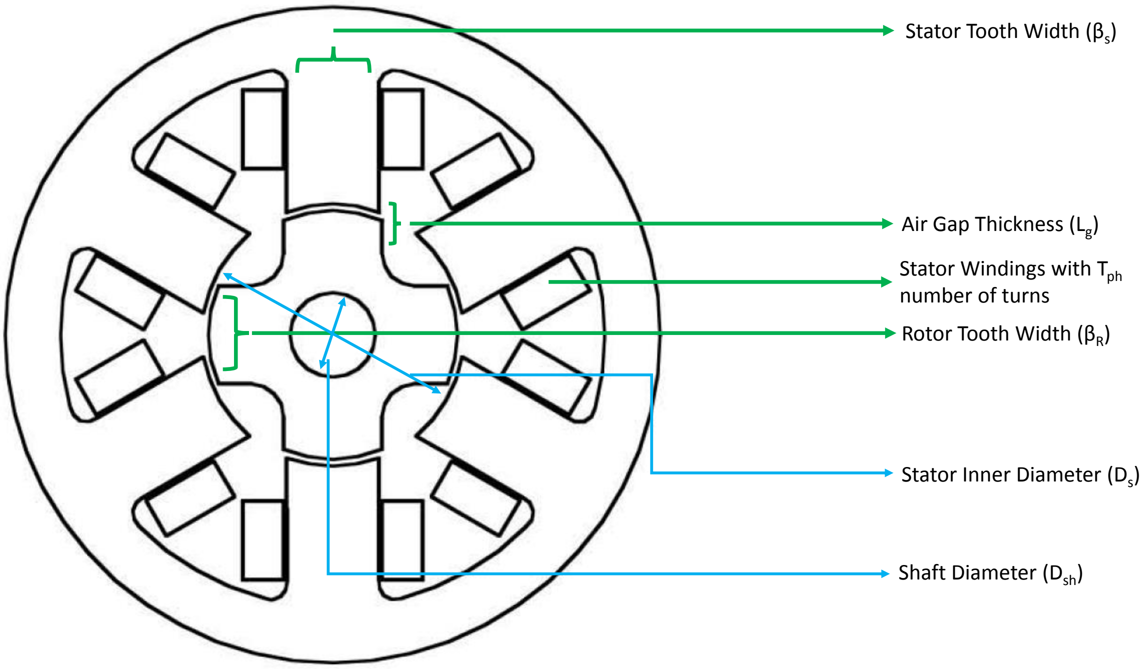

Figure C.6: Construction of SRM

Table C.8: Specifications of Optimised Future Motor

Parameter	Value
Battery Voltage	400 V
Number of rotor poles	4
Number of stator poles	6
Stator tooth width	22 deg
Air gap	0.3 mm
Number of turns per phase	20
Flux Linkage	0.6075 Vs
Saturated aligned inductance	3.75e-5 H
Aligned inductance	5.9e-3 H
Unaligned inductance	1.67e-4 H
Stator Inner Diameter	0.17 m
Axial Length	0.251 m

The length of the motor was calculated using the following approximation relating aligned inductance (L_a), number of turns per phase (T_{ph}), air gap (l_g), stator inner diameter (D), stator tooth width (β), motor axial length (L) and magnetic permeability (μ_0).

$$L_a = \frac{T_{ph}^2}{R_g}$$

Where

$$R_g = \frac{4l_g}{DL\beta\mu_0}$$

D Design of Experiments

D.1 List of Experiments

This section presents the list of experiments run on the future drive-train to obtain a relationship between the motor level parameters and the vehicle level targets.

Table D.1: List of experiments run to obtain Optimal Future drive-train (1/2)

Unaligned Inductance	Aligned Inductance	Saturated Aligned Inductance	Flux Linkage	Resistance of Stator Windings	Battery Voltage
0,000167	0,010325	0,00015	0,6075	1	400
0,00054425	0,0059	0,0000375	0,54675	0,05	400
0,00054425	0,010325	0,000065625	0,577125	0,7625	450
0,00067	0,019175	0,0000375	0,6075	0,7625	600
0,000167	0,010325	0,00015	0,577125	0,05	550
0,000167	0,0236	0,000065625	0,6075	0,2875	400
0,000167	0,019175	0,000065625	0,6075	0,05	600
0,00054425	0,019175	0,000121875	0,486	1	450
0,00029275	0,0059	0,000121875	0,577125	0,7625	550
0,00067	0,0059	0,000121875	0,516375	0,05	450
0,00054425	0,0236	0,0000375	0,577125	0,2875	600
0,00067	0,0059	0,000065625	0,516375	1	550
0,00029275	0,0059	0,00015	0,6075	0,2875	600
0,000167	0,0236	0,00015	0,6075	0,05	400
0,00067	0,0236	0,00009375	0,6075	1	550
0,0004185	0,01475	0,00009375	0,54675	0,525	500
0,000167	0,0236	0,0000375	0,516375	0,05	450
0,00029275	0,0059	0,00015	0,486	0,05	400
0,00054425	0,0059	0,00015	0,486	0,2875	550
0,00067	0,0059	0,00015	0,577125	0,05	600
0,00029275	0,010325	0,000065625	0,516375	0,2875	500
0,000167	0,019175	0,00015	0,486	0,2875	450
0,0004185	0,01475	0,00009375	0,54675	0,525	500
0,00067	0,0059	0,000065625	0,6075	0,05	550
0,00029275	0,0236	0,00015	0,486	0,7625	550
0,000167	0,0236	0,000121875	0,516375	1	600
0,00029275	0,019175	0,000065625	0,577125	1	450
0,00054425	0,019175	0,00015	0,6075	0,7625	400
0,000167	0,0236	0,000065625	0,486	0,7625	400
0,000167	0,0236	0,0000375	0,6075	0,7625	550
0,00054425	0,010325	0,00015	0,6075	1	600
0,00029275	0,0236	0,00015	0,516375	0,05	600
0,00029275	0,0059	0,000121875	0,577125	0,7625	550
0,00054425	0,0059	0,0000375	0,577125	0,525	600
0,00067	0,010325	0,0000375	0,486	0,525	450
0,00067	0,0236	0,0000375	0,516375	0,7625	400
0,00054425	0,019175	0,000121875	0,6075	0,05	550
0,00029275	0,0236	0,000121875	0,6075	0,2875	600
0,000167	0,0059	0,0000375	0,6075	0,7625	400
0,00067	0,0059	0,0000375	0,486	0,05	600

Table D.2: List of experiments run to obtain Optimal Future drive-train (2/2)

Unaligned Inductance	Aligned Inductance	Saturated Aligned Inductance	Flux Linkage	Resistance of Stator Windings	Battery Voltage
0,00054425	0,0236	0,000065625	0,486	0,05	400
0,000167	0,019175	0,0000375	0,486	0,2875	550
0,00054425	0,019175	0,000121875	0,486	1	450
0,00029275	0,0059	0,0000375	0,577125	0,05	600
0,00054425	0,010325	0,000121875	0,516375	0,2875	550
0,00067	0,0059	0,00015	0,6075	1	450
0,00054425	0,010325	0,000065625	0,577125	0,7625	450
0,00067	0,019175	0,00015	0,516375	0,7625	600
0,000167	0,0059	0,000121875	0,486	0,05	600
0,00029275	0,019175	0,000065625	0,516375	0,7625	600
0,00067	0,019175	0,0000375	0,516375	0,2875	550
0,00067	0,0236	0,00015	0,516375	0,05	450
0,00029275	0,0236	0,000121875	0,6075	0,7625	450
0,00067	0,0236	0,00009375	0,486	0,05	600
0,00029275	0,010325	0,00015	0,486	1	600
0,000167	0,010325	0,000121875	0,516375	0,7625	450
0,00067	0,010325	0,00015	0,486	0,7625	400
0,00054425	0,0236	0,0000375	0,6075	1	400
0,00029275	0,010325	0,0000375	0,6075	0,05	400
0,000167	0,019175	0,00015	0,577125	1	550
0,00067	0,0236	0,000065625	0,6075	0,05	450
0,000167	0,010325	0,0000375	0,6075	1	600
0,00054425	0,0059	0,000065625	0,516375	1	400
0,00029275	0,010325	0,0000375	0,486	1	400
0,000167	0,0059	0,000065625	0,486	0,05	400
0,0004185	0,01475	0,00009375	0,54675	0,525	500
0,00029275	0,019175	0,000065625	0,577125	1	450
0,00029275	0,019175	0,000121875	0,516375	0,05	400
0,00067	0,0059	0,0000375	0,6075	1	450
0,00029275	0,0236	0,00015	0,516375	1	400
0,00054425	0,0236	0,0000375	0,486	1	600
0,000167	0,0059	0,000121875	0,577125	0,2875	450
0,000167	0,0059	0,0000375	0,486	0,7625	600
0,00067	0,010325	0,000121875	0,577125	1	550
0,00067	0,0236	0,00015	0,577125	0,2875	550
0,00054425	0,0059	0,00015	0,6075	0,05	400
0,00067	0,010325	0,00009375	0,577125	0,2875	400
0,000167	0,0059	0,00015	0,486	1	450
0,00029275	0,010325	0,000065625	0,516375	0,2875	500
0,00067	0,019175	0,000121875	0,577125	0,2875	400

E Motivations for Results

E.1 Cruise Control Motivations

The simplest method to identify and study wheel phenomena is through wheel slips. The wheel slips for both drive-trains across the full test scenario is shown in Figure E.1.

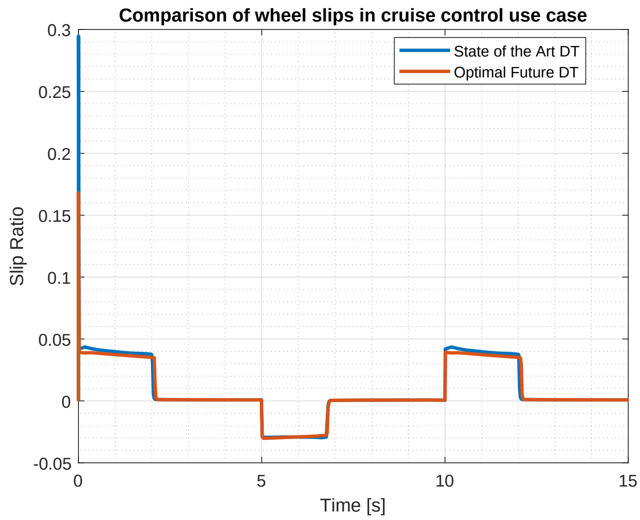

Figure E.1: Wheel slip comparison on Cruise Control use case

As expected the wheel slips follow a trend similar to that of the vehicle's velocity trace. There are two distinct time zones which are of importance, one, the initial region wherein there is a sudden spike of slip ratio (shown in Figure E.2) and two, the region of slip between 0 and 2.5 s (shown in Figure E.3).

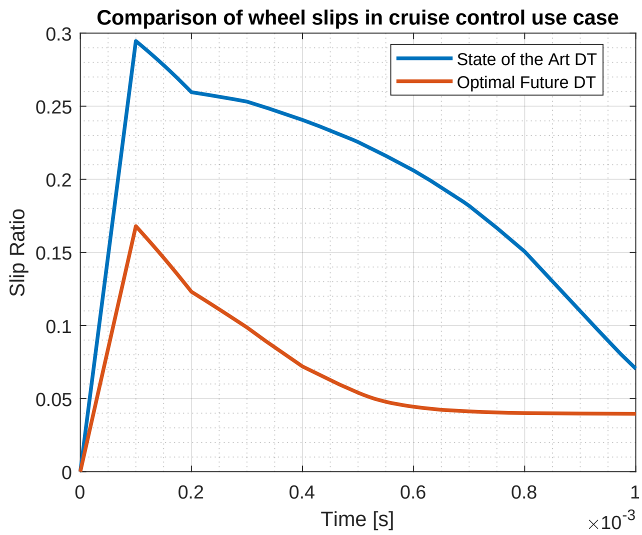

Figure E.2: Wheel slip comparison on Cruise Control use case (0 - 1e-3 s)

It can be seen from the Figures E.2 and E.3 that the slip ratio of the State of the Art drive-train is typically higher than that of the optimised future drive-train. This implies that for the same vehicle velocity the wheels in the State of the Art drive-train have a greater angular velocity when compared to that of the Optimal Future drive-train. These higher slips on the State of the Art drive-train (closer to optimal slip) enable the

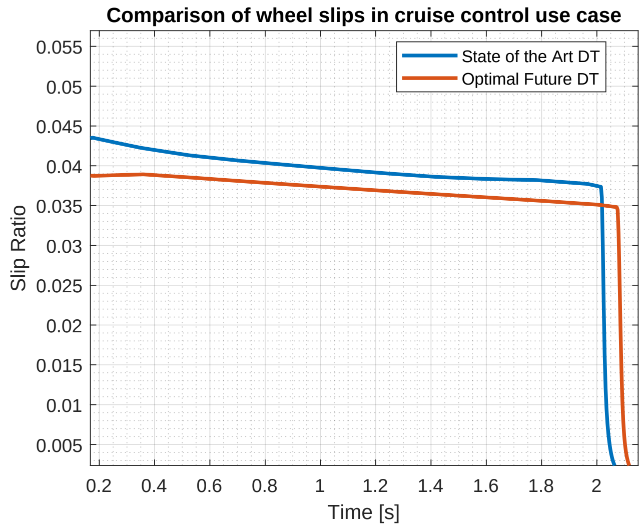

Figure E.3: Wheel slip comparison on Cruise Control use case (0.2 - 2.2 s)

State of the Art drive-train to accelerate quicker than the Optimal Future drive-train, hence the State of the Art drive-train achieves the requested reference velocity earlier than the Optimal Future drive-train. It should also be noted that the slip ratio rises faster in the State of the Art drive-train i.e. wheel angular acceleration is higher in the state of he art drive-train when compared to that of the Optimal Future drive-train.The reasons behind this phenomenon will be described in Section 5.5. The trends from the Figures would imply that each of the drive-trains apply different torques at the wheel with the State of the Art drive train applying a higher torque, this is seen in Figure E.4.

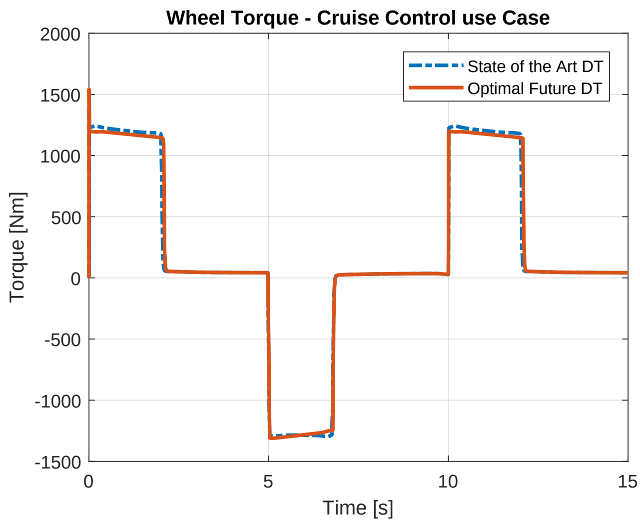

Figure E.4: Wheel torque comparison on Cruise Control use case

Having seen the effect of wheel slip on both the vehicle it is therefore interesting to study the performance of drive-trains when the wheel slip is being controlled. This work is carried out in Section 5.5.

E.2 Traction Control Motivations

It is already known that the optimised future drive-train is high speed and a low torque machine. This would mean a higher angular acceleration at the motor end when compared to the State of the Art drive-train for the same torque request at the wheel.

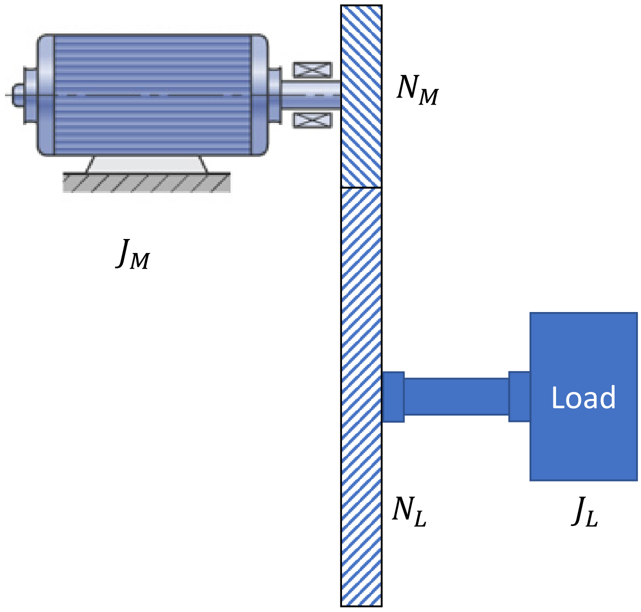

Figure E.5: Motor to Differential Schematic

In the figure E.5, the effect of reflected load inertia at the motor end due to the load is being estimated. The characteristic equations can be given as below. The speed (ω_M) and torque (T_M) of the motor can be related to number of teeth of base and follower gear wheels (N_M & N_L) and load torque (T_L) as,

$$\omega_M = \frac{\omega_L \cdot N_L}{N_M} \tag{E.1}$$

$$T_M = \frac{T_L}{N} \tag{E.2}$$

The reflected load inertia due to gear ratio (J_r), load inertia (J_L), load inertia including gear-box inertia (J_L^*), motor inertia (J_M) and the total torque realisable at the motor end can be related to gear box inertia (J_{GB}) and gear ratio (N) by,

$$J_r = \frac{J_L^*}{N^2} \tag{E.3}$$

where,

$$J_L^* = J_L + J_{GB} \tag{E.4}$$

$$N = \frac{N_L}{N_M} \tag{E.5}$$

The above terms can be related to the total reflected inertia as seen by the motor (J_t) by,

$$J_t = \frac{J_L^*}{N^2} + J_M \tag{E.6}$$

Considering that there exists same torque at the wheel and by keying in the rest of the parameters, it could be deduced that the optimised future drive-train has higher angular acceleration when considered the inertial effects on to the motor as well.